OULUN YLIOPISTO
UNIVERSITY of OULU

Department of Process and Environmental Engineering
Mass and Heat Transfer Process Laboratory

Master's Thesis

Carbon dioxide recovery with activated methyldiethanolamine

In Porvoo, February 4th, 2013

Author: _____
Silja Mustonen
B.Sc. (Eng.), University of Oulu

Supervisor: _____
Riitta Keiski
Prof., Doc., D.Sc. (Tech.), University of Oulu

Advisors: _____
Jussi Laitio
M.Sc. (Eng.), Neste Jacobs Oy

_____
Kari I. Keskinen
Doc., D.Sc. (Tech.), Neste Jacobs Oy

UNIVERSITY OF OULU **Thesis Abstract**

Faculty of Technology

Department	Degree Programme
Department of Process and Environmental Engineering	Process Engineering
Author	**Thesis Supervisor**
Mustonen, Silja Saimi Elisa	Keiski, R. Prof., Doc., D.Sc. (Tech.)

Title of Thesis

Carbon dioxide recovery with activated methyldiethanolamine

Major Subject	Type of Thesis	Submission Date	Number of Pages
Production Technology	Master's Thesis	February 2013	126 + 15 p.

Abstract

Power plants using fossil fuels are producing large amounts of carbon dioxide, which is one of the primary greenhouse gases. Typically the volume of carbon dioxide in flue gases from power plant operation is about 4-14 %. Post-combustion carbon dioxide capture based on aqueous alkanolamine absorption is a widely investigated method in recovering carbon dioxide. Functionality and cost-effectiveness are essentials when applying a technique to a real large scale power plant for reducing emissions. The alkanolamine absorption process consists of an absorber and a stripper column. Carbon dioxide is captured from the flue gas in the absorber and later on released in the stripper as a pure carbon dioxide for further treating. The aqueous alkanolamine can be recycled between the columns. Alkanolamine is acting as a physical and chemical solvent. This means that in addition to the physical dissolution simultaneously a chemical reaction accelerates the mass transfer. To fully understand the process detailed information about mass and heat transfer, chemical reactions and kinetics, phase and reaction equilibriums as well as physical properties of components are needed.

Aqueous piperazine activated methyldiethanolamine is one of the solvents used in the carbon dioxide capture processes. It is known that methyldiethanolamine has several advantages in the gas treating process and piperazine is used as an activator to accelerate the rate of reaction with carbon dioxide in the absorption process without diminishing the advantages. Challenges of the process are concerning high energy demand of the regeneration process occurring in the stripper column and modelling of the process.

In the experimental part of the thesis the aim was to test the ability of a commercial simulation program, Aspen Plus V7.3.2, to model the piperazine activated methyldiethanolamine process. In the simulations it was found that there are some deviations between the solubility results and the literature values likewise between the equilibrium results and literature values. The similarity of the results and the literature values varied widely depending on the concentration of the amines and used temperature. However, the physical properties of unloaded amine solutions were simulated sufficiently well. Since there are no research results or practical experiences available about the whole piperazine activated methyldiethanolamine process, the validity of the results when modelling the whole capture process is uncertain. Nevertheless, the results were promising when considering the capture efficiency and the amine recycling. According to the simulations performed in this work the process to be studied is more energy efficient than the monoethanolamine process.

Place of Storage

University of Oulu, Science Library Tellus

Additional Information

OULUN YLIOPISTO **Tiivistelmä opinnäytetyöstä**

Teknillinen tiedekunta

Osasto	Koulutusohjelma
Prosessi- ja ympäristötekniikan osasto	Prosessitekniikka
Tekijä	**Työn valvoja**
Mustonen, Silja Saimi Elisa	Keiski, R. Prof., Dos. TkT.

Työn nimi

Hiilidioksidin talteenotto aktivoidulla metyylidietanoliamiinilla

Opintosuunta	Työn laji	Aika	Sivumäärä
Tuotantoteknologia	Diplomityö	helmikuu 2013	126 + 15 s.

Tiivistelmä

Fossiilisia polttoaineita käyttävät voimalaitokset tuottavat suuria määriä hiilidioksidia, joka on yksi varteenotettavimmista kasvihuonekaasuista. Voimalaitoksen savukaasuissa hiilidioksidia on tyypillisesti tilavuudeltaan noin 4-14 %. Hiilidioksidin talteenotto savukaasuista (*post-combustion capture*) käyttäen liuottimena alkanoliamiinien vesiliuoksia on eräs tutkittu menetelmä. Toimivuus ja taloudellisuus ovat olennaisia, kun tekniikkaa lähdetään soveltamaan osaksi suuren mittakaavan voimalaitosta päästöjen vähentämiseksi. Hiilidioksidi absorboidaan savukaasuista liuottimeen pesurikolonnissa, absorberissa, ja myöhemmin liuottimen hiilidioksidi erotetaan kaasumaiseksi haihdutuskolonnissa, stripperissä, josta puhdas hiilidioksidi voidaan johtaa jatkokäsittelyyn. Käytettävä alkanoliamiinin voidaan regeneroinnin ansiosta kierrättää. Alkanoliamiini toimii sekä fysikaalisena että kemiallisena liuottimena. Fysikaalisen liukenemisen lisäksi aineensiirtoa tapahtuu siis myös kemiallisen reaktion avulla. Jotta talteenottoprosessi voidaan täysin ymmärtää, tarvitaan yksityiskohtaista tietoa aineen- ja lämmönsiirrosta, kemiallisista reaktioista ja niiden kinetiikasta, faasi- ja reaktiotasapainoista sekä aineiden fysikaalisista ominaisuuksista.

Piperatsiinilla aktivoitu metyylidietanoliamiinin vesiliuos on eräs hiilidioksidin talteenottoon käytetyistä liuottimista. Metyylidietanoliamiinilla tiedetään olevan useita hyötyjä kaasun käsittelyprosesseissa, ja piperatsiinin käyttö aktivaattorina perustuu sen ominaisuuteen kiihdyttää hiilidioksidin absorptioon osallistuvien reaktioiden nopeutta vähentämättä metyylidietanoliamiinin hyötyjä. Prosessin haasteet liittyvät tällä hetkellä stripperissä tapahtuvan regenerointiprosessin korkeaan energiankulutukseen sekä prosessin mallintamiseen.

Tämän työn tavoitteena oli testata kaupallisen simulointiohjelman, Aspen Plus V7.3.2, kykyä mallintaa kyseistä talteenottoprosessia. Simuloitaessa havaittiin liukoisuustulosten sekä tasapainovakioiden arvojen poikkeavan joiltakin osin kirjallisuudessa esitetyistä koetuloksista. Poikkeavuudet vaihtelivat riippuen amiinien konsentraatioista sekä lämpötiloista. Kuitenkin puhtaiden amiiniliuosten fysikaalisia ominaisuuksia ohjelma mallinsi riittävän hyvin. Kirjallisuudessa ei ole tarjolla vertailukohtia kokonaisen prosessin mallinnuksesta, joten niiden tulosten todenmukaisuudesta on mahdotonta antaa varmuutta. Voidaan kuitenkin todeta tulosten olleen lupaavia ottaen huomioon talteenoton tehokkuus sekä amiinin kierrätyksen onnistuminen. Tämän työn simulointien perusteella voidaan todeta, että kyseinen prosessi on regeneroinnin energiankulutukseltaan tehokkaampi kuin monoetanoliamiinin avulla toteutettava prosessi.

Säilytyspaikka

Oulun yliopisto, Tiedekirjasto Tellus

Muita tietoja

Preface

This thesis was conducted as a part of the CLEEN Carbon Capture and Storage Program/Work Package 3: Capture of CO_2 including advanced technologies - project, which is funded by Tekes - the Finnish Funding Agency for Technology and Innovation between August 2012 and January 2013. I would like to express my appreciation for the opportunity to be a part of this project. The work for this thesis was performed at Neste Jacobs Oy in the Competence Center Technology and Process.

I would like to thank my advisors Jussi Laitio and Kari I. Keskinen for all assistance and feedback. Their professional opinions and advices have been indispensable. I would also like to acknowledge Professor Riitta Keiski from the Mass and Heat Transfer Process Laboratory for being my supervisor. My colleagues at Neste Jacobs I would like to thank for the memorable coffee and lunch breaks.

Finally, I would like to acknowledge my family for all the support during this project and throughout my studies, and my friends, thanks to you the phrase "studying is the best time of your life" holds true.

In Porvoo, February 4th, 2013

Silja Mustonen

Table of contents

Thesis Abstract
Tiivistelmä opinnäytetyöstä

Preface 4
Table of contents 5
List of abbreviations 8
List of symbols 9

1 Introduction 12
I Theoretical part 13
2 Post-combustion gas purification 13
3 Absorption 17
3.1 Chemical solvents 17
3.2 Alkanolamines as absorbents 19
3.2.1 Thermal degradation of alkanolamines 22
3.2.2 Formation of heat stable salts 23
3.2.3 Environmental aspects of alkanolamines as absorbents 23
4 Methyldiethanolamine, MDEA 25
5 Activated MDEA 27
5.1 Ionic liquids as activators 28
5.2 Aminoethylethanolamine (AEEA) as an activator 29
5.3 Piperazine (PZ) as an activator 30
6 Mass and heat transfer 33
6.1 Multicomponent mass transfer fundamentals 33
6.2 Mass transfer models 35
6.2.1 The film theory 35
6.2.2 Penetration/surface renewal theory 37
6.3 Heat transfer 39
7 Chemical reactions, equilibrium and kinetics 41
7.1 Reactions of CO_2 with aqueous methyldiethanolamine 41
7.2 Reactions of CO_2 with aqueous piperazine 43
7.3 Reaction of CO_2 with PZ activated aqueous MDEA 43

7.4 Reaction kinetics 49
8 Phase equilibrium 53
8.1 N_2O-CO_2 analogy 54
8.1.1 The diffusion coefficients 55
8.1.2 Henry's law constants 57
8.2 Solubility 57
8.3 Models for phase and chemical equilibrium 59
9 Energy consumption 61
9.1 Heat of absorption 62
9.2 Heat of vaporization 64
9.3 Heat capacities 65
10 Modelling of the absorption/desorption process 66
10.1 Equilibrium stage model 67
10.2 Rate-based model 68
10.3 Modelling of the stripping column 69

II Experimental part 70
11 Modelling with Aspen Plus® 70
12 Modelling of solubility 74
12.1 Modelling results 74
12.2 Interpretation of the solubility results 75
13 Modelling of reaction equilibrium constants and physical properties 77
13.1 Reaction equilibrium constant simulations 77
13.2 Interpretation of the reaction equilibrium constant simulations 79
13.3 Modelling of physical properties 79
13.4 Interpretation of the results of physical property simulations 80
14 Modelling of the regeneration efficiency 82
14.1 Simulation problems 84
14.2 Simulation results 87
14.2.1 Absorber and stripper performances with PZ/MDEA systems 87
14.2.2 Comparison with MDEA and MEA systems 90
15 Modelling of process with amine circulation 96
15.1 About energy consumption 102
15.2 Salt formation 104
15.3 Amines in the exiting flue gas 107

16 Conclusions and proposals for further studies 109
References 111

Appendix 1 Results of the solubility simulations
Appendix 2 Results of the density simulations
Appendix 3 Results of the viscosity simulations
Appendix 4 Results of the surface tension and heat capacity simulations
Appendix 5 Absorber profiles with and without the water washing section
Appendix 6 Stripper profiles
Appendix 7 Stream results of the amine circulation simulation with PZ/MDEA 1
Appendix 8 Stream results of the amine circulation simulation with PZ/MDEA 2
Appendix 9 Stream results of the amine circulation simulation with PZ/MDEA 2_2
Appendix 10 Stream results of the amine circulation simulation with PZ/MDEA 2_3

List of abbreviations

AEEA	Aminoethylethanolamine
Am	Alkanolamine
AmH^+	Protonated amine
Am^+COO^-	Intermediate zwitterion
$AmCOO^-$	Amine carbamate ion
b	Base, OH^- or H_2O
bH^+	Protonated base
CO_2	Carbon dioxide
CO_3^{2-}	Carbonate ion
DEA	Diethanolamine
DMMEA	Dimethylmonoethanolamine
H_2O	Water
H_3O^+	Hydronium ion
HCO_3^-	Bicarbonate ion
HETP	Height Equivalent to a Theoretical Plate (Plate Height)
HSS	Heat stable salt
MAE	Methylaminoethanol
MDEA	Methyldiethanolamine
$MDEAH^+$	Protonated methyldiethanolamine
MEA	Monoethanolamine
NO_2	Nitrogen dioxide
OH^-	Hydroxide ion
PZ	Piperazine
$PZ(COO^-)_2$	Piperazine dicarbamate
$PZCOO^-$	Piperazine monocarbamate
PZH^+	Protonated piperazine
PZH^+COO^-	Protonated piperazine carbamate
PZH^{2+}	Diprotonated piperazine
SO_2	Sulphur dioxide
TEA	Triethanolamine

List of symbols

a	Contact area between gas and liquid phases [m^2/m^3]
a_i	Activity of component i in a solution [-]
c_t	Mixture concentration [$kmol/m^3$]
c_i	Concentration of component i in the liquid phase [$kmol/m^3$]
C_p	The heat capacity of the liquid [kJ/ (mol·K)]
$C_{p,\mathrm{L}}$	The mass-specific heat capacity of liquid [J/ (kg·K)]
d_i	Driving force of component i for mass diffusion in general Maxwell-Stefan equation [1/m]
D_i	Diffusion coefficient of component i [m^2/s]
$Đ_{ij}$	Maxwell-Stefan diffusion coefficient for pair i-j [m^2/s]
E	Enhancement factor for absorption with chemical reaction
E^{PFO}	Pseudo first order enhancement factor
E_a	Activation energy [J/mol]
E_f	Energy flux [W/m^2]
f_i	Fugacity of component i [Pa]
F	Faraday's constant [$9.65 \cdot 10^4$ C/mol]
ΔH_{abs}	Overall heat of absorption [J/mol]
$H_{\mathrm{CO2,H2O}}$	Henry's law constant for CO_2 in H_2O [$(Pa \cdot m^3)/mol$]
H_i	Henry's law constant for component i, solubility of gas in solution [The unit depends on the Henry's law equation that is being used.]
$\overline{H}_i$	Partial molar enthalpy of component i [J/mol]
$\Delta H_\mathrm{R}^\circ$	Standard enthalpy of reaction [J/mol]
H_R	Enthalpy of reaction [J/mol]
$[i]_\mathrm{B}$	Concentration of species i in bulk [$kmol/m^3$]
$[i]_\mathrm{I}$	Concentration of species i at gas liquid interface [$kmol/m^3$]
$[i]^*$	Concentration of species i in a solution in equilibrium with the main body of gas [$kmol/m^3$]
J_i	Molar diffusion flux of component i [mol/ ($m^2 \cdot s$)]
k	Pre-exponential factor [mol/ ($m^3 \cdot s$)]
k_G	Mass transfer coefficient in the gas film [m/s]
k_L	Chemical mass transfer coefficient in the liquid film [m/s]

k_{L}^{o}	Physical mass transfer coefficient in the liquid film [m/s]
k_x	Rate constant for reaction x [second order: m^3/ (kmol·s), pseudo first order: 1/s]
K	Equilibrium constant
K_{G}	Overall gas phase mass transfer coefficient [m/s]
K_{L}	Overall liquid phase mass transfer coefficient [m/s]
L	Characteristic lenght, penetration theory [-]
$\overline{m}_{\mathrm{am}}$	The stoichiometric molality of amine [(mol amine)/ (kg H_2O)]
$\overline{m}_i$	The stoichiometric molality of component i [mol/ (kg H_2O)]
m_i	The true molality of component i [mol/ (kg H_2O)]
n	Number of components [-]
n_i	Amount of substance i [mol]
Δn_i	Change of the amount of substance i [mol]
N	Temperature exponent [-]
N_i	Molar flux of component i [mol/ (m^2·s)]
p_i	Partial pressure of component i in the bulk [Pa]
p_{CO2}	Partial pressure of CO_2 [Pa]
$p_{i\mathrm{I}}$	Partial pressure of component i at gas liquid interface [Pa]
p_i^*	Equilibrium partial pressure of component i [Pa]
Δp	Pressure difference [Pa]
p	Pressure [Pa]
P_E	Electrical power [kW]
q	Conductive heat flux [W/m^2]
Q_{r}	Reboiler duty [kJ/ (mol CO_2) or MJ/ (mol CO_2)]
r_x	Rate of reaction of x [kmol/ (m^3·s)]
R	Universal gas constant [8.314 J/ (mol·K)]
s	Time constant, surface renewal theory [1/s]
t^*	Time, which the small elements stay at the interface, penetration theory [s]
t	Temperature, T/K-273.15 [°C]
T	Temperature [K]
$\dot{V}$	Volumetric flow [m^3/s]
$v_{i,x}$	Stoichiometric factor of reactant i in reaction x

	[$v_{i,x}$ > 0 for a reaction product and $v_{i,x}$ < 0 for a reactant]
$v^{\infty}_i(T)$	Partial molar volume of component *i* infinitely diluted in water
$v_w(T)$	Molar volume of pure liquid water
w_{Am}	The weight fraction of total amine in solution
x_i	Mole fraction of component *i* in the liquid phase [-]
y_i	Mole fraction of component *i* in the gas phase [-]
z_i	Ionic charge of the species *i* [-]

Greek symbols

α	Loading [(mol CO_2)/ (mol amine)]
γ_i	Activity coefficient of component *i* in a solution [-]
δ	Liquid mass transfer boundary layer thickness, film theory [m]
η_{TOT}	Efficiency [-]
μ	Viscosity [Pa·s]
μ_i	Chemical potential of component *i* [J/mol]
v	Characteristic velocity, penetration theory [-]
υ_i	Stoichiometric coefficient of species *i* [-]
ρ	Density [kg/m^3]
φ	Electrical potential [V]
φ_i	Fugacity coefficient of component *i* [-]
$\psi(t)$	Surface age distribution function, surface renewal theory [1/s]

1 Introduction

Carbon dioxide is one of the most worthy greenhouse gases. Fossil fuels are a huge source of carbon dioxide emissions and power plants using fossil fuels as a raw material are producing carbon dioxide emissions constantly in large scales. For example a typical coal fired power plant produces flue gas which based on mole fractions contains about 10-12 % of carbon dioxide.

Recovery of carbon dioxide from the flue gases of power plants can be considered as one of the solutions to diminish the greenhouse gas emissions. There are several methods to perform the recovery but post-combustion carbon dioxide capture via absorption based on chemical solvents is one of the most important technologies. The economical efficiency and the environmental aspects of the recovery process are highly dependent on the solvent used.

Aqueous methyldiethanolamine is one of the most used solvents since it has a low energy requirement but high carbon dioxide absorption capacity. The disadvantage of methyldiethanolamine is a low rate of reaction with carbon dioxide. This can be overcome with the help of activators, which can improve the absorption rate without increasing the energy requirement of the amine regeneration process.

Simulation programs are very important tools when investigating and improving the recovery processes. Absorption and stripping processes can be nowadays modelled with sufficient accuracy in the case of certain amine solvents, but modelling of the methyldiethanolamine process with and without activators have caused difficulties. Accuracy of the modelling processes is extremely important when considering the performance of the overall process.

In the theoretical part of this thesis the backgrounds of the absorption-stripping process and piperazine activated methyldiethanolamine process are introduced. In the experimental part the activities are focused to model the overall process and to test the accuracy of the rate-based model built-up for the new Aspen Plus® V7.3.2.

I Theoretical part

2 Post-combustion gas purification

Carbon dioxide (CO_2) is an acidic gas and a well known greenhouse gas. Its removal from flue gases is essential when reducing emissions and prohibiting the climate effects of global warming. Large amounts of carbon dioxide are produced in power plants using fossil fuels. Cost effective ways to remove CO_2 from flue gases are investigated constantly.

The separation of CO_2 from flue gases started in the 1970s but, as Rao & Rubin (2002) have pointed out, not because of concerns about greenhouse effect. At that time it was a potential economic source of CO_2 mainly for enhanced oil recovery (EOR) operations.

Gas purification is a process where vapour phase impurities are removed from gas streams. Industrially the process is based on a column pair which consists of an absorber and a stripper. When CO_2 is removed from flue gases produced by combustion of fossil fuels and biomass with air, the process type referred is known as a post-combustion capture. According to Olajire (2010) the volume of CO_2 in flue gases from power-plants is typically 4-14 %. Concentration of CO_2 in flue gases depends on the feed type used in a certain power plant. The reported CO_2 concentration can be considered to be low. Large volumes of gas have to be purified in the CO_2 post-combustion capture processes of power plants. Due to this large equipment sizes are demanded and it results in high capital costs. Relatively low partial pressure of CO_2 offers also several design challenges for the post-combustion capture.

Usually the post-combustion capture is based on absorption or adsorption technology, but Kohl & Nielsen (1997) emphasized that the absorption based on chemical solvents is the most important of all gas purification processes. Mofarahi et al. (2008) clarified that this is due to the low CO_2 concentrations in flue gases of power plants. Chemical solvents also provide high capture efficiency, selectivity and the lowest energy use when compared with other existing post-combustion capture methods (Metz, 2005). In

Figure 1 a simplified process scheme with typical process conditions for aqueous amine-based absorption is displayed.

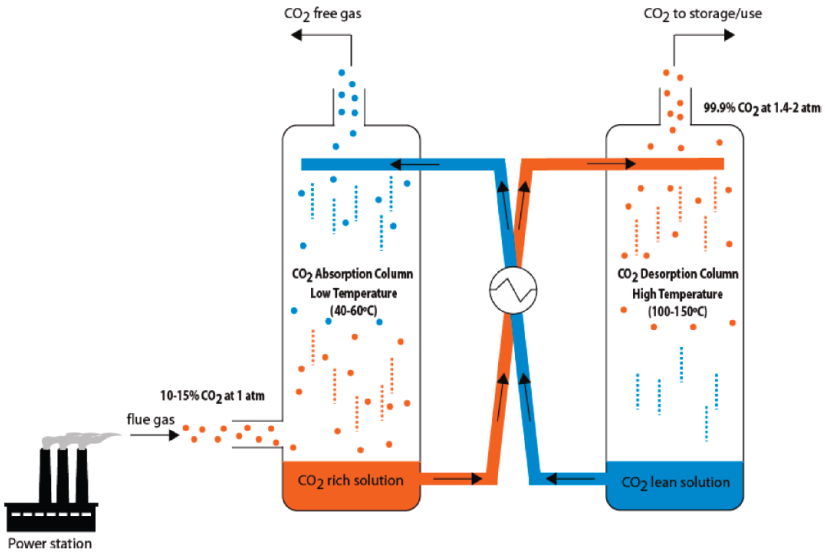

Figure 1 Absorption process using amine-based solvents applied for a post-combustion capture process of CO_2 (Puxty et al., 2009).

Even though the aqueous amine-based systems are the most widely used, the whole process is not as simple as presented in Figure 1. The flue gas to be treated with amine-based solvents must be cooled and purified from other acid gases (NO_2 and SO_2) and particulates before entering the absorber column. The acidic components, which are similar to CO_2, are interacting with the alkaline solvent and can result for example as heat stable salts and hence cause a loss in absorption capacity of the solvent. In Figure 2 a more complex process flow diagram is presented. Some additional equipment like filters, carbon beds and thermally operated reclaimers are needed to ensure the quality of absorption solution because of the formation of degradation products, corrosion products and the presence of particles. (Metz, 2005)

Concentrations of the other acid gases and impurities should be at extremely low levels to prevent them from reacting irreversibly with the solvents. The limits and requirements may vary depending on the plant type and control measures. In the study by Irons et al. (2007) various concentrations which are considered to be acceptable at the atmospheric pressure for further processing are presented for NO_2, SO_2 and particulates. In the report by FLUOR (2004) it is stated that in amine processes the SO_2 and NO_2 levels should be decreased to around 10 ppm and 20 ppm, respectively, at 6 % O_2 v/v (volume of gas per volume of air) measured at dry basis.

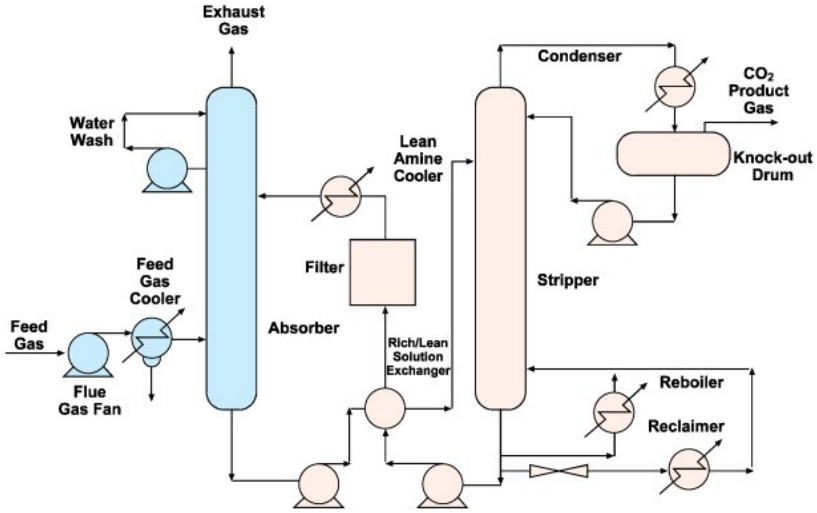

Figure 2 Process flow diagram for CO_2 recovery with additional equipment (Metz, 2005).

Absorption is usually performed in a column with trays, random packing or structured packing. The cooled and purified flue gas enters the absorber from the bottom and amine solution as a solvent is fed from the top. The fluids are contacting counter-current when the solvent flows down the column contacting the gas phase. The solvent, which comes from the bottom of the stripper column and is fed to the top of the absorber, has the lowest CO_2 content in the process and is called lean. The regenerated solvent can never be totally free of CO_2 because it would be too energy demanding to perform the stripping process all the way to the end. In an aqueous alkanolamine solution the CO_2 content is expressed in terms of loading. Loading will be discussed in further detail in Chapter 3.2.

In the absorber CO_2 transfers from the gas phase to the liquid phase due to a chemical potential. When considering the aqueous alkanolamine absorption processes, where the amine solution is a chemical solvent, both physical and chemical absorption are observed.

The gas coming out from the top of the absorber after a washing section is normally not further treated, so the absorber is usually working at the pressures slightly higher than the atmospheric pressure. McCann et al. (2008) have mentioned that the CO_2 free gas released to the atmosphere from the top of the absorber consist mainly of N_2. The amine solution which has the highest loading of CO_2, rich solvent, is exiting the absorber from the bottom and led to the top of the desorption (or stripping) column which is operated

at higher temperatures and pressures. At these higher temperatures the absorbed CO_2 is released due to the shifted chemical equilibria and CO_2 solubility.

The rich/lean solvent heat exchanger is used between the two columns to heat up the rich amine solution and to cool down the lean amine solution. As can be seen from Figure 2 the lean solvent is usually further cooled in a separate cooler before it has reached the absorber temperatures.

Basic idea of stripping is to rise the temperature of the column so high that the endothermic reactions, which are opposite to the ones occurring in the absorption, have the energy needed for them to take place. Energy is needed at the bottom of the stripper to vaporize the liquid. As the steam with a low CO_2 content flows upwards it drives the mass transfer from the liquid phase to the gas phase and releases energy to the liquid phase. As the temperature of the liquid phase rises the conditions for the opposite reactions to occur are improved and CO_2 is released while the heat energy is bound. The energy requirements become higher with higher purity levels of the lean solvent and it may be decreased significantly by increasing the capacity of a chemical absorbent in terms of the amount of CO_2 that can be absorbed and desorbed per unit mass of solution within a range of partial pressures. (McCann et al., 2008, Puxty et al., 2009)

Pure CO_2 can be removed from the top of the desorption column and the regenerated lean amine solution can be circulated back to the absorption column continuously (Mofarahi et al., 2008, Puxty et al., 2009). The pure CO_2 recovered from the top of the stripper is usually further compressed. According to Rochelle (2012) the pressure for geologic storage should be about 150 bar (15000 kPa).

Beside solvent selection, according to Mofarahi et al. (2008), the most important parameters for designing of the CO_2 recovery plant using an absorption method are solvent concentration, solvent circulation rate, reboiler and condenser duty and number of stages in absorber and stripping columns.

3 Absorption

Kohl & Nielsen (1997) described absorption as a process in which a component of a gas phase is transferred to a liquid phase in which it is soluble. Stripping was introduced as a reverse phenomenon. The alkanolamine absorption process is considered to consist of these unit operations.

Solvent absorption can be classified into three different categories when it is applied to a gas purification process. The categories are based on how the absorbent and absorbate are interacting in the process i.e. which kind of solvent is applied. The solvent used can be a physical solvent, a chemical solvent or a mixed physical/chemical solvent. In the first case the gas to be treated is physically absorbed to the physical solvent and can be described with Henry's law. In the second case the gas to be absorbed reacts with the chemical solvent and is this way transferred into the chemical solvent. Kohl & Nielsen (1997) explained the mixed solvent process so that the physical solvent removes the bulk of the acid gas while the chemical solvent purifies the process gas to demanded levels. The three different ways of solvent absorption are described more detailed in Kalliola's Master's thesis (Kalliola, 2007).

3.1 Chemical solvents

From the literature the following information about the characteristics, which a chemical solvent should fulfil, can be gathered. An ideal solvent would have

- high inherent CO_2 capacity per weight of solvent, fast CO_2 absorption kinetics and high heat of CO_2 absorption,
- low vapour pressure and low viscosity,
- low cost,
- non-corrosive, non-toxic and non-hazardous behaviour, and
- no degradation products under the operating conditions of the columns.

A real solvent used as a CO_2 absorbent has the optimized combination of the characteristics. Chemical solvents have a concentration of 10 % to 50 % by weight in aqueous solutions. The concentration of the solvent has an effect on the desired high CO_2 capacity as well as on the undesired high viscosity and increased risk of corrosion.

According to Bishnoi (2000) at the physical absorption of CO_2 into a non-reactive solvent a finite slice of an absorber can be considered. Across this slice the gas and liquid phase concentrations of CO_2 can be considered relatively unchanged and the removal of CO_2 from the gas phase may be written as in Equation (1) and the driving force is the difference between CO_2 concentration at the interface and the bulk solution:

$$r_{CO_2} = k_L^{\circ} a\left([CO_2]_I - [CO_2]_B\right) \quad (1)$$

where a is the contact area between the gas and liquid phases [m^2/m^3],
$[i]_B$ is the concentration of component i in the bulk [$kmol/m^3$],
$[i]_I$ is the concentration of component i in liquid at the interface [$kmol/m^3$],
k_L° is the physical mass transfer coefficient [m/s], and
r_{CO2} is the rate of reaction of CO_2 [$kmol/ (m^3 \cdot s)$].

The subscript I and B refer to the interface and bulk, respectively. The rate of removal into a reactive solvent can be written with the help of an enhancement factor, E:

$$r_{CO_2} = k_L^{\circ} aE\left([CO_2]_I - [CO_2]_B\right) \quad (2)$$

where E is the enhancement factor [-].

There is more information about the enhancement factor in Chapter 10.1. When the absorbed component i will diffuse into the bulk of the liquid before reaction occurs the chemical reaction is very slow and there is no enhancement effect, the situation is called the slow reaction regime. When the reaction is really fast, molecules of the solute react with molecules of the reactant whenever both are present in the same point. Chemical equilibrium exists everywhere in the liquid phase and it is called the instantaneous reaction regime. Between these two extremes the fast reaction regime occurs and there the mass transfer coefficient, k_L, is a function of the reaction rate. (Kohl, 1987) In order to understand Equation (2), we need to have information about the hydraulic parameters, equilibrium conditions and rate of the reactions.

3.2 Alkanolamines as absorbents

Amines are ammonia (NH_3) derivates where one or more hydrogen atoms have been substituted with an alkyl or aromatic group. In an alkanolamine based absorption process they are working as chemical solvents. CO_2 is an acid gas as stated earlier. Amines have a weak basicity and they react with the acid gases converting them into ions and thereby trapping them into the liquid phase. Amine solutions and alkanolamines have been studied as absorbents for several decades. According to Kohl & Nielsen (1997) triethanolamine (TEA) was the first alkanolamine to become commercially available. All the alkanolamines include at least one hydroxyl group and one amine group.

Alkanolamines can be divided into primary (R_1NH_2), secondary (R_1R_2NH) and tertiary ($R_1R_2R_3N$) amines according to how many hydrocarbon chains have been directly attached to the nitrogen atom. R represents a hydrocarbon (alkanol) chain which has replaced a hydrogen atom attached directly to the nitrogen. The hydroxyl group in alkanolamines is reducing the vapour pressure and increasing the water solubility where as the amino group is causing the alkalinity to water solutions and enabling the absorption of CO_2. In Figure 3 some structural formulae for well known alkanolamines are presented. (Kohl and Nielsen, 1997) According to Rufford et al. (2012) the absorption of CO_2 into amine solution is a chemical absorption occurring via a two-step mechanism. First the dissolution of the gas into aqueous solution occurs and then the reaction of the weak acid solution with weakly basic amine follows.

Alkanolamines which have been dominating in aqueous solvents for CO_2 capture processes for a long time are monoethanolamine (MEA) and diethanolamine (DEA), illustrated in Figure 3, but in the last two decades usage of tertiary amines and blended amines have gained some special interest because they allow customized CO_2 removal with minimized energy requirements (Chang et al., 1993). In the review by Vaidya & Kenig (2007) the reason for this kind of development has been explained as follows. When dealing with primary or secondary alkanolamines their reaction with CO_2 to form carbamates is fast, but the heat of absorption associated with the carbamate formation is high. Due to this the costs to regenerate the solvent are also high. When dealing with tertiary alkanolamines the carbamation reaction will not take place because there is no hydrogen atom attached to the nitrogen atom. With tertiary alkanolamines the CO_2

hydrolysis results as bicarbonates. The reaction heat released is lower in this case and this reduces the costs of solvent regeneration.

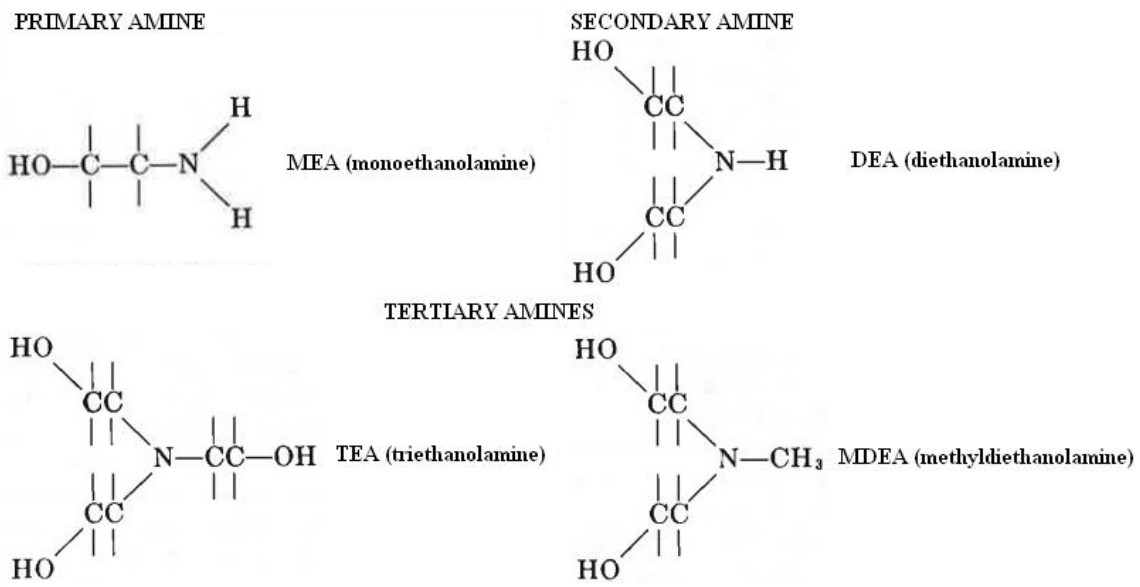

Figure 3 Alkanolamines used in gas purification processes (Kohl and Nielsen, 1997).

Typically the solubility of CO_2 in aqueous amine solutions is described as CO_2 loading as a function of its partial pressure. The ratio of moles of CO_2 taken up by the solution to the total moles of amine in the solution is known as the CO_2 loading, α, (molar capacity, n_{CO2}/n_{amine}). The molar absorption capacity can be normalized to the number of amine functional groups or N atoms present in each molecule (normalized molar capacity, n_{CO2}/n_N). (Puxty et al., 2009)

Si Ali & Aroua (2004) have used the normalized molar capacity to the PZ/MDEA system (mol MDEA+2·mol PZ) in which the stoichiometry of nitrogen atoms is taken into account where as in some of the research articles (Bishnoi, 2000, Bishnoi and Rochelle, 2002b, Derks, 2006, Derks et al., 2010) the total amine concentration have been calculated as equal to the molar concentration of MDEA plus the molar concentration of PZ.

Differences in the CO_2 loading capacity of alkanolamines vary and it is an issue to be considered when choosing the absorbent. With primary and secondary alkanolamines the loading capacity is limited to 0.5 mol of CO_2 per mol of amine where as the loading capacity of tertiary alkanolamine is 1 mol of CO_2 per mol of amine (Vaidya and Kenig, 2007, Feng et al., 2010). The total absorption capacity of a solvent is clearly a

very important issue, but so is a cyclic capacity of a solvent. The rich and lean amine solutions can be found from Figures 1 and 2. The cyclic capacity of a solvent is the difference between CO_2 loadings in the rich and lean solutions (α_{rich} - α_{lean}). (McCann et al., 2008)

Primary, secondary and tertiary amines have a different molecular structure, as Figure 3 showed, and they act differently towards CO_2 in aqueous solutions. Primary and secondary alkanolamines form carbamate species when reacting with CO_2 according to the two steps zwitterion mechanism where as tertiary amines cannot form carbamate since any hydrogen binding with nitrogen atom is not available.

The first step of the zwitterion mechanism is the formation of an intermediate zwitterion (3) and the second step is the formation of a carbamate ion and a protonated base (4). Donaldson & Nguyen (1980) have proposed that tertiary alkanolamines have a base-catalytic effect on the CO_2 hydration (5). This means that the mechanism for catalysis is based on the hydrogen bonding between amine and water, which weakens the H-O bond and increases the nucleophilic reactivity of water towards CO_2 to form a protonated amine and a bicarbonate anion.

$$\mathrm{Am} + \mathrm{CO_2} \leftrightarrow \mathrm{Am^+COO^-} \quad (3)$$

$$\mathrm{Am^+COO^-} + \mathrm{b} \leftrightarrow \mathrm{AmCOO^-} + \mathrm{bH^+} \quad (4)$$

$$\mathrm{Am} + \mathrm{CO_2} + \mathrm{H_2O} \leftrightarrow \mathrm{AmH^+} + \mathrm{HCO_3^-} \quad (5)$$

where Am is an alkanolamine, and
b is a base, normally OH^- or H_2O.

Since no carbamate is formed with tertiary amines and CO_2 can only be absorbed via the slow bicarbonate reaction, the reactivity with CO_2 is lower than with primary or secondary amines but the selectivity is higher. The reactivity and the rate of CO_2 absorption of tertiary amines such as methyldiethanolamine (MDEA), which have high absorption capacity, can be enhanced and high absorption capacity maintained by adding a small amount (low concentration) of an activator which has a fast absorption rate. The activator can be a primary or a secondary amine or a totally different chemical. Activators can also be called accelerators. It has been proven that adding of low

concentration of an activator does not diminish advantages of tertiary amines. (Appl et al., 1982, Boll et al., 2000, Kohl and Nielsen, 1997, Vaidya and Kenig, 2007)

When selecting the alkanolamine for an absorption process there are several important issues to be taken into account from the environmental point of view. According to Puxty et al. (2009) these are resistance to oxidative and thermal degradation, corrosiveness, resistance to degradation by flue gas impurities and toxicity of amines as well as degradation products. For example Veltman et al. (2010) have provided a human and environmental impact assessment which focuses on emissions from MEA based scrubbing solvents mainly concerning natural gas combined cycles. Nevertheless it offers important information about the amine degradation, salt formation and amine mass balance within the process.

3.2.1 Thermal degradation of alkanolamines

Thermal degradation of alkanolamines is an important matter from the economic and environmental point of view. An amine which is resistant to thermal degradation can minimize the economic loss of amine and the environmental impact of the degradation products. Thermal degradation of amines at 100-150 °C limits the maximum temperature/pressure used in the process, especially in the stripper, and therefore the energy performance of the solvent regeneration. Primary, secondary and tertiary amines as well as amines with ring structures and mixed amines are degrading at high temperature differently. MEA and DEA degrade through oxazolidinones, MDEA degrades by elimination and transalkylation and PZ degrades by ring opening and closing. Thermal degradation can generate products that are more volatile than the parent amines. (Rochelle, 2012)

The degradation of blended amine solutions differs from solutions containing only one type of amine. A reactive secondary amine can pick up "arms" from the tertiary amine. For example PZ will react with MDEA to produce N-methylpiperazine and DEA. In thermal degradation about one mole of PZ disappears for every mole of MDEA that degrades. More detailed information about the oxidation and thermal degradation of the PZ/MDEA system can be found from the Ph.D. Dissertation by Closmann (2011).

Usually thermal degradation requires amine carbamate or protonated amine as a reactant. Therefore CO_2 loading or an amine salt such as sulfate or formate will increase

the rate of amine degradation. Thermal degradation should be avoided by stripping the amine solution to a very low CO_2 loading. This is possible with tertiary amines that make only bicarbonate whereas primary and secondary amines produces carbamates and it makes it difficult to strip the amine solution to low loadings. (Rochelle, 2012)

3.2.2 Formation of heat stable salts

The amine system is designed to form soluble salts in the reaction of amine with acid gas (CO_2) [amine + acid gas → salt] in the absorber and the reverse reaction occurs in the stripper [salt + heat → amine + acid gas] to remove the acid gas from the solution. According to Weiland and Sivasubramanian (2004) an amine heat stable salt (HSS) is a thermally unregenerable protonated form of amine. Bicine, formate and sulfate are some of the known heat stable salts. For example if there is formic acid produced in the process, MDEA reacts with it to form a formate, which is a HSS and no change occurs in the regeneration column [salt + heat → no change]. Heat stable salts are products of the neutralization reaction between alkaline amine and organic or inorganic acid, which are stronger than CO_2. Species like SO_x or NO_x, which are impurities of the flue gas, can form these stronger acids but also amine degradation products can cause the formation. Even a relatively small amount of heat stable salts in the process can significantly influence the performance of the absorber and stripper because of the irreversible reaction with amine. In addition heat stable salts increase the conductivity and the corrosion in the system since they lower the pH.

3.2.3 Environmental aspects of alkanolamines as absorbents

From Figure 2 it could be seen that there are two flows exiting the amine absorption plant, the treated exhaust gas and the produced CO_2. Usually the reclaimer produces also a waste stream. Thus, environmental concerns are focused to these three outlet streams. The produced CO_2 is left out from the further discussion since it is assumed to be almost pure CO_2 and it is going for downstream operations. Amines are volatile to some extent and they exhibit a vapour pressure above the aqueous solution so they can vaporize into the flue gas exiting from the top of the absorber. Typical flue gas contains oxygen and this can cause oxidation of amine in the absorber packing at 40-60 °C or at 100-150 °C in the hot solution leaving the cross heat exchanger. The greatest rate of thermal degradation occurs in the stripper and reboiler at 120-150 °C. Nguyen et al. (2010, 2011) have compared volatilities of different amines in their two articles. MDEA, PZ and their mixture have low volatilities where as MEA has relatively high

volatility. Usually amine losses are reduced by washing stages on the top of the absorber. In the washing stages water is recycled, amine is absorbed and a bleed is returned back to the absorber. With the proper operation of wash water stages amine levels as low as 0.01-0.05 ppm can be achieved in the exiting gas. (Svendsen et al., 2011)

During the operation of an absorption plant the absorbent will produce degradation products continuously. The degradation products can be divided into volatile, low volatility and non-volatile components. The volatile products are usually at least partially water soluble so they can be separated from the flue gas in the washing section, too. However there is a change that these substances will go straight through. One solution is to remove a small stream from the top of the washing section and to tread the removed wash water in a biological water treatment plant. Non-volatile degradation products must be removed also. This can be done in the reclaimer either continuously or intermittently. In normal operation the reclaimer waste is not considered as a big problem. Absorption plant will inevitably emit some of the absorbent, activator and degradation products and also accidental spills are possible. It is thus important that these emissions are not detrimental to the surroundings. (Svendsen et al., 2011)

4 Methyldiethanolamine, MDEA

Monoethanolamine (MEA) has been dominating as the alkanolamine absorbent used for gas treating for a long time but as a conventional alkanolamine it is known to have some disadvantages. Feng et al. (2010) listed a few of these disadvantages. The most noticeable of them are the corrosiveness of amine solutions especially with high amine concentrations and loadings, the easy degradation of amines at high temperatures of the regeneration process and the volatility which can cause amine losses in the gas stream. Since the disadvantages of conventional solvents, new alkanolamines and their mixtures have been investigated. Methyldiethanolamine has proven to be one of the options since it has lower volatility and it is less alkaline. MEA is a strong Lewis base where as MDEA is a weak base. As presented before MDEA does not form carbamate with CO_2 like primary and secondary amines. Since carbamates have a great impact on the corrosivity of amine solutions MDEA is a good choice for the amine solvent. MDEA works as a chemical solvent when used as an absorbent similar to other alkanolamines.

Methyldiethanolamine, which is also known as N-methyldiethanolamine, is the most widely used tertiary amine (Boll et al., 2000, Derks, 2006). MDEA can be produced from methylamine and ethylene oxide as a mixture of MEA and DEA (MAK, 2002). In Table 1 some information and common properties of MDEA are presented. According to Kohl & Nielsen (1997) the usage of MDEA as an amine absorbent first gained interest due to its ability to selectively absorb hydrogen sulphide in reasonable operating conditions. In 1981 MDEA was first researched as a CO_2 absorbent (Xu et al., 1992). As a tertiary amine, MDEA reacts with CO_2 according to a mechanism presented in the reaction equation (5).

Appl et al. (1982) introduced some advantages of MDEA. They pointed out that MDEA has low energy requirement, high CO_2 absorption capacity and high thermal stability. Boll et al. (2000) have roughly estimated that 80 kg of steam is required for the regeneration of 1 m^3 of solvent for bulk CO_2 removal. The disadvantage of MDEA is that it has a low rate of reaction with CO_2 i.e. the absorption of CO_2 into MDEA is quite slow, but this can be increased with the usage of activators as mentioned before.

Table 1 Properties of MDEA, PZ and aqueous PZ (Dow).

Property	MDEA	PZ, anhydrous	PZ, 68% aqueous
Molecular formula	$C_5H_{13}NO_2$	$C_4H_{10}N_2$	-
Molar mass [g/mol]	119.16	86.14	-
CAS number	105-59-9*	110-85-0	-
Melting point [°C]	-21	106**	48
Boiling point [°C]	247.3	146**	117.8
Density @ 20°C [g/cm^3]	1.038-1.041*	-	1.034
Viscosity @ 20°C MDEA/ 60°C PZ [cP]	101	-	22.5
Vapour pressure 20°C [kPa]	< 0.0013	-	0.4666

*(MAK, 2002)
**(ScienceLab)

In the gas treating process there is always formed some degradation products of alkanolamines. Tertiary amines are known to degrade by two mechanisms, by transalkylation and elimination. All tertiary amines can transalkylate. The transalkylation reactions are catalyzed by CO_2 or acid loading to protonate the tertiary amine i.e. degradation of tertiary amines is proportional to the CO_2 loading. In the case of MDEA these thermal degradation products are lower amines, for example DEA, MAE (methylaminoethanol) and DMMEA (dimethylmonoethanolamine), which can further act as an activator for carbon dioxide removal (Boll et al., 2000). The secondary amines that are produced can further degrade by carbamate polymerization (Rochelle, 2012).

Humans can inhale or have skin contact with MDEA primarily via occupational exposure. MDEA is considered to be slightly toxic if swallowed and severely irritating to eyes. It is practically non-irritating to skin, but repeated contact may cause skin burns. MDEA like most of the tertiary amines and compounds containing quarternary carbon has a low biodegradability and especially in marine environment its biodegradability is low and it is considered to be slightly toxic to aquatic organisms on an acute basis. (Eide-Haugmo et al., 2009, Dow, 2010a)

5 Activated MDEA

Activators are used with aqueous MDEA to enhance the overall process by allowing higher amine concentrations and improving the CO_2 absorption rate. Activators also reduce corrosion potential to carbon steel and foaming tendency (Boll et al., 2000, Xu et al., 1992) and they can be used to vary the formulation of a solvent so that it can meet specific site requirements (Kohl and Nielsen, 1997). Usually the used activators are small amounts of primary or secondary amines (Boll et al., 2000, Derks, 2006, Kohl and Nielsen, 1997). Derks (2006) clarified the principle for the process enhancement in his thesis as follows: "The enhancement is based on the relatively high rate of reaction of CO_2 with the primary or secondary alkanolamine combined with the low heat of reaction of CO_2 with the tertiary alkanolamine."

The first commercial process using activators with the aqueous solution of MDEA was introduced by BASF Aktiengesellschaft in the 1970s and piperazine was used as an activator in that process (Kohl and Nielsen, 1997, Appl et al., 1982).

The activated alkanolamine solutions have higher rates of absorption in the absorber and low heat of regeneration in the desorber. Astarita et al. (1983) proposed that the general mechanism for promoted solution is based on two chemical steps (6) and (7), and it can well be described as a homogenous catalytic reaction:

$$CO_2 + \text{promoter} \rightarrow \text{intermedia te} \quad (6)$$

$$\text{intermedia te} + OH^- \rightarrow HCO_3^- + \text{promoter} \quad (7)$$

A lot of research dealing with different activators mixed with the aqueous solution of MDEA has been made recently. In Table 2 several activators used with MDEA are listed. From the table it can be seen that many kinds of primary and secondary amines as activators have been tested, but recently for example functionalized ionic liquids have gained some interest, too.

Table 2 Activators used to enhance the absorption of CO_2 to aqueous MDEA solutions.

Activator	**Reference**
Piperazine (PZ)	(Appl et al., 1982, Zoghi et al., 2012)
Monoethanolamine (MEA)	(Kohl and Nielsen, 1997, van Loo et al., 2007)
Diethanolamine (DEA)	(Kohl and Nielsen, 1997, van Loo et al., 2007)
Diisopropanolamine (DIPA)	(van Loo et al., 2007, Zoghi et al., 2012)
2-Amino-2-methyl-1-propanol (AMP)	(van Loo et al., 2007, Zoghi et al., 2012, Huang et al., 2011)
Diglycolamine (DGA)	(van Loo et al., 2007, Zoghi et al., 2012, Pacheco et al., 2000)
Aminoethylethanolamine (AEEA)	(Zoghi et al., 2012)
Monomethylethanolamine (MMEA)	(van Loo et al., 2007)
1-Butyl-3-methylimidazolium Tetrafluoroborate ([bmim][BF_4])	(Ahmady et al., 2012)
Tetramethylammonium Glycinate ([Gly])	(Feng et al., 2010)
Tetraethylammonium Glycinate([N_{2222}][Gly])	(Feng et al., 2010)
Tetramethylammonium Lysinate ([N_{1111}][Lys])	(Feng et al., 2010)
Tetraethylammonium Lysinate ([N_{2222}][Lys])	(Feng et al., 2010)
Ferrofluids	(Komati and Suresh, 2008)
Enzyme Carbonic Anhydrase	(Penders-van Elk et al., 2012)
Immobilised Activators (Benzyl Amine Groups)	(Schubert et al., 2001)

5.1 Ionic liquids as activators

Ionic liquids are materials consisting entirely of ions and they are often described as molten salts. They can be designed to have special properties like hydrophobicity, which is a key character for an ionic liquid to be used as a CO_2 absorbent. Ionic liquids should have a low water solubility to be able to work properly in the absorption process (Giardina et al., 2010). Some ionic liquids have shown to be good CO_2 absorbents and the capacity can be improved. In functionalized ionic liquids there is a functional group added for this purpose.

Baugh et al. (2012) have found that certain ionic liquids can be used as chemisorbents for CO_2 in cyclic CO_2 separation processes but usage of ionic liquids as accelerators of carbon dioxide absorption into aqueous MDEA have recently gained interest as well. When using ionic liquids as activators it has been thought that ionic liquids enhance the physical absorption of CO_2 into MDEA, but Ahmady et al. (2012) discovered in their

work that there is a change in the activation energy and this indicates that with ionic liquids there is a component with a catalytic effect on the reaction. For example Feng et al. (2010) have investigated that tetramethylammonium lysinate ($[N_{1111}][Lys]$) enhanced MDEA shows similar absorption capacities to those of MEA activated MDEA while the absorption load was smaller. These solutions also have regeneration efficiency over 90 %. The challenges of ionic liquids are the high viscosity which causes high operation costs for circulation and the unknown corrosion behaviour.

5.2 Aminoethylethanolamine (AEEA) as an activator

Aminoethylethanolamine or 2-(2-aminoethylamino)ethanol is an unhindered diamine and its structural formula is presented in Figure 4. Diamines contain two amino groups which may offer a higher CO_2 absorption capacity than 1 (mol CO_2)/ (mol amine).

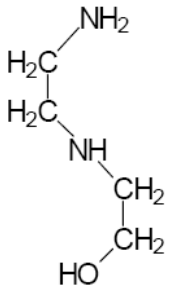

Figure 4 Chemical formula of AEEA.

Bonenfant et al. (2005, 2007) have investigated aqueous AEEA+MDEA solutions. In their investigations MDEA was playing the part of an activator, but they still made some interesting observations. They acknowledged that adding MDEA did not accelerate the absorption rate of CO_2, but absorption itself was slightly increased and desorption was highly enhanced. Zoghi et al. (2012) included AEEA in their comparison of different MDEA activators. In the conditions they used, AEEA was shown to be the best activator for the enhancement of CO_2 absorption in a low activator/MDEA ratio. Piperazine was the second best activator in their tests, but when increasing its ratio to MDEA the enhancement factor became higher. In order to decide which activator is better more research in different conditions should be performed with AEEA.

AEEA is highly corrosive. For humans it can cause severe eye damages and skin burns. It is acutely harmful for aquatic organisms and in laboratory animals it has caused malformations/developmental toxicity and fertility impairing effects. (Dow, 2011)

5.3 Piperazine (PZ) as an activator

Piperazine is a cyclic diamine belonging to the group of ethyleneamines. It has two secondary amine groups and no alcohol group as can be seen from Figure 5. Pure piperazine has a relatively high melting point at atmospheric pressure, as could be seen from Table 1, which makes it difficult to handle and commercial piperazine is usually sold as aqueous solutions (Dow, 2001). In Table 1 some additional properties of piperazine were also presented.

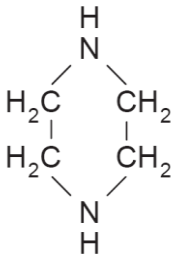

Figure 5 Structural formula of piperazine (PZ) (Derks, 2006).

In gas treating PZ has been used as an additive for tertiary amines well over 20 years. Appl et al. (1982) discovered in their patent that piperazine is a more efficient accelerator than other conventional activators with MDEA. Bishnoi & Rochelle (2002a) came to the same conclusion 20 years later. Piperazine has two main advantages in the absorption process. Firstly it is extremely reactive towards CO_2 and this way accelerates the absorption process and secondly as a diamine it contains two reactive amine groups per molecule both of which can attach to CO_2. This results in high CO_2 carrying capacity. Appl et al. (1982) also calculated that by using an activator with MDEA, the amounts of solvent circulation and the height of absorption towers can be reduced, thanks to the higher loading capacity of the mixed solvent.

When CO_2 dissolves into the liquid a good activator immediately reacts rapidly with it. Then the activator shuttles CO_2 as carbamate into the interior of the liquid where it dissociates back into the free amine and transfers CO_2 to MDEA. The activator diffuses back to the interface for more CO_2. The so called shuttle mechanism is presented in Figure 6 and more detailed information can be found from the technical newsletter by Optimized Gas Treating, Inc. ("Piperazine - Why It's Used and How It Works", 2008).

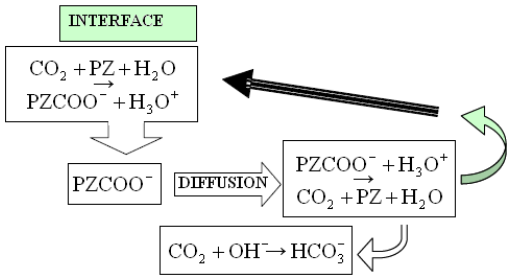

Figure 6 Schematic of the shuttle mechanism ("Piperazine - Why It's Used and How It Works", 2008).

Concentration of an amine solution has an impact on absorption and desorption performances as mentioned in Chapter 3.1. Commonly piperazine as an activator is used at low concentrations. The total amine concentration of aqueous MDEA/PZ solutions may also be limited by viscosity issues. In Table 3 many concentrations used in the literature are gathered.

Thermal degradation of PZ differs from the other amines since PZ is a cyclic diamine. PZ degrades by ring opening, which is catalyzed by protonation in loaded CO_2 solutions. The initial product is aminoethylaminoethylpiperazine (AEAEPZ) and it can further degrade by cyclic urea formation. The cyclic urea can again react with PZ to produce oligomers and fragments. (Rochelle, 2012) According to Closmann et al. (2009) the PZ/MDEA amine blend offers a solvent which is more resistant to thermal and oxidative degradation at typical absorption/stripping conditions than plain amines.

Table 3 Amine concentrations of aqueous MDEA solutions where PZ is used as an activator. Calculated stoichiometric molalities are taken from the work by Ermatchkov & Maurer (2011) and marked with *.

Reference	$\overline{m}_{MDEA}$ [mol/kg]	$\overline{m}_{PZ}$ [mol/kg]	M_{MDEA} [kmol/m^3]	M_{PZ} [kmol/m^3]	MDEA/PZ wt %
(Xu et al., 1998)*	8.1-8.7	0.2-1.5	4.28	0-0.515	
(Liu et al., 1999)*	1.6-11	0.2-3.3	1.53-4.77	0-1.55	
(Bishnoi and Rochelle, 2002b)*	7.74	1.16	4	0.6	45/5
(Si Ali and Aroua, 2004)*	2.2-2.5	0.01-0.1	1.8-1.98	0.01-0.4	
(Derks, 2006, Derks et al., 2010)*	0.6-7.7	1.1-1.8	0.5-4.0	0.6-1.5	
(Pérez-Salado Kamps et al., 2003)	2	2			
(Chen, 2011, Closmann et al., 2009)	7	2			42/8.6
(Speyer et al., 2010)	2.0-8.0	1.0-4.0			
(Samanta and Bandyopadhyay, 2011)			1.89-2.41	0.24-0.95	
(Lu et al., 2005, Lu et al., 2007)			2.0	0.5	
(Idem et al., 2009)					27/3, 24/6, 21/9
(Böttger et al., 2009)	2.2-7.83	1.97-2.07			18.5/12, 30/10, 44/8.5

Alkanolamines with ring structures have typically shown the highest toxicity of the most common alkanolamines, but piperazine makes the exception. In the piperazine activated CO_2 absorption process piperazine releases to environment may occur at the regeneration, mainly as gas or vapour, and when the plants are cleaned. The cleaning takes place at intervals of 3-5 years and process waters including significant amounts of piperazine can be released to wastewater streams. Due to the gas washing humans can inhale piperazine after emissions to air or intake contaminated foodstuff after emissions to air and surface water. Human contact with piperazine may cause severe irritation or chemical burns. In nature piperazine is slightly toxic to fish. Piperazine biodegrades relatively slowly, but its bioaccumulation potential is low. From wastewater piperazine can be removed by regular wastewater treatment process and in the atmosphere piperazine can be assumed to be rapidly degraded by photolysis in air. (Schenkel and Day, 2005, Dow, 2010b, Eide-Haugmo et al., 2009)

6 Mass and heat transfer

Mass transfer is a complex process in the absorber and desorber columns. It is dependent for example on the length of the mass transfer zone, solubility and diffusivity of CO_2 in and through the solvent, and the chemical reactivity between CO_2 and the chemical solvent. In addition all of those have an impact on the rate of mass transfer.

Mass transfer with chemical reaction occurs whenever two phases, which are not at chemical equilibrium with each other, are brought to contact. Mass transfer with chemical reaction should gain interest when one of the three following steps is rate-controlling for the overall phenomena.

1. Diffusion of the reactants from the interface towards the bulk of the phase 2.
2. Chemical reaction within the phase 2.
3. Diffusion of reactants initially present within the phase 2, and/or of reaction products, within the phase 2 itself, due to concentration gradients which are set up by the chemical reaction.

When alkanolamine solutions are used for CO_2 removal, mass transfer and analogous chemical reactions occur whatever the used amine is. (Astarita, 1967)

According to Astarita et al. (1983) in absorption and desorption chemical reaction maintains high driving force for mass transfer in the liquid phase and at a given level of driving force, the actual rate of mass transfer may be significantly larger when chemical reactions are taking place. In absorption mass transfer with chemical reaction increases absorbent capacity and solubility of CO_2 into the solvent (Thiele and Löning, 2006).

6.1 Multicomponent mass transfer fundamentals

Maxwell-Stefan equation can be used to describe the diffusion in a multicomponent system and usually all simplified models like Fick's law can be derived from it. The general form of the Maxwell-Stefan equation can be presented (Taylor and Krishna, 1993, Thiele and Löning, 2006):

$$d_i = \sum_{\substack{j=1 \\ j \neq i}}^{n} \frac{x_i N_j - x_j N_i}{c_t Đ_{ij}} = \sum_{\substack{j=1 \\ j \neq i}}^{n} \frac{x_i J_j - x_j J_i}{c_t Đ_{ij}} \qquad i = 1,2,...,n \tag{8}$$

where c_t is the mixture concentration [kmol/m^3],
d_i is the driving force for component i [1/m],
$Đ_{ij}$ is the Maxwell-Stefan diffusion coefficient for component pair i-j [m^2/s],
J_i is the molar diffusion flux of component i [mol/ (m^2·s)],
N_i is the molar flux of component i [mol/ (m^2·s)], and
x_i is the mole fraction of component i in the liquid phase [-].

In CO_2 absorption with an aqueous amine solution there are electrolytes participating in the system. These electrolytes must be taken into account, so an additional force caused by the electrostatic potential gradient $\nabla \varphi$ is inserted and the Maxwell-Stefan equation can be written:

$$d_i = \frac{x_i}{c_t RT} \nabla_{T,P} \mu_i + x_i z_i \frac{F}{c_t RT} \nabla \varphi \qquad i = 1,2,...,n \tag{9}$$

where F is the Faraday constant = 9.65*10^7 C/kmol,
R is the universal gas constant = 8.314 J/ (mol·K),
T is temperature [K] ,
z_i is the ionic charge of species i [-], and
$\nabla_{T,P}\ \mu_i$ is the isothermal and isobaric chemical potential gradient of component i [J/ mol].

For aqueous electrolyte solutions the nth component is usually assumed to be water (Krishna and Wesselingh, 1997).

When observing gas-liquid systems two absorption coefficients can be defined; k_L and k_G. k_L refers to the quantity of material transferred through the liquid film and k_G to the material transferred through the gas film. The quantity of material transferred from the main body of the gas to the interface must be equal to the quantity transferred from the interface to the main body of the liquid (Kohl and Nielsen, 1997). Because of that the following relationship can be written:

$$N_i = k_G (p_i - p_{iI}) = k_L ([i]_I - [i]_B) \tag{10}$$

where k_G is the mass transfer coefficient in the gas film [m/s],
k_L is the chemical mass transfer coefficient in the liquid film [m/s],
p_i is the partial pressure of component i in the gas [Pa], and
p_{iI} is the partial pressure of component i in gas at interface [Pa].

The overall mass transfer coefficients can be defined (Kohl, 1987):

$$N_i = K_G\left(p_i - p_i^*\right) = K_L\left([i]^* - [i]_B\right) \tag{11}$$

where K_G is the overall gas phase mass transfer coefficient [m/s],
K_L is the overall liquid phase mass transfer coefficient [m/s],
$[i]^*$ is the concentration of component i in a solution in equilibrium with the main body of gas [kmol/m^3], and
p_i* is the partial pressure of i in equilibrium with a solution having the composition of the main body of liquid [Pa].

6.2 Mass transfer models

There are several models developed to describe the mass transfer between two phases in an absorption process. The most used theories are the two film theory and the penetration theory or the surface renewal theory. All of the models are using some decisive parameters and they simplify the hydrodynamic behaviour significantly. Usually in chemical absorption the chemical reactions are so fast that they have an effect on the mass transfer in the film. Because mass transfer and reactions occur simultaneously it causes concentration gradients and thus it enhances the mass transfer. The reactions occurring can be assumed to be instantaneous and hence equilibrium can be considered to be achieved or the reactions can be incorporated into the model using detailed reaction kinetics for both the film and the bulk phase. Sometimes it can be presumed that the equilibrium of the reaction is achieved in the bulk phase and detailed reaction kinetics is applied only for the film. The influence of the chemical reaction on mass transfer can be accounted for by enhancement factors. (Thiele and Löning, 2006)

6.2.1 The film theory

The simplest hydrodynamic model is known as the two-film theory. The theory is considered as steady-state since no changes occur as a function of time. In the two-film theory, depicted in Figure 7, it is assumed that gas and liquid are in equilibrium at the

interface. There is supposed to be a thin film at the gas-liquid interface which separates the interface from the main bodies of the two phases.

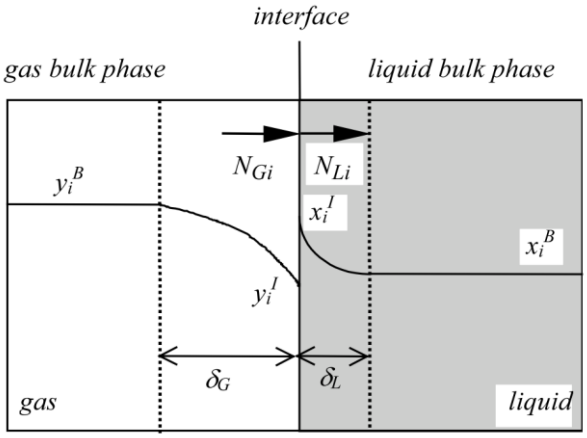

Figure 7 A graphical model for the two-film theory (Noeres et al., 2003).

Through this thin stagnant film of thickness δ mass transfer can only take place by molecular diffusion while the rest of the bulk phases are assumed to be perfectly well mixed with no concentration gradients. This results in one-dimensional diffusion transport normal to the interface at the film region. (Astarita et al., 1983, Kohl and Nielsen, 1997, Lewis and Whitman, 1924, Bishnoi, 2000)

The film thickness model (12) represents a model parameter which can be estimated by using mass transfer coefficient correlations. These correlations can be found from literature, i.e. Taylor and Krishna (1993), and they govern the mass transfer dependence on physical properties and process hydrodynamics.

$$k_L^o = \frac{D}{\delta} \tag{12}$$

where D is the diffusion coefficient [m^2/s], and
δ is the liquid mass transfer boundary layer thickness [m].

The disadvantage of the two-film theory is that on the basis of Equation 12 k_L° is proportional to the diffusivity D whereas empirical mass transfer coefficient correlations indicate that k_L° is proportional to the square root of D. Therefore the two-film theory might not predict the influence of diffusivity values on the enhancement factor correctly. (Astarita et al., 1983)

6.2.2 Penetration/surface renewal theory

Penetration theory can be considered as a more complex model of the fluid mechanisms and it was first proposed by Higbie in 1935. In the penetration theory it is assumed that there are small liquid elements continuously moving from the bulk of the liquid phase to the interface. At the interface the small liquid elements are staying for the time t^* after which the elements move back to the bulk of the liquid phase and get mixed with it. During t^* an element stays at the interface and can be considered as a fixed body which means that there is no appreciable velocity gradient. Due to the fixed body absorption into the surface elements is taking place by molecular diffusion alone. Contrary to the two-film theory in penetration theory diffusion is an unsteady phenomenon. The mass transfer coefficient in the penetration theory can be written as:

$$k_{\mathrm{L}}^{o} = 2\sqrt{\frac{D}{\pi t^{*}}} \tag{13}$$

where t^{*} is the time which elements stay at the interface [s].

Since t^* is generally not known, the value of k_{L}° must be given in the following form

$$\frac{k_L^o}{v} = (\text{constant})\left(\frac{\mu}{\rho D}\right)^{-0.5}\left(\frac{Lv\rho}{\mu}\right)^{-0.5} \tag{14}$$

where v is some characteristic velocity [-],
L is characteristic length [-],
μ is the liquid viscosity [Pa·s], and
ρ is the liquid density [kg/m^3].

The dimensionless groups appearing in Equation (14) are the Stanton number, the Schmidt number and the Reynolds number (Astarita et al., 1983).

In the penetration theory the assumption that all surface elements stay on the surface for the same length of time t^* is unsatisfactory and this has led to the development of the surface renewal theory which was presented by Danckwerts in 1951. In this theory the interface is assumed to be formed by a variety of elements. Each one of these elements has been brought to the surface some time t before the instant observation. Surface

element distribution is described by a distribution function $\psi(t)$ which is defined by the condition that $\psi(t)dt$ is the fraction of the interface area formed by elements with "age" comprised between t and $(t+dt)$. The distribution function satisfies the following condition:

$$\int_0^\infty \psi(t)dt = 1 \tag{15}$$

where $\psi(t)$ is the surface age distribution [1/ s].

In the surface renewal theory s is regarded as the rate of surface renewal and the mass transfer rate can be considered as:

$$k_L^o = \sqrt{Ds} \tag{16}$$

where s is the surface renewal frequency [1/ s].

As it can be seen from Equations (13) and (16), k_L° is proportional to $(D)^{0.5}$, which indicates that the penetration theory and the surface renewal theory are more realistic than the film theory (Astarita et al., 1983, Bishnoi, 2000). The penetration and surface renewal theories are unsteady state theories and the basic idea of them is presented in Figure 8.

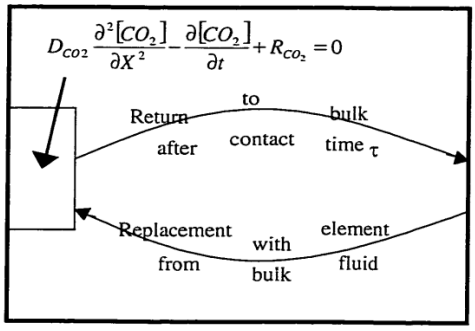

Figure 8 The basic idea of the unsteady state theories (Bishnoi, 2000).

6.3 Heat transfer

Absorption is one of the chemical engineering practises which involve simultaneous mass and heat transfer across phase interfaces. Heat transfer can affect the mass transfer by three temperature sensitive parameters; solubility, reaction rate constant and binary mass transfer coefficient. Temperature gradients in the region of the phase interface affect phase equilibria and chemical reaction rates. When there is a temperature gradient heat transfer and mass transfer are interacting in two ways. Firstly there is an additional enthalpy transport in addition to the conductive heat flux q. This is due to species fluxes:

$$E_f = q + \sum_{i=1}^{n} N_i \overline{H}_i \tag{17}$$

where E_f is the energy flux [W/m^2],
q is the purely conductive heat flux [W/m^2], and
$\overline{H}_i$ is the partial molar enthalpy of component i [J/mol].

The second term of Equation (17) accounts for the convective enthalpy transfer due to the diffusing species. The conductive heat flux q plays a role analogous to the molar diffusion fluxes J_i. It should be remembered that there is a continuity of the energy flux across the vapour-liquid interface. Secondly there is a direct contribution to the heat flux induced by species diffusion known as the Dufour effect and the opposite phenomena of thermal diffusion known as the Soret effect. Usually the Dufour effect is not considered as important phenomenon in chemical engineering applications. The film theory can also be applied for the simultaneous mass and heat transfer. (Taylor and Krishna, 1993)

Enthalpy of the solution can be considered as a combination of enthalpies associated to reactions involved in the dissolution of CO_2 into aqueous amine solution. Enthalpy of reaction x occurring in the liquid phase can be expressed:

$$\Delta H_{\mathrm{R}x} = \Delta H^{\circ}_{\mathrm{R}x} + \sum_i \nu_{i,x} \overline{H}_i \tag{18}$$

where ν_x is a stoichiometric coefficient for reaction x [-],

ΔH_{Rx} is the enthalpy of reaction x [J/ mol], and
ΔH°_{Rx} is the standard enthalpy of reaction x [J/ mol].

The partial molar enthalpies of species can be calculated by temperature differentiation of activity coefficient and in the case of water by activity (Arcis et al., 2009). Reaction equilibrium constants are temperature dependent and the dependency usually follows Equation (60). The standard heat of reaction can be calculated according to the Gibbs-Helmholtz equation (also known as the van't Hoff's equation) with the help of equilibrium constants:

$$\frac{d \ln K_x}{dT} = \frac{\Delta H^{\circ}_{Rx}}{RT^2} \qquad \text{or} \qquad \frac{d \ln K_x}{d\frac{1}{T}} = -\frac{\Delta H^{\circ}_{Rx}}{R} \tag{19}$$

where K_x is the equilibrium constant of reaction x.

The equation presented above (19) can be applied directly only to equilibrium constants that are defined in terms of temperature independent standard states such as molalities but not molarities (Olofsson and Hepler, 1975). Kim et al. (2009a, 2009b) have used the contributions of each of the key reactions to determine the overall heat of absorption as the sum of individual heat contributions. The changes in the number of moles of the key component, Δn_i, per mole of total amount of CO_2 absorbed, Δn_{CO2}, form the individual contributions:

$$\Delta H_{abs} = -\Delta H_{des} = \sum \frac{\Delta n_i}{\Delta n_{totalCO_2}} \Delta H_{Rx} \tag{20}$$

where ΔH_{abs} is the overall heat of absorption [J/ mol], and
n_i is the amount of substance i [mol].

According to Kohl & Nielsen (1997) the heats of reactions for amines and acid gases are not constant and generally they decrease as the acid gas concentration increases in the solution.

7 Chemical reactions, equilibrium and kinetics

MDEA and PZ belong to tertiary and secondary amines, respectively. Several equilibrium reactions can be observed when carbon dioxide is absorbed into aqueous solutions containing PZ and MDEA.

7.1 Reactions of CO_2 with aqueous methyldiethanolamine

In Chapter 3.2 the mechanism in which the amine enhances the reaction rate of CO_2 by a homogenous catalytic effect was described and presented (5). A hydrolysis catalyzed reaction occurs only in aqueous solutions since direct reaction of tertiary amines with CO_2 is not possible. The reaction of MDEA to form a protonated amine and a bicarbonate anion is presented below (Derks, 2006, Wang et al., 2004):

$$CO_2 + MDEA + H_2O \leftrightarrow MDEAH^+ + HCO_3^- \quad (21)$$

There are three reactions to be considered when aqueous MDEA reacts with CO_2. The first one is presented above, the second one is the hydration of CO_2 (22) and the third one is the bicarbonate formation (23) (Ko and Li, 2000, Zhi and Kai, 2009).

$$CO_2 + 2H_2O \leftrightarrow H_3O^+ + HCO_3^- \quad (22)$$

$$CO_2 + OH^- \leftrightarrow HCO_3^- \quad (23)$$

The rate of reaction (22) is generally known to be very low and may usually be neglected. The reaction (21) is usually represented as a second order with respect to the amine and CO_2 concentrations. The rate expressions for the reactions and the overall reaction rate can be written as:

$$R_{CO_2-MDEA} = k_{MDEA}[MDEA][CO_2] \quad (24)$$

$$R_{CO_2-OH^-} = k_{OH^-}[OH^-][CO_2] \quad (25)$$

$$R_{OV} = R_{CO_2-MDEA} + R_{CO_2-OH^-} \quad (26)$$

where R_x is the rate of reaction x [kmol/m^3·s], and
k_x is the rate constant for reaction x
[second order: m^3/(kmol·s), pseudo first order: 1/s].

In the above equations the concentration of CO_2 can be obtained from the Henry's law (Zhi and Kai, 2009):

$$[CO_2] = \frac{p_{CO_2}}{H_{CO_2}} \tag{27}$$

where p_{CO2} is the partial pressure of carbon dioxide [Pa], and
H_{CO2} is the Henry's law constant of CO_2 in aqueous MDEA [(Pa·m^3)/mol].

Some kinetic data of MDEA from the literature is gathered in Table 4. The reaction rate constant equation is based on the Arrhenius type equation (53).

Table 4 Summary of the MDEA kinetic data.

Reference	T [K]	MDEA [kmol/m^3]	P_{CO2} [atm]	Reaction rate constant k_{MDEA} [m^3/(kmol·s)]	Method
(Rinker et al., 1995)	293-342	0.8-2.6	1	$2.91*10^7\exp(-4579/(T/K))$	Wetted-sphere absorber
(Versteeg and van Swaaij, 1988a)	293-333	0.2-2.4	<1	$1.19*10^8\exp(-5103/(T/K))$	Stirred tank
(Ko and Li, 2000)	303-313	1.0-2.5	0.5-1	$4.01*10^8\exp(-5400/(T/K))$	Wetted wall column
(Pani et al., 1997)	296-343	0.8-4.4	1-2	$4.68*10^8\exp(-5461/(T/K))$	Stirred tank
(Zhi and Kai, 2009)	300-313	0.8-2.6	<1	$2.15*10^8\exp(-5190/(T/K))$	Wetted wall column
(Kierzkowska-Pawlak and Chacuk, 2010)	293-333	0.8-1.7	0.26-1	$2.07*10^9\exp(-5913/(T/K))$	Stirred tank

Based on the Arrhenius equations for reaction rates presented in Table 4 the values for reaction rate constants at the temperature of 298 K have been calculated and the values are presented in Table 5.

Table 5 Values for reaction rates at 298 K from different literature sources.

Reference	Rinker et al. (1995)	Ko & Li (2000)	Zhi & Kai (2009)
$k_{298,MDEA}$ [m3/(kmol-s)]	6.17	5.41	5.86
Reference	Versteeg & Swaaij (1988)	Pani et al. (1997)	(Kierzkowska-Pawlak and Chacuk, 2010)
$k_{298,MDEA}$ [m3/(kmol-s)]	4.35	5.14	4.99

From Table 5 it can be seen that there is variation between the observed values. Reaction rate constants in the lower section have been evaluated with a stirred tank and it can be seen that those are slightly smaller than the values in the upper section, which were achieved by using a wetted wall type of an absorber.

7.2 Reactions of CO_2 with aqueous piperazine

Theoretically piperazine as a diamine may absorb two moles of CO_2, which may favour rapid formation of carbamates. The reaction mechanism between PZ and CO_2 follows the so called zwitterion mechanism presented in Chapter 3.2. It includes the formation of zwitterion intermediate (PZH^+COO^-) which is then deprotonated by a base to produce piperazine carbamate ($PZCOO^-$) and protonated piperazine (PZH^+). More detailed information about the reaction of CO_2 with piperazine can be found from the literature (Bishnoi and Rochelle, 2000, Derks et al., 2005, Derks et al., 2006b, Ermatchkov et al., 2003).

7.3 Reaction of CO_2 with PZ activated aqueous MDEA

Several different kinds of presentations about the chemical reactions of CO_2 into aqueous PZ/MDEA systems can be found from the literature. The reaction system presented by Bishnoi (2000) has also been used by other research groups (Bishnoi and Rochelle, 2002b, Edali et al., 2010, Idem et al., 2009, Pérez-Salado Kamps et al., 2003, Lu et al., 2007, Samanta and Bandyopadhyay, 2011) and it is presented below in Table 6. K_i refers to the equilibrium constant for reaction i and k_i is the forward rate coefficient for reaction i.

Table 6 Reaction scheme for CO_2 absorption in piperazine activated aqueous MDEA.

Reaction description	Reaction	Reaction number
Formation of protonated amine and a bicarbonate anion:		
	$CO_2 + MDEA + H_2O \overset{K_{MDEA}, k_{MDEA}}{\leftrightarrow} MDEAH^+ + HCO_3^-$	(28)
Formation of piperazine carbamate:		
	$CO_2 + PZ + H_2O \overset{K_{PZ}, k_{PZ}}{\leftrightarrow} PZCOO^- + H_3O^+$	(29)
	$CO_2 + PZ + MDEA \overset{K_{30}, k_{30}}{\leftrightarrow} PZCOO^- + MDEAH^+$	(30)
Formation of piperazine dicarbamate:		
	$CO_2 + PZCOO^- + H_2O \overset{K_{PZCOO^-}, k_{PZCOO^-}}{\leftrightarrow} PZ(COO^-)_2 + H_3O^+$	(31)
	$CO_2 + PZCOO^- + MDEA \overset{K_{32}, k_{32}}{\leftrightarrow} PZ(COO^-)_2 + MDEAH^+$	(32)
Formation of bicarbonate:		
	$CO_2 + OH^- \overset{K_{OH^-}, k_{OH^-}}{\leftrightarrow} HCO_3^-$	(33a)
	$CO_2 + 2H_2O \overset{K_{33b}, k_{33b}}{\leftrightarrow} HCO_3^- + H_3O^+$	(33b)
Formation of carbonate:		
	$HCO_3^- + H_2O \overset{K_{34}}{\leftrightarrow} CO_3^{2-} + H_3O^+$	(34)
PZ protonation:		
	$PZ + H_3O^+ \overset{K_{35}}{\leftrightarrow} PZH^+ + H_2O$	(35)
Monocarbamate protonation:		
	$PZCOO^- + H_3O^+ \overset{K_{36}}{\leftrightarrow} PZH^+COO^- + H_2O$	(36)
MDEA protonation:		
	$MDEA + H_3O^+ \overset{K_{37}}{\leftrightarrow} MDEAH^+ + H_2O$	(37)
Water dissociation:		
	$2H_2O \overset{K_{38}}{\leftrightarrow} H_3O^+ + OH^-$	(38)
PZ diprotonation:		
	$PZH^+ + H_3O^+ \overset{K_{36}}{\leftrightarrow} H_2O + PZH_2^{2+}$	(39)

Reactions (28)-(33a) can be assumed to be reversible and their reaction rates are infinite. Reactions (34)-(38) can be assumed to be reversible too, but since they involve only proton transfer they can be considered to be instantaneous with respect to mass transfer and thus are at equilibrium. (Edali et al., 2010, Idem et al., 2009, Samanta and Bandyopadhyay, 2011) Reaction (33b) is presented here since the formation of bicarbonate is included in the solubility simulations with Aspen Plus in Chapter 12 in that form. Derks et al. (2010) and Ermatchkov & Maurer (2011) presented the reaction system in a different form but the basic idea was similar. They presented also a reaction

mechanism for piperazine diprotonation (39), but usually diprotonated piperazine is neglected from further investigations (Derks et al., 2005).

Water is mainly left out of the kinetic and equilibrium calculations since it is considered to be constant across the boundary layer and can be therefore lumped with the apparent rate and equilibrium constants (Bishnoi, 2000, Bishnoi and Rochelle, 2002a).

The six first introduced reactions are kinetically controlled and the overall reversible rate of reaction can be considered for each of them. The overall reaction rates are presented below:

$$R_{\mathrm{MDEA}} = -k_{\mathrm{MDEA}}\left([\mathrm{MDEA}][\mathrm{CO_2}] - \frac{[\mathrm{MDEAH^+}][\mathrm{HCO_3^-}]}{K_{\mathrm{MDEA}}}\right) \tag{40}$$

$$R_{\mathrm{PZ}} = -k_{\mathrm{PZ}}\left([\mathrm{PZ}][\mathrm{CO_2}] - \frac{[\mathrm{PZCOO^-}][\mathrm{H_3O^+}]}{K_{\mathrm{PZ}}}\right) \tag{41}$$

$$R_{30} = -k_{30}\left([\mathrm{PZ}][\mathrm{CO_2}][\mathrm{MDEA}] - \frac{[\mathrm{PZCOO^-}][\mathrm{MDEA^+}]}{K_{30}}\right) \tag{42}$$

$$R_{\mathrm{PZCOO^-}} = -k_{\mathrm{PZCOO^-}}\left([\mathrm{PZCOO^-}][\mathrm{CO_2}] - \frac{[\mathrm{PZ(COO)_2^-}][\mathrm{H_3O^+}]}{K_{\mathrm{PZCOO^-}}}\right) \tag{43}$$

$$R_{32} = -k_{32}\left([\mathrm{PZCOO^-}][\mathrm{CO_2}][\mathrm{MDEA}] - \frac{[\mathrm{PZ(COO)_2^-}][\mathrm{MDEA^+}]}{K_{30}}\right) \tag{44}$$

$$R_{\mathrm{OH^-}} = -k_{\mathrm{OH^-}}\left([\mathrm{OH^-}][\mathrm{CO_2}] - \frac{[\mathrm{HCO_3^-}]}{K_{\mathrm{OH^-}}}\right) \tag{45}$$

The rate constant k_{PZ} is considered as the global rate coefficient for the formation of zwitterion and zwitterion deprotonation. Similarly the rate constant k_{PZCOO^-} is considered as the global rate coefficient for the formation of piperazine carbamate because the effect of MDEA on the reaction of PZ with CO_2 is assumed to be the same as the effect of MDEA on the reaction of $PZCOO^-$ with CO_2. (Bishnoi and Rochelle, 2002a, Idem et al., 2009, Samanta and Bandyopadhyay, 2011) The equilibrium constants for kinetically controlled reactions are calculated by the ratio of the species in the bulk solution:

$$K_{\mathrm{MDEA}} = \frac{[\mathrm{MDEAH^+}][\mathrm{HCO_3^-}]}{[\mathrm{MDEA}][\mathrm{CO_2}]} \tag{46}$$

$$K_{\mathrm{PZ}} = \frac{[\mathrm{PZCOO^-}][\mathrm{H_3O^+}]}{[\mathrm{PZ}][\mathrm{CO_2}]} \tag{47}$$

$$K_{\mathrm{PZCOO^-}} = \frac{[\mathrm{PZ(COO)^-}][\mathrm{H_3O^+}]}{[\mathrm{PZCOO^-}][\mathrm{CO_2}]} \tag{48}$$

$$K_{\mathrm{OH^-}} = \frac{[\mathrm{HCO_3^-}]}{[\mathrm{OH^-}][\mathrm{CO_2}]} \tag{49}$$

As mentioned before water is left out from the kinetics thus in order to avoid having H_3O^+ as a species in the model:

$$R_{\mathrm{PZ}} = -k_{\mathrm{PZ}}\left([\mathrm{PZ}][\mathrm{CO_2}] - [\mathrm{PZCOO^-}]\frac{K_{\mathrm{W}}}{K_{\mathrm{PZ}}[\mathrm{OH^-}]}\right) \tag{50}$$

$$R_{\mathrm{PZCOO^-}} = -k_{\mathrm{PZCOO^-}}\left([\mathrm{PZCOO^-}][\mathrm{CO_2}] - [\mathrm{PZ(COO)_2^-}]\frac{K_{\mathrm{W}}}{K_{\mathrm{PZCOO^-}}[\mathrm{OH^-}]}\right) \tag{51}$$

where the equilibrium constant for water is

$$K_{\mathrm{W}} = [\mathrm{H_3O^+}][\mathrm{OH^-}] \tag{52}$$

The water dissociation reaction and its temperature dependency have been investigated widely by Olofsson & Hepler (1975).

The forward reaction rate coefficients are usually estimated from the Arrhenius type of equation:

$$k = k_{25^\circ\mathrm{C}} \cdot \exp\left[-\frac{E_{\mathrm{a}}}{R}\left(\frac{1}{T} - \frac{1}{298.15\mathrm{K}}\right)\right] \tag{53}$$

where E_{a} is the activation energy [J/mol].

The forward rate constant correlation values for piperazine related reactions are presented in Table 7.

Table 7 Forward rate constant correlations performed with a wetted wall contractor for piperazine related reactions**.**

Reference	Rate constant	$k_{25°C}$ [m^3/(kmol·s)]	ΔH_a [kJ/kmol]	T [K]	MDEA [kmol/m^3]	PZ [kmol/m^3]
(Bishnoi and Rochelle, 2000)	k_{PZ}	5.37*10^4	3.36*10^4	298-333	-	0.06-0.2
(Samanta and Bandyopadhyay, 2007)	k_{PZ}	5.8*10^4	3.5*10^4	298-313	-	0.2-0.8
(Samanta and Bandyopadhyay, 2007)	k_{PZCOO^-}	5.95*10^4	3.55*10^4	298-313	-	0.2-0.8
(Bishnoi and Rochelle, 2002a)	k_{PZCOO^-}	4.70*10^4	3.36*10^4	298-313	4	0.6
(Samanta and Bandyopadhyay, 2011)	k_{30}	1.75*10^4	8.75*10^4	298-313	1.89-2.41	0-0-95
(Bishnoi and Rochelle, 2002a)	k_{30}	1.46*10^4	8.43*10^4	295-343	4	0.6
(Samanta and Bandyopadhyay, 2011)	k_{32}	1.55*10^4	8.75*10^4	298-313	1.89-2.41	0-0-95
(Bishnoi and Rochelle, 2002a)	k_{32}	1.27*10^4	8.43*10^4	295-343	4	0.6

Some correlations for k_{MDEA} were presented in Table 3 and the correlation for k_{OH^-} is presented as follows (Pinsent et al., 1956):

$$\log_{10}\left(\frac{k_{OH^-}}{\mathrm{m^3/(kmol\cdot s)}}\right) = 13.635 - \frac{2895}{(T/\mathrm{K})} \tag{54}$$

The correlations presented by Rinker et al. (1995) for k_{MDEA} (Table 4) and by Pinsent et al. (1956) for k_{OH^-} (54) have been used in the recent studies (Edali et al., 2010, Samanta and Bandyopadhyay, 2011).

The instantaneous proton transfer reactions are assumed to be at equilibrium and they can be presented using respective species concentrations as follows:

$$K_{34} = \frac{[CO_3^{2-}][H_3O^+]}{[HCO_3^-]} \tag{55}$$

$$K_{35} = \frac{[PZH^+]}{[PZ][H_3O^+]} \tag{56}$$

$$K_{36} = \frac{\left[\mathrm{PZH^+COO^-}\right]}{\left[\mathrm{PZCOO^-}\right]\left[\mathrm{H_3O^+}\right]} \tag{57}$$

$$K_{37} = \frac{\left[\mathrm{MDEAH^+}\right]}{\left[\mathrm{MDEA}\right]\left[\mathrm{H_3O^+}\right]} \tag{58}$$

$$K_{38} = \left[\mathrm{H_3O^+}\right]\left[\mathrm{OH^-}\right] \tag{59}$$

The equilibrium constants are temperature dependent. The dependency can be expressed with the generalized equation of temperature dependency (60) or with the equations presented in Table 8 below, from which part follows the form of the equation (60).

$$\ln K = A + \frac{B}{(T/\mathrm{K})} + C \cdot \ln(T/\mathrm{K}) + D \cdot (T/\mathrm{K}) + \left(\frac{E}{(T/\mathrm{K})}\right)^2 \tag{60}$$

All chemical equilibrium constants presented in Table 8 are defined in the mole fraction scale with as reference state infinite dilution in water for all species except water. Mathematically all constants can be defined as in Equation (61). The coefficients for Equation (60) for molality based chemical equilibrium constants can be found from the literature (Ermatchkov and Maurer, 2011, Pérez-Salado Kamps et al., 2003). Molality, m, can be defined as (mol amine) / (kg water).

On the molality scale the chemical equilibrium is defined in terms of component activity or activity coefficient and mole fraction:

$$K_x(T) \equiv \prod_i a_i^{\nu_{i,x}} = \prod_i (x_i \gamma_i)^{\nu_{i,x}} \tag{61}$$

where a_i is the activity of component i in a solution [-],
x_i is the mole fraction of component i in the liquid phase [-],
γ_i is the activity coefficient of component i in a solution [-], and
$\nu_{i,x}$ is the stoichiometric factor of reactant i in reaction x
[$\nu_{i,x}>0$ for a reaction product and $\nu_{i,x}<0$ for a reactant].

Equilibrium constants K_{33b}, K_{34} and K_{38} can be assumed to be valid for the temperature range of 273.15 K-498.15 K (Derks, 2006). The temperature ranges for the rest of

equations has not been reported clearly, but usually the experimental results are gathered at low temperatures (below 333.15 K).

Table 8 Temperature dependency of the mole fraction based equilibrium constants.

Equilibrium constant (mole fraction based)	Equation	Reference
$K_{\mathrm{MDEA}} = \frac{x_{\mathrm{MDEA^+}} x_{\mathrm{HCO_3^-}}}{x_{\mathrm{MDEA}} x_{\mathrm{H_2O}} x_{\mathrm{CO_2}}}$	$K_{\mathrm{MDEA}} = \frac{K_{\mathrm{OH^-}}}{K_{37}}$	(Edali et al., 2010)
$K_{\mathrm{PZ}} = \frac{x_{\mathrm{PZCOO^-}} x_{\mathrm{H_3O^+}}}{x_{\mathrm{PZ}} x_{\mathrm{H_2O}} x_{\mathrm{CO_2}}}$	$\ln(K_{\mathrm{PZ}}) = -29.31 + \frac{5615}{(T/\mathrm{K})}$	(Bishnoi, 2000)
$K_{\mathrm{PZCOO^-}} = \frac{x_{\mathrm{PZ(COO^-)_2}} x_{\mathrm{H_3O^+}}}{x_{\mathrm{PZCOO^-}} x_{\mathrm{H_2O}} x_{\mathrm{CO_2}}}$	$\ln(K_{\mathrm{PZCOO^-}}) = -30.78 + \frac{5615}{(T/\mathrm{K})}$	(Bishnoi, 2000)
$K_{\mathrm{OH^-}} = \frac{x_{\mathrm{HCO_3^-}}}{x_{\mathrm{OH^-}} x_{\mathrm{CO_2}}}$	$\log_{10}(K_{\mathrm{OH^-}} K_{38}) = 179.648 + 0.019244 \cdot (T/\mathrm{K}) - 67.341 \cdot \log_{10}(T/\mathrm{K}) - \frac{7495.441}{(T/\mathrm{K})}$	(Read, 1975)
$K_{33\mathrm{b}} = \frac{x_{\mathrm{HCO_3^-}} x_{\mathrm{H_3O^+}}}{x_{\mathrm{H_2O}}^2 x_{\mathrm{CO_2}}}$	$\ln(K_{33\mathrm{b}}) = 231.465 - \frac{12092.1}{(T/\mathrm{K})} - 36.7816 \ln(T/\mathrm{K})$	(Posey and Rochelle, 1997)
$K_{34} = \frac{x_{\mathrm{CO_3^{2-}}} x_{\mathrm{H_3O^+}}}{x_{\mathrm{H_2O}} x_{\mathrm{HCO_3^-}}}$	$\ln(K_{34}) = 216.049 - \frac{12431.7}{(T/\mathrm{K})} - 35.4819 \cdot \ln(T/\mathrm{K})$	(Edwards et al., 1978, Harned and Scholes, 1941, Posey and Rochelle, 1997)*
$K_{35} = \frac{x_{\mathrm{H_2O}} x_{\mathrm{PZH^+}}}{x_{\mathrm{PZ}} x_{\mathrm{H_3O^+}}}$	$\ln\left(\frac{1}{K_{35}}\right) = -11.91 - \frac{4351}{(T/\mathrm{K})}$	(Bishnoi and Rochelle, 2000, Pagano et al., 1961, Samanta and Bandyopadhyay, 2011)
$K_{36} = \frac{x_{\mathrm{PZH^+COO^-}} x_{\mathrm{H_2O}}}{x_{\mathrm{PZCOO^-}} x_{\mathrm{H_3O^+}}}$	$\ln\left(\frac{1}{K_{36}}\right) = -8.21 - \frac{5286}{(T/\mathrm{K})}$	(Bishnoi, 2000)
$K_{37} = \frac{x_{\mathrm{MDEA^+}} x_{\mathrm{H_2O}}}{x_{\mathrm{MDEA}} x_{\mathrm{H_3O^+}}}$	$\ln\left(\frac{1}{K_{37}}\right) = -9.4165 - \frac{4234.98}{(T/\mathrm{K})}$	(Posey and Rochelle, 1997)
$K_{38} = \frac{x_{\mathrm{H_3O^+}} x_{\mathrm{OH^-}}}{x_{\mathrm{H_2O}}^2}$	$\ln(K_{38}) = 132.899 - \frac{13445.9}{(T/\mathrm{K})} - 22.4773 \cdot \ln(T/\mathrm{K})$	(Harned and Robinson, 1940, Posey and Rochelle, 1997)

* According to Edwards et al. (1978) the first term is 220.067.

7.4 Reaction kinetics

When designing absorption and desorption columns a lot of detailed information is needed for accurate design. One part of the information needed is the reaction kinetics. In the literature various researchers have been investigating the kinetics of absorption whereas desorption has gained less interest. Usually theory of absorption with a reversible chemical reaction is applied for desorption. Xu et al. (1995) came to the

conclusion that kinetics of absorption of CO_2 into aqueous solutions of activated MDEA can be applied to desorption.

Older articles (Xu et al., 1992, Zhang et al., 2001a) have proposed that the reaction of activated MDEA solution with CO_2 follows a mechanism which can be regarded as rapid pseudo-first-order reversible reactions of PZ with CO_2 in parallel with the reaction of MDEA with CO_2. Nevertheless Bishnoi & Roxelle (2002a) questioned this in their more recent study and since then their proposal has been applied also by other research groups (Idem et al., 2009, Samanta and Bandyopadhyay, 2011).

The pseudo first-order kinetic assumes that the concentration of the amine is uniform across the cross section of the liquid boundary layer. This assumption simplifies the kinetics because it transforms the second-order reaction expression of CO_2 with amine into the first-order expression.

Xu et al. (1992, 1995) studied the absorption and desorption of CO_2 into aqueous solution of activated MDEA. They presented that a reaction, in which MDEA reacts with CO_2 in a liquid film and forms unstable weakly bonded CO_2-nitrogen atom complex, is the dominant reaction of absorption of CO_2 into an activated MDEA solution. Simultaneously PZ as an activator reacts with CO_2 in a liquid film to form an intermediate. It is assumed that the reaction of PZ with CO_2 is rapid and in parallel with the reaction of MDEA and CO_2. In equilibrium in the liquid phase a hydrolytic reaction occurs forming protonated PZ and bicarbonates. The reaction system formed mainly by those three equations can be considered as two parallel rapid pseudo-first-order reversible reactions with the assumption of constant conversions of MDEA and PZ. When the diffusion equation in a liquid film is combined with a rapid pseudo-first-order parallel reversible reaction the chemical absorption and desorption rates for aqueous activated MDEA solutions can be expressed as (Xu et al., 1992, Xu et al., 1995):

$$\begin{aligned} N_{CO_2} &= k\left(p_{CO_2} - p^*_{CO_2}\right) \\ &= H_{CO_2}\left[D_{CO_2}\left(k_{MDEA}c_{MDEA} + k_{PZ}c_{PZ}\right)\right]^{1/2}\left(p_{CO_2} - p^*_{CO_2}\right) \end{aligned} \tag{62}$$

$$\begin{aligned} N_{CO_2} &= k\left(p^*_{CO_2} - p_{CO_2}\right) \\ &= H_{CO_2}\left[D_{CO_2}\left(k_{MDEA}c_{MDEA} + k_{PZ}c_{PZ}\right)\right]^{1/2}\left(p^*_{CO_2} - p_{CO_2}\right) \end{aligned} \tag{63}$$

Bishnoi & Rochelle (2002a) have questioned the work by Xu et al. (1992) and Zhang et al. (2001a). They figured out that the absorption rate did not follow the pseudo-first-order behaviour except at very low loadings. All carbamate and bicarbamate reactions approached instantaneous behavior at high loadings. In Figure 9 the results of Xu et al. (1992) are presented. Bishnoi & Rochelle (2002a) concluded that there is no information about the effect of PZ available since the measured enhancement was not significantly different from the enhancement in the MDEA solutions. According to them Figure 9 shows that the data is best described as pseudo first-order absorption into unpromoted MDEA. The figure also illustrates that piperazine would have a negative effect on the enhancement factor. That is unreasonable, so an experimental error can be assumed to have occurred.

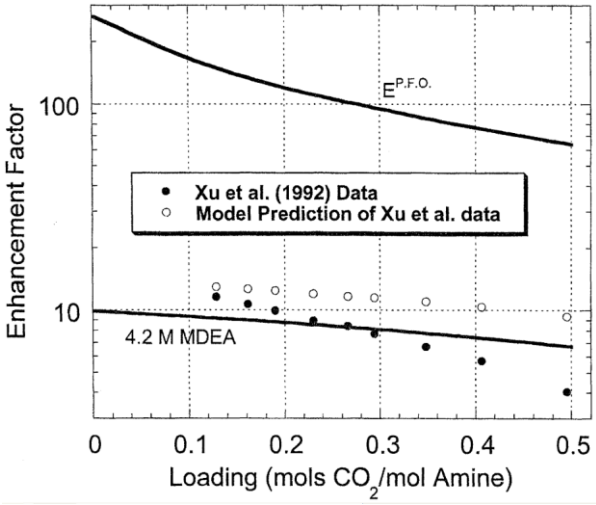

Figure 9 Enhancement factors for 0.1 M piperazine / 4.21 M MDEA at 40 °C (Bishnoi and Rochelle, 2002a). $E^{P.F.O}$ is the pseudo-first-order enhancement factor.

Bishnoi & Rochelle (2002a) came to the conclusion that with low loadings (<0.14) the reaction of PZ to form monocarbamate (29) is the dominant action, at moderate loadings the dominant reaction is the reaction of monocarbamate to form dicarbamate (31) and at high loadings the solution behaves like plain MDEA with instantaneous carbamate reactions. Samanta & Bandyopadhyay (2011) agreed with Bishnoi & Rochelle (2002a) in the fact that the measurents of Xu et al. (1992) might be erroneous. They validated their opinions with too low PZ concentrations that Xu et al. (1992) used in their research. The PZ concentrations studied are too low for commercial CO_2 processes. In addition Xu et al. (1992) performed the research with almost pure CO_2. That results in high partial pressure of CO_2 and leads to almost complete depletion of PZ at the gas-liquid interface. Bishnoi & Rochelle (2002a) tried different kinetic models

to fit the data. At low CO_2 loadings all ionic species are at very low concentrations and only chemical reactions (29) and (30) are taken into account. Also the forward reactions are considered since the concentrations of reaction products are low. It has been noticed that MDEA participates in the reaction of CO_2 and piperazine to form carbamate (30). At higher loadings also the reactions (31) and (32) are taken into account. Samanta & Bandyopadhyay (2011) and Derks (2006) came to the same conclusion that the formation of PZ dicarbamate and equilibrium between PZ carbamate and its protonated species play an important role in increasing the CO_2 loadings.

8 Phase equilibrium

Phase equilibrium determines the distribution of molecular species between vapour and liquid phases. When the phases are in equilibrium the fugacity in both phases (V and L) is equal for each component:

$$f_{i\mathrm{V}} = f_{i\mathrm{L}} \tag{64}$$

The deviation from ideality can be expressed with the fugacity coefficients of the mixture in vapour (V) and liquid (L) phases:

$$\varphi_{i\mathrm{V}} \equiv \frac{f_{i\mathrm{V}}}{y_i p} \tag{65}$$

$$\varphi_{i\mathrm{L}} \equiv \frac{f_{i\mathrm{L}}}{x_i p} \tag{66}$$

where φ_i is the fugacity coefficient of component i [-], and
p is the pressure [Pa].

The vapour-liquid equilibrium condition results in the extended Henry's law for molecular solutes (67) and in the extended Raoults's law for solvents (68).

$$\varphi_{i\mathrm{V}} y_i p = H_i x_i \gamma_i \exp\left(\frac{v_i^{\infty}\left(p - p^*_{\mathrm{SOLVENT}}\right)}{RT}\right) \tag{67}$$

$$\varphi_{i\mathrm{V}} y_i p = p_i^* x_i \gamma_i \exp\left(\frac{v_{\mathrm{w}}\left(p - p_i^*\right)}{RT}\right) \tag{68}$$

where y_i is the mole fraction of component i in the vapour phase [-],
$\varphi_{i\mathrm{V}}$ is the fugacity coefficient of i in the vapour phase [-],
p is the system total pressure [Pa],
x_i is the mole fraction of i in the liquid phase [-],
γ_i is the activity coefficient of component i [-],

$v_i^{\infty}(T)$ is the partial molar volume at infinite dilution of component i in the solvent at the system temperature T and at the vapour pressure of the solvent, $p^*_{SOLVENT}$, and

$v_w(T)$ is the molar volume of pure liquid water at the system temperature T and at the vapour pressure of the component i, p^*_i.

The activity coefficient of a solute species, γ_i, may be calculated with the Pitzer's molality-scale based equation for the excess Gibbs energy of aqueous solutions. Interaction parameters of the equation for the PZ/MDEA system can be found from the literature (Ermatchkov and Maurer, 2011, Pérez-Salado Kamps et al., 2003).

8.1 N_2O-CO_2 analogy

To model the Henry's law constant for CO_2 a physical solubility data of CO_2 in aqueous alkanolamine solutions is needed. Carbon dioxide's solubility to aqueous alkanolamines cannot be directly measured since it reacts with alkanolamines. CO_2 and N_2O have similarities in molecular properties i.e. in mass and structure so Clarke (1964) introduced a method to determine the diffusion coefficient and the physical solubility of CO_2 by using N_2O since N_2O does not react with alkanolamines so only mass transfer is occurring. Nowadays the method is known as the N_2O-CO_2 analogy. The Henry's law constant and the diffusion coefficient of CO_2 in a reactive solvent (aqueous alkanolamine solution) can be calculated from the following equations:

$$\frac{H_{CO_2,amine}}{H_{N_2O,amine}} = \frac{H_{CO_2,water}}{H_{N_2O,water}} \tag{69}$$

$$\frac{D_{CO_2,amine}}{D_{N_2O,amine}} = \frac{D_{CO_2,water}}{D_{N_2O,water}} \tag{70}$$

where $H_{N2O,water}$ is the Henry's law constant of N_2O in water,

$H_{CO2,water}$ is the Henry's law constant of CO_2 in water,

$H_{N2O,amine}$ is the Henry's law constant of N_2O in the aqueous alkanolamine solution, and

$H_{CO2,\ amine}$ is the Henry's law constant of CO_2 in aqueous alkanolamine solution.

The N_2O-CO_2 analogy to estimate the physical solubility and the diffusivity of CO_2 in alkanolamine systems has been used for example by (Samanta et al., 2007, Versteeg and van Swaaij, 1988b, Al-Ghawas et al., 1989)

8.1.1 The diffusion coefficients

In Table 9 the diffusivities of N_2O and CO_2 in water are correlated as a function of temperature.

Table 9 Temperature correlations for N_2O and CO_2 diffusion coefficients in water.

Reference	$D_{N2O,water}$ [m^2/ s]	$D_{CO2,water}$ [m^2/ s]
(Versteeg and van Swaaij, 1988b)	$5.07\cdot10^{-6}\exp\left(-\frac{2371}{(T/\mathrm{K})}\right)$	$2.35\cdot10^{-6}\exp\left(-\frac{2119}{(T/\mathrm{K})}\right)$
(Samanta et al., 2007)	$9.72\cdot10^{-6}\exp\left(-\frac{2582}{(T/\mathrm{K})}\right)$	$8.13\cdot10^{-6}\exp\left(-\frac{2488}{(T/\mathrm{K})}\right)$

Pacheco (1998) presented a correlation for the diffusion coefficient of N_2O [cm^2/s] in amine solution in a modified form of the Stokes-Einstein equation:

$$\left(\frac{D_{N_2O}}{\mathrm{cm}^2/\mathrm{s}}\right) = 5.533\cdot10^{-8}\frac{(T/\mathrm{K})}{\left(\frac{\mu_L}{\mathrm{cP}}\right)^{0.545}} \tag{71}$$

where μ_L is the viscosity at the liquid phase [cP].

For the viscosity calculations of aqueous alkanolamine solutions Glasscock (1990) has proposed the following correlation (72), which is assumed to be valid in the range of 20 to 50 °C and for MDEA concentrations up to 50 wt% (Pacheco, 1998):

$$\ln\left(\frac{\mu}{\mathrm{cP}}\right) = A + \frac{B}{(T/\mathrm{K})} + C(T/\mathrm{K}) \tag{72}$$

where μ is the viscosity [cP]

$$A = -19.52 - 23.40w_{Am} - 31.24w_{Am}^2 + 36.17w_{Am}^3 \tag{73}$$

$$B = 3912 + 4894w_{Am} + 8477w_{Am}^2 - 8358w_{Am}^3 \tag{74}$$

$$C = 0.02112 + 0.03339w_{Am} + 0.02780w_{Am}^2 - 0.04202w_{Am}^3 \tag{75}$$

and where w_{Am} is the weight fraction of total amine in solution.

Bishnoi (2000) used the correlation (72) also for the PZ/MDEA mixture. Some experimental viscosity and density data of an aqueous PZ/MDEA solution has been published in the literature (Derks et al., 2008, Muhammad et al., 2009, Paul and Mandal, 2006b, Samanta and Bandyopadhyay, 2011).

The method to calculate the diffusion coefficient of MDEA in aqueous solutions has been studied experimentally by Rowley in 1999 in solutions from 0-50 wt% MDEA and temperatures from 25 °C to 100 °C and he figured out the following correlation reported by Bishnoi (Bishnoi, 2000):

$$\left(\frac{D_{\mathrm{MDEA}}}{\mathrm{m^2/s}}\right) = d_0 + d_1 w_{\mathrm{Am}} + d_2 w_{\mathrm{Am}} \tag{76}$$

where

$$d_0 = 4.272 \cdot 10^{-4(T/\mathrm{K})^2} - 2.8582 \cdot 10^{-2(T/\mathrm{K})} - 22.036 \tag{77}$$

$$d_1 = 4.88 \cdot 10^{-3(T/\mathrm{K})^2} - 3.4444(T/\mathrm{K}) + 576.98 \tag{78}$$

$$d_2 = -7.92 \cdot 10^{-3(T/\mathrm{K})^2} + 5.1699(T/\mathrm{K}) - 822.13 \tag{79}$$

Also Snijder et al. (1993) have made some experiments to determine the diffusion coefficient of MDEA and they presented the original form for the correlation from which the correlation (80) has been presented by (Pacheco, 1998).

$$\left(\frac{D_{\mathrm{MDEA}}}{\mathrm{cm^2/s}}\right) = 0.0207 \exp\left(-\frac{2360.7}{(T/\mathrm{K})} - 24.727 \cdot 10^{-5} \cdot \frac{c_{\mathrm{MDEA}}}{(\mathrm{mol/m^3})}\right) \tag{80}$$

Diffusion coefficients for PZ are usually calculated using the diffusion coefficient of MDEA. The diffusion coefficient of MDEA is corrected for molar mass by multiplying with an appropriate factor. Two kinds of factor have been used in the literature; 1.2 by Bishnoi (2000, 2002a) and 1.38 by Samanta and Bandyopadhyay (2011). The diffusion coefficients of ionic species have been assumed to be equal to that of PZ (Bishnoi and Rochelle, 2002a, Samanta and Bandyopadhyay, 2011).

8.1.2 Henry's law constants

In Table 10 the Henry's law constants of N_2O and CO_2 in water are correlated as a function of temperature. Similar correlation are presented also by other authors (Pacheco, 1998, Versteeg and van Swaaij, 1988b).

Table 10 Temperature correlations for N_2O and CO_2 Henry's law constants in water.

Reference	$H_{N2O,water}$ [kPa·m^3/kmol]	$H_{CO2,water}$ [kPa·m^3/kmol]
(Versteeg and van Swaaij, 1988b)	$8.55 \cdot 10^6 \exp\left(-\frac{2284}{(T/\mathrm{K})}\right)$	$2.82 \cdot 10^6 \exp\left(-\frac{2044}{(T/\mathrm{K})}\right)$
(Samanta et al., 2007)	$4.86 \cdot 10^6 \exp\left(\frac{-2117}{(T/\mathrm{K})}\right)$	$6.17 \cdot 10^6 \exp\left(\frac{-2276}{(T/\mathrm{K})}\right)$

When considering the Henry's law constant of N_2O in the PZ/MDEA solutions the data is scarcer. In the literature (Al-Ghawas et al., 1989, Versteeg and van Swaaij, 1988b) only a few correlations for aqueous MDEA solutions have been presented. Samanta et al. (2007) presented a correlation which can describe the physical solubility of N_2O to an aqueous solution of PZ/MDEA.

8.2 Solubility

Solubility of gases in liquids are usually given in the terms of Henry's law constant H, which is dependent on temperature but relatively independent of system pressure at moderate pressure levels for systems where the Henry's law applies i.e. where the concentration of dissolved gas is small and the temperature and pressure are not close to the critical values of the gaseous component (Kohl, 1987). The law states that solubility of gas in liquid is directly proportional to its partial pressure in the gas phase:

$$p_i = Hx_i \tag{81}$$

where p_i is the partial pressure of component i in the gas phase [Pa], and
x_i is the mole fraction of component i in the liquid phase.

In Equation (81) the Henry's law constant has the units of pressure since the mole fraction is dimensionless. It should be noted that the units of the Henry's law constant may vary depending on the equation used. In the case of chemical absorption the Henry's law applies only to the unreacted gas dissolved into the solution. The physical

solubility of CO_2 into aqueous alkanolamine solutions is the equilibrium between gaseous CO_2 molecules and CO_2 molecules in the solution:

$$CO_2(g) \leftrightarrow CO_2(aq) \tag{82}$$

The equation (82) is purely physical. The dissolution must occur prior to further reaction of CO_2 to be able to occur in the liquid phase. An accurate thermodynamic model to describe the solubility of CO_2 in aqueous solutions of MDEA+PZ can only be developed with sufficient experimental data. Solubility of carbon dioxide into aqueous solutions of MDEA and PZ has been investigated more or less in recent years and the results can be found from the literature (Si Ali and Aroua, 2004, Bishnoi and Rochelle, 2002b, Böttger et al., 2009, Derks, 2006, Derks et al., 2006a, Derks et al., 2010, Ermatchkov and Maurer, 2011, Pérez-Salado Kamps et al., 2003, Speyer et al., 2010). In general solubility is investigated with low CO_2 loadings but with various amine concentrations and conditions. Low CO_2 loadings are encountered at the top of the industrial absorption towers and in systems involving flue gases such as in power plants (Si Ali and Aroua, 2004). Solubility is usually described as the partial pressure of CO_2 as the function of CO_2 loading in the solution (mol CO_2) / (mol amine).

Si Ali and Aroua (2004) have investigated carbon dioxide solubility into aqueous PZ/MDEA solutions at the temperatures and CO_2 partial pressures ranging from 40 °C to 80 °C and 0.1 kPa to 100 kPa. In their research they kept the total amine concentration constant so they were able to compare the results with pure MDEA. The results are gathered in Figure 10. The effect of PZ concentration on the ultimate CO_2 loading was found to be dependent on both the CO_2 partial pressure as well as the solution temperature. From the results it can be seen that the addition of PZ increased the solubility of CO_2 in the region of low CO_2 partial pressure compared to pure MDEA. When observing the trends of activated MDEA solutions it can be discovered that the CO_2 loading increases with increasing CO_2 partial pressure, decreasing absorption temperature and increasing PZ concentration.

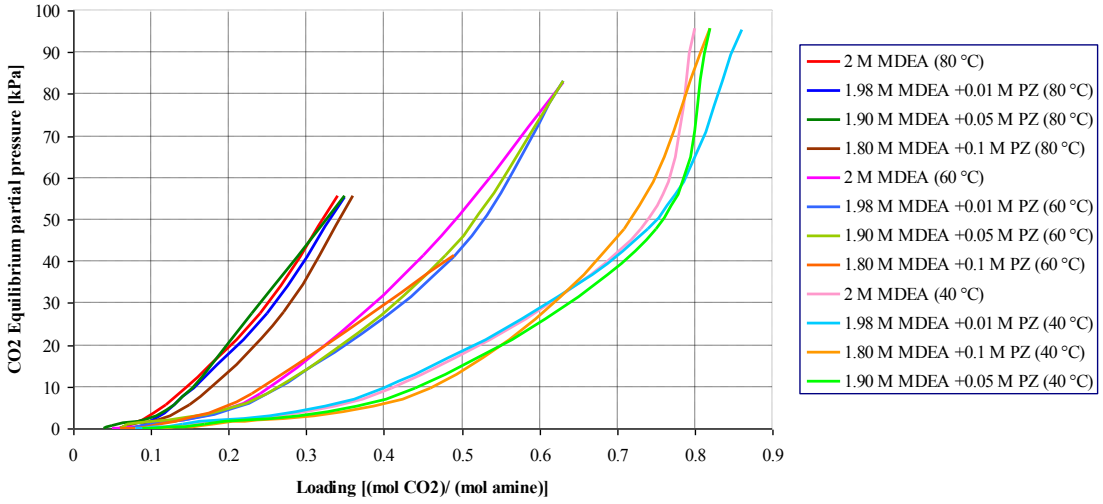

Figure 10 CO_2 partial pressures as the function of loading.

At the equilibrium the partial pressure of CO_2 over a loaded amine solution determines the operating window of the absorber and the stripper.

8.3 Models for phase and chemical equilibrium

Good predictions on the vapour liquid equilibria can be obtained by using rigorous thermodynamic models. The system to be considered is a multi-electrolyte and multi-solvent system. The liquid phase is highly non-ideal due to the presence of ions and polar molecules whereas the gas phase does not present significant non-idealities since the pressures of interest are not so high and the reactions are assumed to occur in the liquid phase. There are thermodynamic models available in the literature to approach this kind of systems and they can be divided into three groups.

The first group includes the simplest models. They are called non-rigorous models and they utilize simple mathematical relations for phase equilibria and a fitted chemical equilibrium constant. One example of the models belonging to this group is the Kent-Eisenberg model (Kent and Eisenberg, 1976). In this model two of the equilibrium constants are fitted to experimental partial pressures of CO_2. The model is unsuitable for the prediction of the speciation and exact energy balances cannot be performed because of fitting of the equilibrium constants. Despite the shortages, these models may be suitable for early phase studies and they have been quite popular due to the simplicity. (Hessen et al., 2010)

The second and third groups are more rigorous. One is based on the excess Gibbs energy (activity) and the other is based on the Helmholtz energy (equation of state). The selection of models based on the activity is quite large and the complexity of them is varying. One of the widely used models is the Desmukh-Mather (Deshmukh and Mather, 1981) model which utilizes the extended Debye-Hückel expression to predict all the activity coefficients except for water, which is assumed to behave ideally. More recent models are the electrolyte-NRTL model (e-NRTL) and the extended UNIQUAC model. (Hessen et al., 2010)

The nonrandom, two-liquid (NRTL) equation was first developed by Renon and Prausnitz (1968). It was originally a non-electrolyte model, but it was expanded to electrolyte-NRTL model by Chen et al. (1982, 1986). The e-NRTL model can be considered as a local composition model. (Hessen et al., 2010, Prausnitz, 1977) It has been applied for the MDEA solutions by several authors (Austgen et al., 1989, Hessen et al., 2010, Kim et al., 2009a, Zhang and Chen, 2010) and it has also been applied for the PZ/MDEA alkanolamine solution (Bishnoi and Rochelle, 2002b).

Electrolyte equation of state has been applied for the PZ/MDEA systems in the works of Derks et al. (2006, 2006a, 2010). The basic model for the quaternary MDEA-PZ-H_2O-CO_2 system can be understood as the combination of subsystems involved as illustrated in Figure 11.

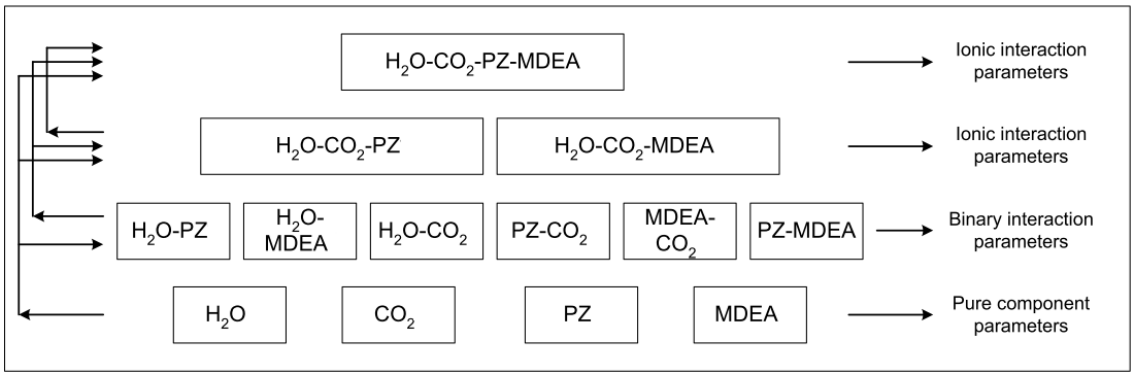

Figure 11 Schematic build-up of the electrolyte equation of state equilibrium model.

9 Energy consumption

Energy is required in the CO_2 recovery process based on amine absorption mainly to regenerate the rich amine solution and for the compression of CO_2. To a lesser extent electricity is needed for liquid pumping and in the flue gas fan. Energy consumed consists mainly of the energy needed in the endothermic reactions opposite to the absorption reactions. The steam generated in a reboiler at the bottom of the stripping column provides the latent and the sensible heat required for desorption of CO_2. The steam also acts as the diluent gas to maintain the partial pressure of CO_2 in the gas phase low enough for stripping to take place. As the energy needed in the blowers can be fixed according to the flow rates and the absorber pressure drop the energy needed in the reboiler changes significantly with process conditions. As mention in Chapter 2 the heat exchanger between the two columns offers an economical way to use the heat of the hot stripper bottoms to heat up the cool absorber bottoms. Due to the fact that the solution to be regenerated must be heated to temperatures above 100 °C and due to the high latent heat of water vaporization (2260 kJ/kg at 100 °C) it is obvious that the heating has a significant role in the energy consumption (Baugh et al., 2012). The stripper conditions are limited by the thermal degradation of amines. Higher temperature and pressure in the stripper would be energetically preferred since the thermal compression is more efficient than mechanical compression. The maximum and optimum operating temperature of the amine regenerator is therefore determined by thermal degradation and the formation of heat stable salts.

The capacity of the solvent is explained in Chapter 2. High capacity of solvent reduces the sensible heat requirements with temperature swing absorption and thus is a desirable characteristic. Solvent with a fast rate of reaction with CO_2 yield richer solution in the absorber. Richer solutions are more easily stripped and the energy requirements for stripping are reduced. (Oyenekan, 2007) As one of the main goals of this work is to minimize the energy needed in the regeneration the aspects affecting to it should be clarified. The reboiler duty, Q_r, can be considered as the sum of three terms: the heat required for desorbing the CO_2, $Q_{desorption}$, the heat required to generate the steam, Q_{steam}, and the heat required to raise the temperature of CO_2-loaded solution to the boiling point, $Q_{sensible}$ (Oyenekan, 2007):

$$Q_{\mathrm{r}} = Q_{\mathrm{desorption}} + Q_{\mathrm{steam}} + Q_{\mathrm{sensible}} \tag{83}$$

where Q_{r} is the reboiler duty [kJ/(mol CO_2) or MJ].

Many of the solvent properties are affecting the reboiler duty; loading of lean and rich solutions, alkanolamine type and concentration, and composition of mixed alkanolamines. Sakwattanapong et al. (2005) have indicated that the reboiler duties of mixed alkanolamines are between the heat duties of their parent alkanolamines. They also pointed out that the level of reboiler duty depends on the quantity of stripped CO_2 as well as from the quantity of lean solution exiting the stripper. A higher amount of CO_2 product and purer exiting lean solution results in higher reboiler duties.

9.1 Heat of absorption

The heat of absorption results from the temperature rise in the solution that is caused by the physical solution of CO_2 into the solvent and the exothermic reactions of CO_2 with alkanolamines. The same amount of energy is the minimum that must be fed to the stripping column in order to reverse the reaction. The temperature dependency of the heat of absorption and the impact of acid gas loading on it are often neglected even though it has been shown in the literature that at the conditions of an absorber and a desorber there might be a difference in the absorption heat larger than 25-30 % (Kim and Svendsen, 2011). The heat of absorption can be calculated from experimental solubility measurements by using the Gibbs-Helmholtz equation:

$$\left(\frac{\partial \ln p_{\mathrm{CO_2}}}{\partial (1/T)} \right)_{P,x} = \frac{\Delta H_{\mathrm{abs}}}{R} \tag{84}$$

In the equation above the fugacity of CO_2, f_{CO2}, can be used instead of the partial pressure. Enthalpies of absorption calculated with the equation (84) are differential in loading, α, but integral in temperature. According to Kim et al. (2009b) direct calorimetric measurements can provide accurate values for the enthalpy of absorption, ΔH_{abs}, combining the heat effect due to physical dissolution of gas in the solvent and chemical reaction between CO_2 and amine. The different measurement and calculation methods affect the values of heat of absorption and there might be $\pm$ 10 % inaccuracy between the values.

Currently, only a little information about the enthalpy of reaction of CO_2 in mixed solutions of PZ and MDEA is available. Schäfer et al. (2002) and Oyenekan and Rochelle (2007) have studied about the heat of CO_2 absorption in PZ/MDEA solutions and Oyenekan and Rochelle (2007) reported the heat of CO_2 desorption in rich and lean loadings and also at absorber and stripper conditions to be 62 kJ/(mol CO_2). Some useful experimental data was found from the Ph.D. Dissertation by Chen (2011). In Figure 12 a comparison of the heat of CO_2 absorption for two different PZ/MDEA solutions over the range of lean and rich CO_2 loading are presented. The heats of absorption of CO_2 at mid loadings were found to be -72 kJ/(mol CO_2) for the 7 m MDEA/2 m PZ (42 wt % MDEA/8.6 wt % PZ) and -68 kJ/(mol CO_2) for the 5 m MDEA/5 m PZ. The lean, mid and rich loadings are corresponding CO_2 partial pressures of 0.5, 1.5 and 5 kPa respectively and the experiments were performed at 313 K. The amount of PZ and MDEA are presented based on the molality.

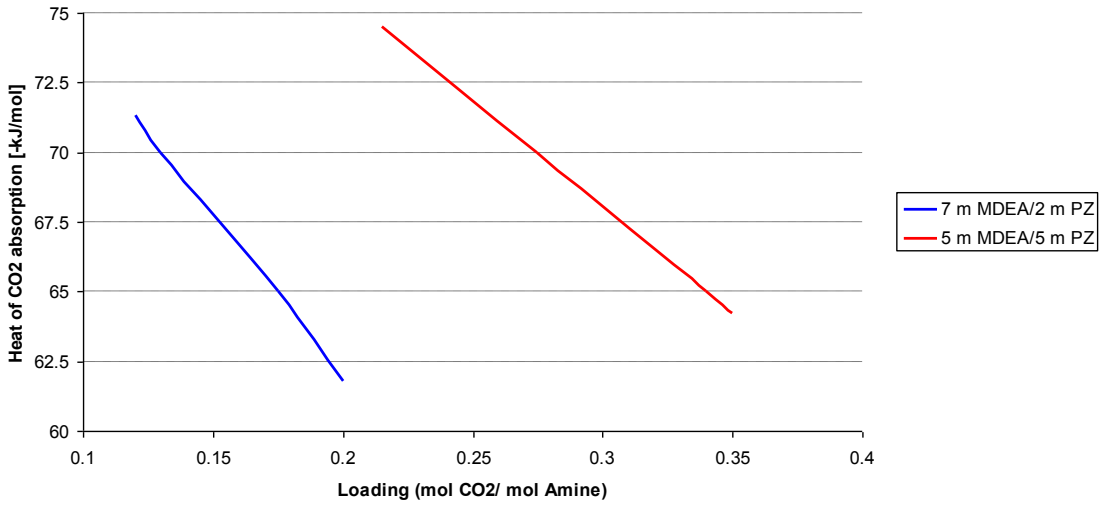

Figure 12 Comparison of the heat of CO_2 absorption in aqueous PZ/MDEA solutions (Chen, 2011).

Kim and Svendsen (2011) have performed a comparative study of the heats of absorption for amine solutions at different temperatures and with different loadings. The results for single MDEA and single PZ are presented in Figures 13 and 14. From the results it can be concluded that the enthalpy of absorption varies with different solvent types, acid gas loadings and temperatures. The figures present that MDEA has a lower heat of absorption than PZ. Except that MDEA shows a very strong temperature

dependency at loadings below 0.2. The loading capacity for MDEA is much lower at 293 K than at 313 K which can be considered as an advantage at the regeneration stage.

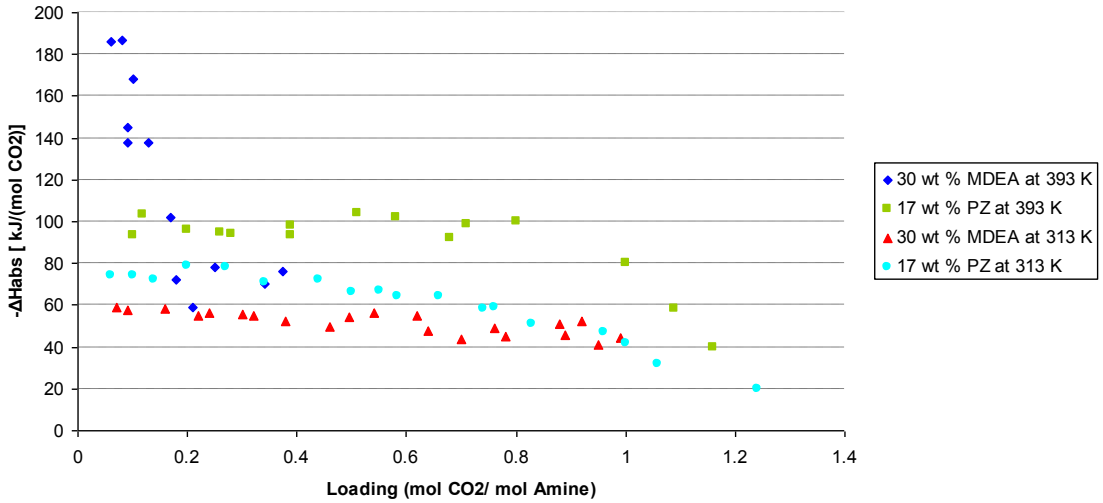

Figure 13 Heats of absorption of CO_2 at 313 and 393 K in aqueous PZ and aqueous MDEA (Kim and Svendsen, 2011).

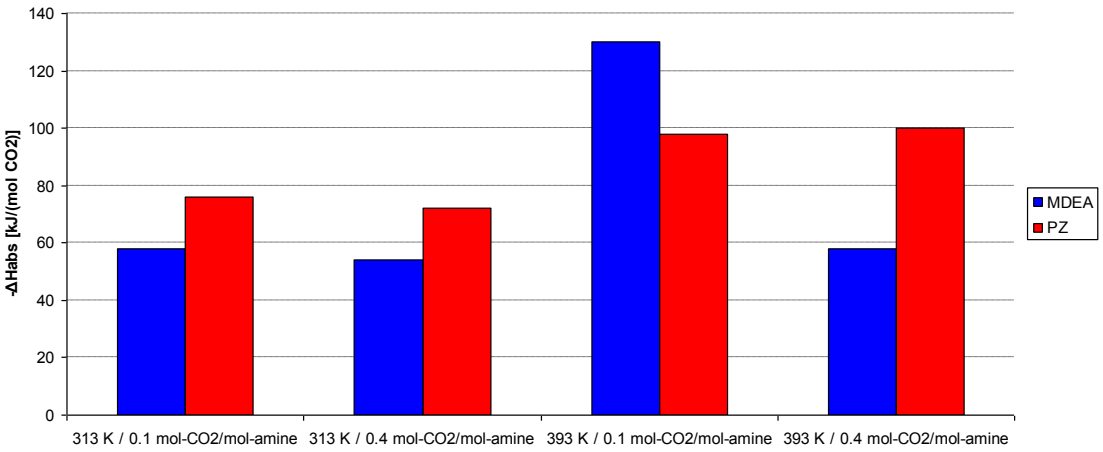

Figure 14 Heats of absorption with PZ and MDEA at 313 K and 393 K for loadings between 0.1 and 0.4 (mol CO_2/mol amine).

9.2 Heat of vaporization

Nguyen et al. (2010) have researched amine volatilities in CO_2 capture. They also calculated some heats of vaporization according to the Gibb's Helmholtz relations:

$$\frac{d\left(\ln P_{\text{amine}}\right)}{d\left(1/T\right)} = \frac{-\Delta H_{\text{vaporization}}}{R} \tag{85}$$

In the research the experiments were performed at 40 °C and 60 °C. In the solution of 7 m MDEA/2 m PZ the estimated heats of vaporization were 102 kJ/mol for MDEA and 135 kJ/mol for PZ.

9.3 Heat capacities

Heat capacities of aqueous PZ/MDEA solutions have been measured by Chen et al. (2010). The results of their work are of sufficiently acceptable accuracy. From the literature experimental measurements of heat capacities of aqueous PZ/MDEA loaded with CO_2 was not found. Oexmann (2011) has reported an equation developed by Hillard in 2008 for the heat capacity of CO_2-loaded solutions:

$$C_{p,\mathrm{L}} = c_{Cp,0} + c_{Cp,1}t + c_{Cp,2}t^2 + c_{Cp,3}\alpha + c_{Cp,4}\alpha^2 + c_{Cp,5}\overline{m}_{\mathrm{Am}} + c_{Cp,6}\overline{m}_{\mathrm{Am}}^2 + c_{Cp,7}t\alpha + c_{Cp,8}t\overline{m}_{\mathrm{Am}} + c_{Cp,9}\alpha\overline{m}_{\mathrm{Am}} + c_{Cp,10}t\alpha\overline{m}_{\mathrm{Am}} \quad (86)$$

where $C_{p,\mathrm{L}}$ is the mass-specific heat capacity of liquid [J/ (kg·K)],

$\overline{m}_{\mathrm{Am}}$ is the molality of amine [(mol amine)/ (kg H_2O)], and

t is the liquid temperature in Celsius, T/K -273.15 [°C].

In Table 11 the conditions to calculate the coefficients for Equation (86) are presented and the coefficients are presented in Table 12.

Table 11 Conditions of PZ/MDEA solution to calculate the heat capacity of loaded solution.

$\overline{m}_{\mathrm{Am}}$	t	α
11 (2/7) *m*	40-120 °C	0.1-0.25

Table 12 Coefficient to calculate the heat capacity of loaded PZ/MDEA solution.

$c_{Cp,0}$	$c_{Cp,1}$	$c_{Cp,2}$	$c_{Cp,3}$	$c_{Cp,4}$	$c_{Cp,5}$	$c_{Cp,6}$	$c_{Cp,7}$	$c_{Cp,8}$	$c_{Cp,9}$	$c_{Cp,10}$
3.304E+03	3.599E+00	3.369E-03	2.080E+03	0	0	0	6.398E+00	0	0	0

10 Modelling of the absorption/desorption process

When considering the absorption and desorption columns an effective mass transfer area is an essential parameter. A good way to provide contact area for mass transfer is the use of packing. It can be assumed that there is a film around the packing formed by the liquid in the column. This thin film increases the contact area between the gas and liquid phases. Besides packing, another good way to provide contact area between the gas and liquid phases is to use sieve trays or sprays. Large industrial reactive separation processes are usually divided into smaller elements, stages, which can identify real trays or segments of a packed column. These stages are related via mass and energy balances.

Modern absorbers and strippers using aqueous amines as solvents are designed to use effective trays like sieve or valve types and improved packing shapes like Pall rings of high-performance proprietary designs. Common tower packing types are presented in the work by McCabe et al. (2001). There are no specific guidelines for the choice between trays and packing and the choice is usually arbitrary because both types can do an adequate job. Sieve tray columns can be assumed to be the most popular type for both absorbers and strippers in conventional and large commercial plants whereas packed columns are preferred for small installations, corrosive service, liquids with a tendency to foam, very high liquid-gas ratios and applications in which a low pressure drop is desired. For CO_2 removal, as a special application, packed columns are often preferred. In columns applied for CO_2 recovery processes a high degree of CO_2 removal is desired and the low efficiency of trays may result in tall columns which are not feasible. (Kohl and Nielsen, 1997) Olarije (2010) has reported that when an amine absorption technology is used in a power plant capture of CO_2, the flue gas is bubbled counter current through the amine solvent in a packed absorber column. Kohl and Nielsen (1997) have presented a selection guide for gas-liquid contactors at page 7. According to the guide a randomly packed column would be more preferable than a structured column because of high liquid rates and corrosive fluids.

Modelling of an absorption process can be performed in several different levels. Usually a process model can be considered to be formed by several sub-models. The sub-models can be formed for mass transfer, reaction and hydrodynamics (mixing). There are several ways to select the stage model. The evolution and the complexity of stage

models can be presented for example as in Figure 15. The modelling can be started with classical equilibrium model with no reaction and infinite mass transfer. Accuracy of the equilibrium model can be increased by considering the reaction kinetics even though it is physically inconsistent. A rate-based approach can be achieved by considering the mass transfer kinetics whereas the accuracy of this rate-based approach can be improved by taking into account additional effects like the electrolyte influence. On optimal process design is a combination of rigour and simplicity.

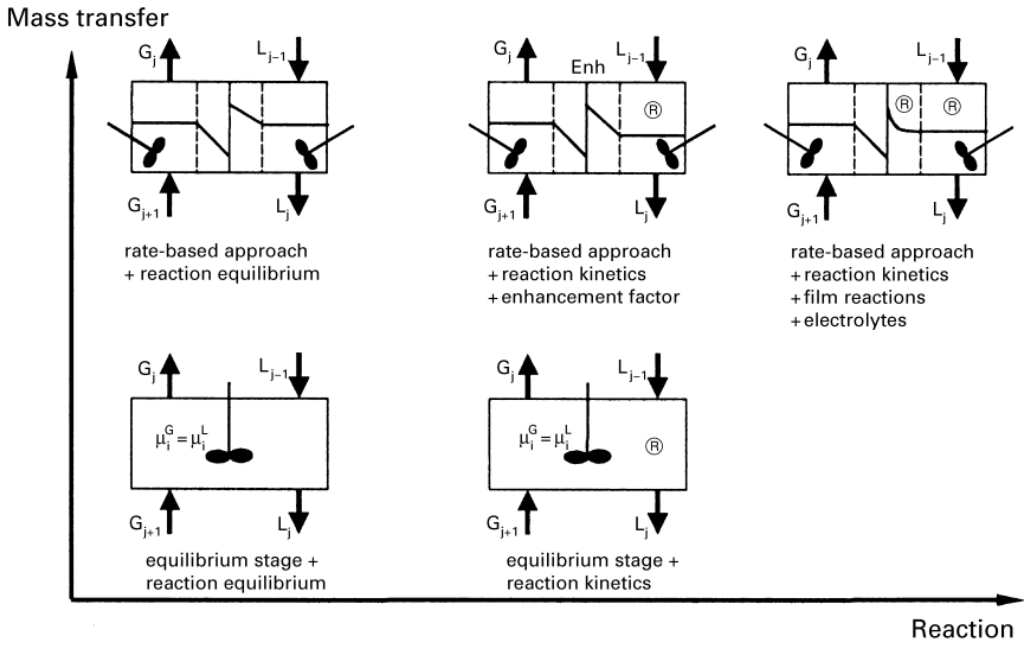

Figure 15 Complexities of different stage models (Kenig et al., 2001).

10.1 Equilibrium stage model

Equilibrium stage model is a simple model, which assumes that each gas-vapour stream leaving a tray or a packing segment is in a thermodynamic equilibrium with the corresponding liquid stream leaving the tray or the packing segment. In practise this equilibrium only truly holds at the interfaces separating vapour and liquid phases. Stage efficiencies are used to try to account for deviations from equilibrium, but these empirical factors are very limited and prediction methods are often unreliable. In packed columns, HETP is often used in the place of the equilibrium stage, but it can also be difficult to predict accurately. More about the efficiencies can be found from the doctoral thesis by Ilme (1997). When modelling a reactive separation process with this model the chemical reaction has to be separately taken into account. It can be done either via rate expressions integrated into the mass and energy balances or via reaction equilibrium equations. As mentioned before in this work, acceleration of mass transfer

caused by chemical reaction can be taken into account by an enhancement factor (Noeres et al., 2003).

A parameter to rigorously model the phenomena occurring at the gas-liquid interface is known as the enhancement factor, E. The enhancement factor describes how much more effective the mass transfer becomes at the presence of a chemical reaction and it can be defined with the ratio of actual liquid phase mass transfer coefficient, k_L, to the mass transfer coefficient under the same conditions without chemical reaction in the liquid, k_L°:

$$E = \frac{k_L}{k_L^o} \tag{87}$$

Enhancement factors can be obtained by fitting experimental results or they can be derived theoretically. The equations to calculate the enhancement factor varies depending on the mass transfer model used and the nature of the chemical reaction it is describing. The enhancement factor may include information about the amount of substances and concentrations, reaction kinetics, diffusivities of reactants and products, reversibility of the reactions and hydrodynamics at the interface. (Danckwerts, 1970, Kohl, 1987) Enhancement factors are usually exact only for a few simple reaction types (Kucka et al., 2003). According to Noeres et al. (2003) it is not possible to derive the enhancement factors properly from binary experiments and problems usually arise if reversible, parallel or consecutive reactions are taking place.

10.2 Rate-based model

In comparison with the equilibrium model, a rate-based model for describing a column stage is fundamental and rigorous approach which avoids the approximations of efficiency and HETP entirely. In this approach actual rates of multicomponent mass and heat transfer and chemical reactions as well as specific features of electrolyte species are considered directly. The acceleration effect of chemical reaction is taken into account without application of enhancement factors. The rate-based model can be based on different theoretical models described in Chapters 6.2.1 and 6.2.2, but the two-film theory is advantageous since there is a broad spectrum of information available in the literature. (Noeres et al., 2003)

In rate-based modelling the reaction rates are implemented as source terms into the transport equations describing film phenomena and into the balances describing liquid bulk behaviour. The bulk phase and the film region equations based on the two-film theory are presented for example in the work of Kucka et al. (2003).

10.3 Modelling of the stripping column

The optimal stripper design is crucial when minimizing the operation costs. Nevertheless most studies concerning the absorption/stripping processes have focused on the absorption process and it has been assumed that desorption process works as the opposite. In the literature, articles about stripping with MEA can be found. Some of them are listed in the work by Oyenekan (2007) in which he modelled strippers with different aqueous amines. He introduced some stripper configurations for minimizing the operation costs and he also studied the effects of variables like operating temperature or pressure as well as the effect of solvent, heat of absorption and capacity to the energy consumption.

The desorption conditions are crucial when concerning the stripper performance. High pressure would be beneficial when considering the further use of the recovered CO_2. As the vapour used in the regeneration is produced in the reboiler at the bottom of the stripping column the maximum pressure is limited. At normal amine concentrations the boiling points of amine solutions correspond to the boiling point of pure water as determined by the pressure. The temperature of 120 °C corresponds to a pressure around 200 kPa. In general also high desorber temperature is desirable but the limitation comes from the thermal degradation of amine solvents. At the top of the stripping column there are higher amounts of CO_2, which cause the temperature to decrease about 10-20 °C.

II Experimental part

11 Modelling with Aspen Plus®

Aspen Plus is a process modelling environment developed by Aspen technology, Inc. It can be used for example for conceptual design, optimization and performance monitoring. In this work the Aspen Plus V7.3.2 simulation program is used. The mathematical model behind the calculations in Aspen rate-based distillation, the rate-based mode of RadFrac, consists of material balances, energy balances, mass transfer, energy transfer, phase equilibrium and summation equations. In this new version of Aspen Plus a model for rate-based CO_2 capture in absorber-stripper systems using an aqueous PZ/MDEA system can be applied with updated databank to PURE26 (Aspen Technology, 2010-2012). In the system developed by Aspen Plus also the removal of hydrogen sulphide is possible, but in this work it is left out of further discussions.

In the rate-based PZ/MDEA model the thermophysical properties and reaction kinetic models are based on Aspen Technology's own recent work and on works by Bishnoi and Rochelle (2000, 2002a). The asymmetric electrolyte NRTL method (ENRTL-RK) is used to compute liquid properties and the PC-SAFT (Perturbed-Chain Statistical Associating Fluid Theory) equation of state is used to compute vapour properties. In the model CO_2, N_2, O_2, CO_2, CO and H_2 are treated as solutes to which Henry's law is applied and water, PZ and MDEA are treated as solvents. In the Aspen Plus there are two reaction sets built-up, one where all the ionic reactions are assumed to be at equilibrium and another where some of the reactions are kinetically controlled.

The equilibrium equation set used in the equilibrium model of Aspen Plus is presented in Table 13. Some of the reactions are presented in a different form than in the theoretical part of this thesis.

Table 13 Equilibrium equations used in Aspen Plus "P-M".

Equilibrium reaction	Reaction number
$2H_2O \overset{K_{38}}{\leftrightarrow} H_3O^+ + OH^-$	(38)
$CO_2 + 2H_2O \overset{K_{33b}}{\leftrightarrow} HCO_3^- + H_3O^+$	(33b)
$HCO_3^- + H_2O \overset{K_{34}}{\leftrightarrow} CO_3^{2-} + H_3O^+$	(34)
$PZH^+ + H_2O \overset{K_{88}}{\leftrightarrow} PZ + H_3O^+$	(88)
$PZ + HCO_3^- \overset{K_{89}}{\leftrightarrow} PZCOO^- + H_2O$	(89)
$HPZCOO^- + H_2O \overset{K_{90}}{\leftrightarrow} PZCOO^- + H_3O^+$	(90)
$PZCOO^- + HCO_3^- \overset{K_{91}}{\leftrightarrow} CO_2 + PZ(COO^-)_2 + H_2O$	(91)
$MDEAH^- + H_2O \overset{K_{92}}{\leftrightarrow} MDEA + H_3O^+$	(92)

The equilibrium constants for the reactions presented in Table 13 are calculated from the standard Gibbs free energy change in Aspen Plus. Some of the data used are gathered from the literature and some can be obtained from the databank of Aspen Plus.

The reaction set consisting of kinetically controlled reactions as well as equilibrium reactions is discussed below. In the calculation of reactions occurring in the electrolyte solution, the reactions involving only proton transfer (34)-(38) has been assumed to be at equilibrium as mentioned in Chapter 7.3. The reactions which are kinetically controlled (28)-(33) have been replaced by the equations presented in Table 14. The reduced power law expression (93) has been used to calculate the rates of the reactions. The pre-exponential factors as well as the activation energies used are given in Table 14.

$$r_x = kT^N \exp\left(-\frac{E_a}{RT}\right)\prod_{i=1}^{n}(x_i\gamma_i)^{\nu_{i,x}} \qquad (93)$$

where N is the temperature exponent = 0, and
k is the pre-exponential factor [mol/(m^3·s)].

In Table 14 the kinetic parameters for reactions (94) and (95) are derived from the work by Rinker et al. (1997). The kinetic parameters for reactions (96)-(99) are derived from the studies by Bishnoi and Rochelle (2000, 2002a). The kinetic parameters for

reaction (100) are taken from the work by Pinsent et al. (1956), and the kinetic parameters for corresponding reversible reaction (101) are calculated by using kinetic parameters of reaction (100) and the equilibrium constant of the reversible reactions (100) and (101).

Table 14 Equations for kinetically controlled reactions used in Aspen Plus.

Reaction replaced	New reaction	k [mol/(m^3·s)]	E_a [cal/mol]	Reaction number
(28)	$CO_2 + MDEA + H_2O \xrightarrow{k} MDEAH^+ + HCO_3^-$	6.85E+10	9029	(94)
(28)	$MDEAH^+ + HCO_3^- \xrightarrow{k} CO_2 + MDEA + H_2O$	6.62E+17	22131	(95)
(29)	$CO_2 + PZ + H_2O \xrightarrow{k} PZCOO^- + H_3O^+$	1.70E+10	319	(96)
(29)	$PZCOO^- + H_3O^+ \xrightarrow{k} CO_2 + PZ + H_2O$	3.40E+23	14160	(97)
(31)	$CO_2 + PZCOO^- + H_2O \xrightarrow{k} PZ(COO^-)_2 + H_3O^+$	1.04E+14	8038.3	(98)
(31)	$PZ(COO^-)_2 + H_3O^+ \xrightarrow{k} CO_2 + PZCOO^- + H_2O$	3.20E+20	8692	(99)
(33)	$CO_2 + OH^- \xrightarrow{k} HCO_3^-$	1.33E+17	13249	(100)
(33)	$HCO_3^- \xrightarrow{k} CO_2 + OH^-$	6.63E+16	25656	(101)

In the rate-based simulations the reaction set "P-M-REA" is used. The reaction set includes reactions 34, 38, 88, 90, 92 and 94-101 presented in Tables 13 and 14.

In some parts of the simulations pure CO_2 stream is used and in some parts flue gas streams are used as a feed stream. The typical flue gas composition of coal fired power plant is presented in Table 15 and this composition is used in certain solubility simulations. The flue gas composition presented in Table 15 is taken from a coal fired power plant of 565 MW. The technology used in the power plant allows the removal of 80 % of nitrogen oxides, 85-90 % of sulphur oxides and 99.9 % of dust.

Table 15 The typical composition of coal fired power plant. The slip-NH_3 and dust are not taken into account when modelling the solubility.

	kg/s	kmol/s	mol %	dry V %
SO_2	0.08880	1.386E-06	0.0065	0.007
N_2	424.50000	15.154	71.4813	79.800
O_2	30.33000	0.843	3.9764	5.000
CO_2	118.80000	2.699	12.7312	14.200
Ar	7.22000	0.181	0.8538	0.952
NOx (NO_2)	0.06430	1.398E-03	0.0066	0.007
SO_3	0.01350	1.69E-04	0.0008	0.001
H_2O	41.80000	2.320	10.9434	0.000
	622.81660	21.199	100	99.967
Not taken into account:				
Slip-NH_3	0.00171			0.001
Dust	0.02670			
	622.84501			99.968

12 Modelling of solubility

In this work the solubility of CO_2 into aqueous PZ/MDEA solution was simulated by using Aspen Plus V7.3.2 and the results were compared with experimental results presented in the literature. The solubility simulations were performed with the flash system presented in Figure 16. The flash is acting as an equilibrium stage where the reaction set P-M occurs. The equilibrium reaction set, P-M, includes the reactions presented in Table 13. In the flash the entering streams were allowed to achieve the equilibrium in desired conditions. In the solubility simulations pure CO_2 was used instead of flue gas. The amine concentration of the feed stream and the ratio between MDEA and PZ were determined according to the literature references and the amount of CO_2 feed was varied. Both the stream and the flash were at desired temperature and the amount of exiting streams were determined so that the vapour fraction in the vessel was low (0.000001).

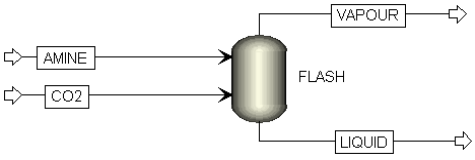

Figure 16 Flash system used in the solubility simulations.

12.1 Modelling results

The equilibrium solubility is usually illustrated with figures where the partial pressure of CO_2 is in the vertical axis and the solubility of CO_2 into the liquid (the molar ratio of CO_2 and amine at the liquid phase) is in the horizontal axis. Selected simulation results are gathered in Figure 17 and more detailed figures can be found from Appendix 1. When considering absorption and stripping processes the most interesting results are at CO_2 loadings less than 0.5 (mol CO_2)/ (mol amine) in the liquid phase. The results by Vahidi et al. (2009) are not so important in this case because they only have a few measure points below $\alpha < 0.5$. The accuracy of the simulations and experiments is important when it comes to the regeneration of the amine. Only one research group (Speyer et al. 2010) has explored the solubility at the desorption temperatures (393.15 K) and the experimental results show a bit smaller partial pressures of CO_2 than the simulation. If the partial pressure of CO_2 is underestimated it leads to the underestimation of CO_2 released in the stripping and to be able to separate the wanted amount of CO_2 the temperature should be raised.

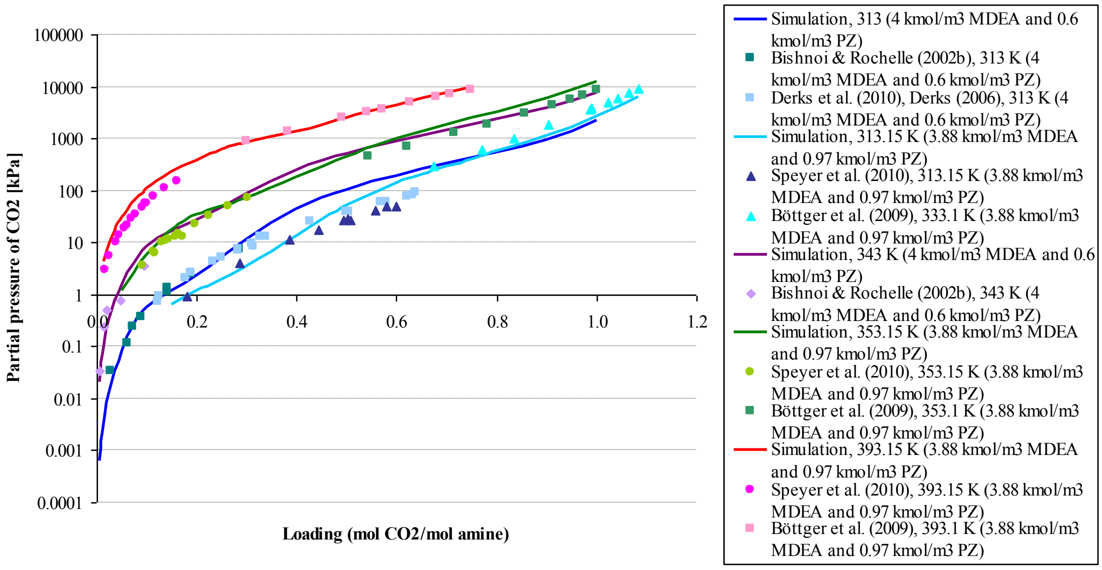

Figure 17 Solubility simulations with pure CO_2.

In addition the effect of the amine concentration and the effect of the ratio between MDEA and PZ were illustrated by performing additional simulations without literature references. Those results are presented in Figure 18.

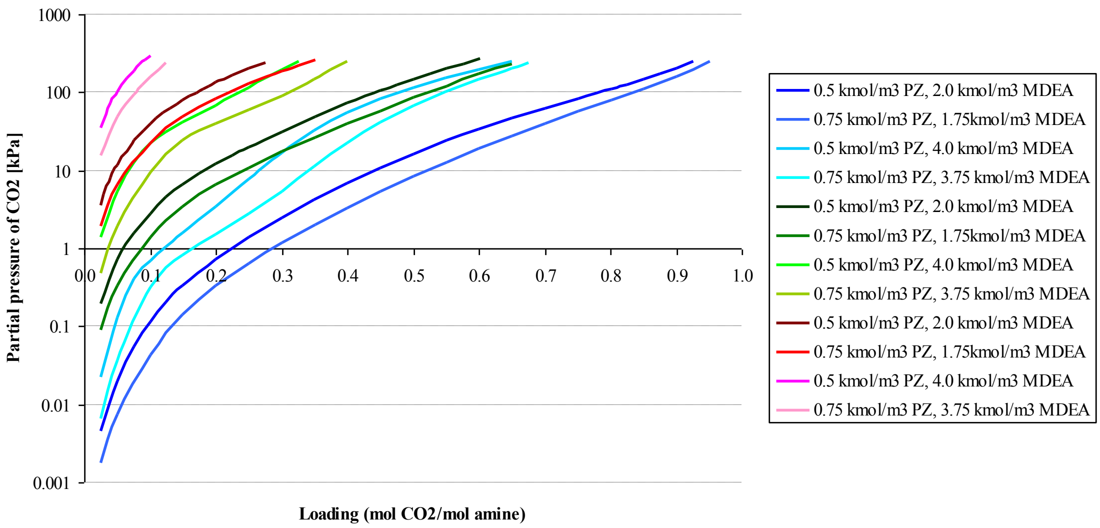

Figure 18 Comparison between different amine concentration and MDEA-PZ ratios in three different temperature; a) blue: 313.15 K b) green: 353.15 K c) red: 393.15K.

12.2 Interpretation of the solubility results

Solubility of CO_2 into the aqueous amine solutions was investigated in the temperature range of 303.15-393.15 K. The amount of CO_2 fed to the system was varied so that the simulation results were achieved at wanted loadings i.e. the mole ratio between CO_2 and total amine (mol MDEA + mol PZ) in the exiting liquid stream varied between 0-1.4.

The mole ratio was determined with the apparent concentrations which mean that both the molecular and the ionic components were taken into account. As a common comment from the results it can be concluded that the CO_2 loading increases with CO_2 partial pressures and decreases with the temperature.

Comparison of the simulation results and certain experimental findings (Bishnoi and Rochelle, 2002b, Böttger et al., 2009, Pérez-Salado Kamps et al., 2003, Speyer et al., 2010) affirm that they are corresponding to each other relatively well whereas there is variation between the simulation results and the experimental results of Vahidi et al. (2009) especially at the lower amine concentrations but also with high CO_2 loadings at low temperatures with all amine concentrations. The experimental results by Derks et al. (2006, 2010) are corresponding the simulation results well at the lower loadings but the difference becomes at the loadings bigger than 0.4. Similar deviation can be obtained in the experimental results by Speyer et al. (2010) at low temperature and high amine concentration. The experimental results by Liu et al. (1999) are quite well in line with the simulation in each temperature. The only noticeable difference appears at high CO_2 loadings.

Figure 18 discloses that with the constant amine concentration the solubility of CO_2 diminishes with raising temperature whereas with constant temperature the solubility of CO_2 diminishes with raising amine concentration. When comparing different amine concentrations it can be noticed that with higher concentrations the amount of dissolved CO_2 is higher and it also seems that a higher amount of PZ compared to the amount of MDEA results in higher amounts of dissolved CO_2. When considering the regeneration process, high temperatures and high amine concentrations are more beneficial since the separation is easier with bigger CO_2 partial pressures. When comparing amine solutions at high temperatures the amine solution with a lower PZ content has a higher vapour pressure and CO_2 is easier to remove from the solution i.e. the addition of PZ inflicts an increase in the reboiler duties. It has been studied by Zhang et al. (2001b) that the optimum weight ratio of MDEA to PZ for CO_2 removal is 50/5 at a total amine concentration of 3.0 kmol/m^3.

13 Modelling of reaction equilibrium constants and physical properties

13.1 Reaction equilibrium constant simulations

Reaction equilibrium constants were investigated within a temperature range from 313.15 K to 393.15 K. The concentrations of amines in the amine stream were 4 kmol/m^3 of MDEA and 0.6 kmol/m^3 of PZ and the CO_2 flow was determined so that the wanted loading was achieved (α = 0.1). An additional water stream was fed to the flash tank to keep the pH of the liquid stream constant. In the modelling of the equilibrium constants the simulation scheme was similar to the solubility modelling and it is presented in Figure 19. The same equilibrium reaction system P-M (Table 13) was used in the flash column.

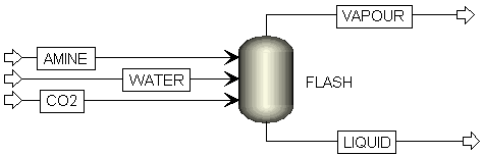

Figure 19 Flash system for reaction equilibrium constant simulations.

Due to the additional water the real amine concentration in the system was extremely low. The amount of excess water was determined so that the pH of the liquid stream was ~7.90. The vapour fraction of the flash tank was set to 0.000001 and the temperature was adjusted for each run. The temperature dependencies of the reactions 33b, 34, 38, 88, 90 and 92 (or the temperature dependency of the reverse reaction) were presented in Table 8. In the equilibrium model of Aspen Plus the reactions 89 and 91 are in such a form that no previous temperature dependencies of their equilibrium constants are presented in this work. A correlation for the temperature dependency is needed to be able to compare the simulation results with the literature values at different temperatures. Reaction 89 can be derived by combining reactions 29 and 33b whereas reaction 91 can be derived similarly from reactions 31 and 33b. However Derks (2006) has presented the temperature dependencies of reactions 89 and 91 based on the results of Ermatchkov et al., (2003) in the mole fraction based on (102) and (103). Those correlations can be assumed to be valid within a temperature range of 273.15-333.15 K.

$$K_{89} = -4.6185 + \frac{3616.1}{(T/\mathrm{K})} \tag{102}$$

$$K_{91} = 0.36150 + \frac{1322.3}{(T/\mathrm{K})} \tag{103}$$

The correlations presented in Table 8 were applied to calculate the estimated values in Figure 20. In Figure 21 the estimated values are calculated according to the correlations presented above. In both of the figures the mole fraction based equilibrium constants are calculated based on the mole fractions calculated by Aspen Plus.

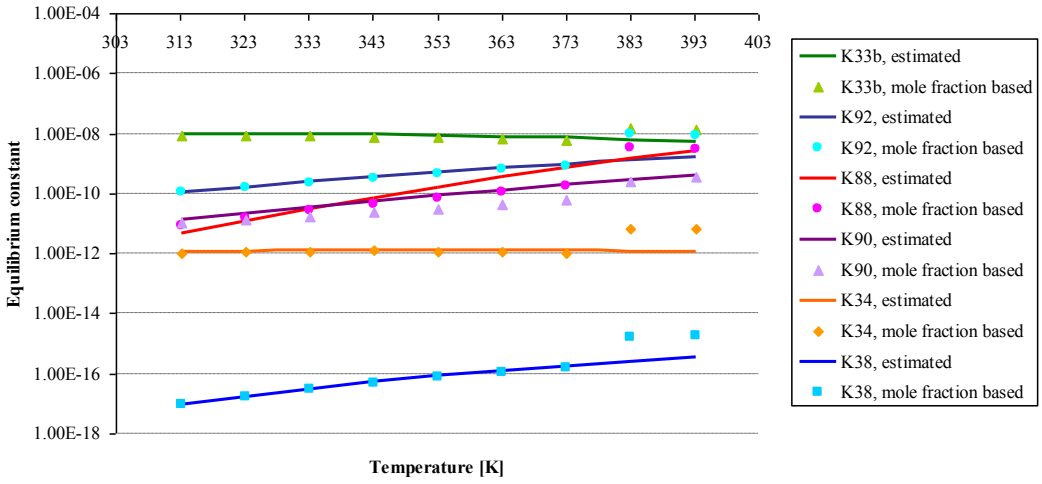

Figure 20 Temperature dependency of the mole fraction based reaction equilibrium constants.

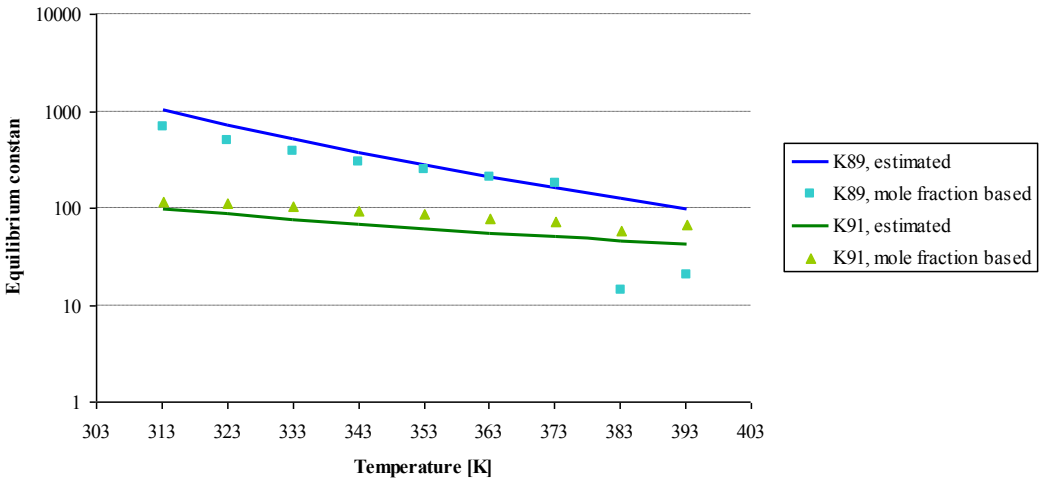

Figure 21 Temperature dependency of the mole fraction based reaction equilibrium constants.

13.2 Interpretation of the reaction equilibrium constant simulations

Figures 20 and 21 illustrating the results of the reaction equilibrium constant simulations show that the results are quite well in line with the values calculated from the temperature dependency correlations until the temperature of 373.15 K that is the boiling point of water at atmospheric pressure. At higher temperatures than 373.15 K a clear leap can be obtained at the values of Aspen Plus based equilibrium constants. When taking into account the logarithmic scale of the axis the leap can be considered to be noticeable. A few of the equilibrium constant correlations presented in Table 8 are valid only for relatively low temperatures but the temperature dependency correlations for equilibrium constants K_{33b}, K_{34} and K_{38} are reported to be valid until 498.15 K. From this point of view it can be concluded that the accuracy of the equilibrium constants obtained from Aspen Plus is uncertain at high temperatures. This may lead to inaccuracies when modelling the regeneration process which occurs at these higher temperatures. The leap in the values of equilibrium constants seems to be beneficial for the regeneration process, since the equilibria are moving towards pure amines and pure CO_2. The equilibrium reactions included in the rate-based model are reactions 34, 38, 88, 90 and 92. The correlations and simulation results are well in line in the case of carbonate formation (34) and water dissociation (38). The equilibrium constants which have the biggest deviation from the estimated values are the reactions involving PZ (89, 90). The equilibrium constant of MDEA protonation reaction (92) also seems to be well in line with the estimation. These findings lead to a conclusion that the reaction mechanisms and impacts of PZ should gain some additional interest. It should be noticed that in real amine absorption process the pH varies within the process and this affects the equilibrium constants.

13.3 Modelling of physical properties

The ability of Aspen Plus V7.3.2 to model physical properties of aqueous PZ/MDEA solutions was investigated briefly. The accuracy of the physical properties has an effect on the dimensioning of the equipment as well as mass transfer. High surface tension of the amine solvent facilitates the separation of the phases where as it also hinders the physical absorption of CO_2 into the amine solvent. Viscosity and density of the solvent affect the mass transfer coefficients in the liquid film and heat capacity is an important factor when modelling heat transfer. As a conclusion physical properties and their accuracy are important factors when modelling mass transfer in the absorber and in the desorber as well as when modelling equipments like pumps and heat exchangers.

In the simulations only aqueous amine solutions were investigated since no literature references about physical properties of CO_2 loaded PZ/MDEA solutions were found. Nevertheless, in general it can be said that the CO_2 loading in aqueous amine solutions has an effect on physical properties. Usually density, viscosity and surface tension increase while the loading of CO_2 increases where as the heat capacity decreases. In the modelling the vapour fraction of the flash tank was again determined to be small (0.000001) and the concentration of the amine solution as well as the temperature were determined according to the literature references.

Simulations of density and viscosity of the aqueous PZ activated MDEA solutions were compared with three literature reference (Derks et al., 2008, Muhammad et al., 2009, Paul and Mandal, 2006b). The results of the density simulations are presented in Appendix 2 and the results of the viscosity simulations are presented in Appendix 3. Simulations of surface tension were compared to two literature references (Muhammad et al., 2009, Paul and Mandal, 2006a) and they are presented in Appendix 4 and simulations of heat capacity were performed according to Chen et al. (2010) and they are also presented in Appendix 4.

13.4 Interpretation of the results of physical property simulations

Derks et al. (2008) have simulated densities and viscosities at two different temperatures with several different PZ and MDEA concentrations whereas Muhammad et al. (2009), Paul and Mandal (2006b) and Samanta and Bandyopadhyay (2011) have measured densities and viscosities with constant amine concentrations at different temperatures. Nevertheless, the amine concentrations in these two latter experimental studies are so different that they are not easily comparable and they are presented in separate figures.

From the findings it can be concluded that the density of aqueous amine solutions decreases as the temperature increases, and the density increases as the concentration of the amine in the solution increases. From Figure 1 in Appendix 2 it can be seen that the density simulation results are corresponding to the experimental results best at the amine concentrations below and slightly above 30 % by weight. Another interesting issue to be noticed can be seen from Figure 3 in Appendix 2 in which the simulation of density and experimental results by Paul and Mandal (2006b) are acting as opposite to

each other whereas the simulation and the experimental results by Samanta and Bandyopadhyay (2011) are quite well in line with each other. According to the simulation and work by Samanta and Bandyopadhyay (2011) the density of the liquid decreases as the mass fraction of PZ increases while the total amine mass faction is kept constant. According to that it may be concluded that there might occur an error in the article by Paul and Mandal (2006b).

From Appendix 3 it can be seen that the viscosities according to the experimental results and the simulations are following the trend of viscosity of aqueous amine solutions reported in the literature; the viscosity of aqueous amine solution decreases while the temperature increases. The findings also disclose that the viscosity increases as the concentration of the amine in the solution increases, similarly to the density. When observing the results of viscosity simulations and experimental results it seems that there is almost a systematic deviation between the simulation results and the experimental results (Muhammad et al., 2009) but when considering the experimental results by Paul and Mandal (2006b) they are of the same order as the simulations but the slope is different.

Both surface tension simulations seem to be well in line with the experimental results as can be seen from Appendix 4. The results demonstrate that the increase in temperature and in amine concentration decreases surface tension. When taking into account the small scale of the surface tension axis it can be concluded that the simulations and experimental results are corresponding to each other with sufficient accuracy. Heat capacity simulations are also quite well in line with the experimental results within the measured temperature range. As a conclusion from all the physical property simulations it can be concluded that the Aspen Plus models the physical properties of aqueous PZ/MDEA solutions with sufficient accuracy.

14 Modelling of the regeneration efficiency

Regeneration process is consuming most of the energy used in the CO_2 capture process and that is why the understanding of the regeneration process is an important factor when considering the whole process, but of course the performance of the absorber is important too since the concentration of the rich amine stream affects the performance of the stripper, not to mention the overall CO_2 percentage captured in the process. Modelling of the regeneration efficiency and the reboiler duty was performed with the systems presented in Figures 22 and 23. In Figure 22 the system is quite simple since the lean amine solution is not recycled back to the absorber. CO_2 is absorbed by the lean amine solution from flue gas (which composition and flows are presented in Table 17) in an absorber. Both of the feed streams are at the temperature of 50 °C and at atmospheric pressure (101.325 kPa). At the top of the absorber there is a washing section to decrease the amounts of amines in the exiting flue gas stream. Usually the amount of washing liquid varies between 10 m^3/h and 15 m^3/h per cross-sectional area (m^2). In the simulations the amount of water circulation is 30 kg/h in both of the cases just to model the effect of the washing section. The amount of H_2O make-up stream (H2O-MU) is 10 % of the total water circulation i.e. about 3 kg/h of the washing water eddies through the absorber and the whole process. Then the CO_2 rich amine solution is fed via a pump, where the pressure is doubled (202.65 kPa), and a heater, where the temperature is raised to 120 °C, to a stripper where the CO_2 is separated from the amine solution. Connected to the stripper there is a reboiler which provides the energy for the regeneration process and a condenser which decreases the amount of water in the exiting CO_2 stream.

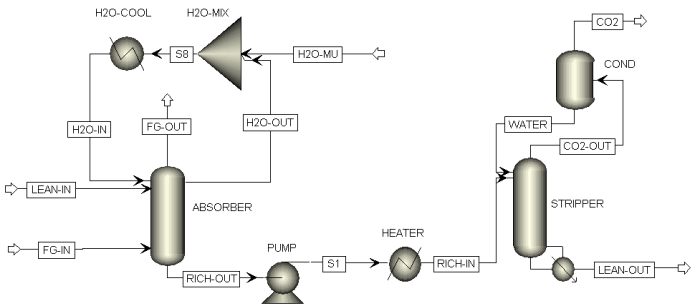

Figure 22 Simulation flowsheet in Aspen Plus with a water washing section in the absorber.

In Figure 23 the same process is presented without the washing section in the absorber. The results of the two processes with and without the washing section are compared to figure out the benefits of the washing at the top of the absorber.

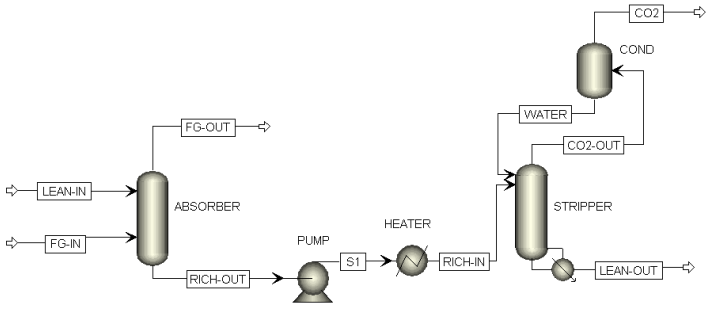

Figure 23 Simulation flowsheet in Aspen Plus without a water washing section in the absorber.

The initial parameters used in the PZ/MDEA simulations are presented in Table 16. The columns were not sized in detail, because there was not any specific case or reference junction to be studied. For this reason the parameters were mostly set according to the simulation example provided by Aspen Plus. The simulations were performed with two different amine solutions. At first the composition of the amine solution fed to the absorber was chosen according to Zhang et al. (2001b) so that the total amine concentration of the lean amine solution was 3.0 kmol/m^3 and the mass ratio of MDEA to PZ was 10/1, which results in 0.365 kmol/m^3 PZ and 2.635 kmol/m^3 MDEA (henceforward referred as PZ/MDEA 1) and secondly according to Bishnoi (2000) and Derks (2006) so that the concentrations of PZ and MDEA were 0.6 kmol/m^3 and 4.0 kmol/m^3, respectively (henceforward referred as PZ/MDEA 2).

Performances of the absorber and stripper were investigated by changing the ratio of CO_2 and amine solution fed into the absorber, which also results in a changed loading in the RICH-OUT stream. In all of the simulations the flue gas flow was kept constant (46 kg/h) and the amine flow was varied. The effect of the reboiler duty into the regeneration efficiencies were simulated with a flow ratio which resulted in approximately 90 % CO_2 capture efficiency in the absorber.

Table 16 Configurations used in the PZ/MDEA rate-based simulations.

ABSORBER	RadFrac	Calculation Type	Rate-based Standard convergence
		Rate-based Distillation Setup	Maximum number of iterations 50
		Top Pressure	101.325 kPa
		Number of Stages	20
		Reaction Set	Stages 1-20 P-M-REA (Chapter 11)
		Holdups	Stages 1-20; Liquid holdup 0.0005 m^3
		Packing Type	FLEXIPAC® 250Y, metal
		Column diameter	0.125 m (0.2 m with 0.6 M PZ/4.0 M MDEA)
		Packing section height	0.42 m/15m with washing section 15.42 m without washing section
		Mass Transfer Coefficient Method	HanleyStruc (2010)
		Interfacial Area Method	HanleyStruc (2010)
		Flooding Method	Wallis
		Heat Transfer Coefficient Method	Chilton and Colburn
		Film Resistance Options	Discrxn for liquid film, Film for vapour film
		Discretization Points	5
		Flow Model	VPlug
		Estimates	Temperature estimates at stages 1 and 20, flow estimates when needed
		Convergence	Maximum iterations 50
STRIPPER	RadFrac	Calculation Type	Rate-based Strongly non-ideal liquid/Standard convergence
		Rate-based Distillation Setup	Maximum number of iterations 100
		Top Pressure	202.65 kPa
		Number of Stages	21
		Reaction Set	P-M-REA (Chapter 11); P-M for condenser and reboiler (Chapter 11)
		Holdups	Stages 1-20; Liquid holdup 0.0001 m^3
		Packing Type	FLEXIPAC® 250Y, metal
		Column diameter	0.125 m
		Packing section height	5 m
		Mass Transfer Coefficient Method	HanleyStruc (2010)
		Interfacial Area Method	HanleyStruc (2010)
		Flooding Method	Wallis
		Heat Transfer Coefficient Method	Chilton and Colburn
		Film Resistance Options	Discrxn for liquid film, Film for vapour film
		Discretization Points	5
		Flow Model	VPlug
		Estimates	Temperature and flow estimates for all stages
		Convergence	Maximum iterations 100
CONDENSER	Flash2	Temperature	313.15 K
		Pressure	202.65 kPa
		Reaction Set	P-M (Chapter 11)
PUMP	Pump	Discharge Pressure	202.65 kPa
HEATER	Heater	Outlet Temperature	393.15 K
		Outlet Pressure	202.65 kPa
		Valid Phases	Vapor-Liquid
Convergence		Default Convergence Method for Tears	Broyden
Setup		Flash Error Tolerance	1.00E-06

As can be seen from Table 16 both the absorber and stripper columns were modelled as packed columns. The separation is treated as a mass and heat transfer process in the Aspen Plus Rate-Based distillations. The number of theoretical stages is offered in order

to enable the calculations. The number of stages divides the packing into segments. The segments are used to evaluate mass and heat transfer rates between contacting phases. By providing more stages a more accurate approximation of real structured packing can be achieved. When the number of segments is changed both the temperature and composition profile can change. According to Peng et al. (2002) the number of stages can be considered as a parameter that accounts for back mixing in the distillation column. With extremely small segment, i.e. with large number of stages, no back mixing occurs in the distillation column and the separation succeeds. Solving the rate-based model is always complicated and the addition in the number of theoretical stages may cause convergence problems. In this thesis 20 theoretical stages are used. Numbering of the theoretical stages is usually started from the bottom of the column, but Aspen Plus considers the first theoretical stage to be at the top of the column.

Similar simulation systems were built for aqueous MEA and MDEA solvents to compare the performances with the PZ/MDEA processes. Amine concentrations for the solvents were chosen after typical concentrations used in the literature; 30 % by weight for MEA and 45 % by weight for MDEA (henceforward referred as MEA and MDEA, respectively). In the process using plain MDEA the RICH-IN stream was heated to 120 °C and in the MEA process to 115 °C. Since no detailed sizing was performed with the PZ/MDEA cases the comparison was performed with similar columns. Due to this for example in the case of MEA smaller columns would have been sufficient. When observing the results of the simulations it should be taken into account that the column sizes are not optimized for the certain cases.

14.1 Simulation problems

During the simulation of the CO_2 recovery process there occurred convergence problems especially when using the rate-based calculation method. The simulations were performed with flue gas containing fewer substances than the original plan was. The sulphur oxides, nitrogen oxide and argon were added after the simulation had converged with the simpler system. Nevertheless the extra components slowed the simulation and caused still some convergence problems so it was decided to run the simulations with the flue gas containing only water, nitrogen, carbon dioxide and oxygen, the composition used is presented in Table 17.

Table 17 Flue gas composition used in the modelling.

	kg/h	kmol/h	mol %
N_2	31.9045	1.138898	72.1070
O_2	2.027288	0.0633551	4.0112
CO_2	8.927086	0.202843	12.8426
H_2O	3.141131	0.174359	11.0392
	46	1.579455	100

To help and speed up the overall convergence Murphree efficiencies were set for the absorber and stripper, but the following error occurred: "MURPHREE EFFICIENCY CAN NOT BE USED WITH TRUE SPECIES APPROACH FOR ELECTROLYTIC COLUMNS WHEN USING GIBBS FREE ENERGY TO COMPUTE REACTION EXTENTS". As a conclusion Murphree efficiencies could not be used with the system used in this thesis.

The flash error tolerance was set to 1E-06 to be tighter than in columns (1E-05) to help the overall convergence. The absorber converged relatively easily with the chosen parameters after changing the damping method, depending on the simulation from mild to severe, and increasing the number of maximum iterations. The damping method was also varied in the case of the stripper, but still some convergence problems occurred with it.

In the case used for simulations no internal condenser is used in the RadFrac regeneration column. The stripper converged with the internal partial-vapour condenser in some rare cases. In those cases the CO_2 stream leaving the stripper included a large percentage of water, which is an unwanted feature, but the system was so shaky that even the smallest change in parameters caused the convergence to fail. With the partial-vapour-liquid condenser the stripper column did not converge at all. Due to that an "external" condenser was added by using a flash tank to separate the CO_2 and extra water and the water is returned to the top of the column. Occasionally the convergence method for the stripper was set as strongly non-ideal liquid which means that Aspen Plus uses the non-ideal algorithm and the standard initialization method, otherwise the standard convergence method was used. The damping level was varied when calculating the regeneration column as mentioned before and the number of maximum iterations was increased to 100. Estimates of temperature and flows were used to aid convergence.

First two temperature estimates were given after which the system was run with the equilibrium calculation method for the regeneration column. From these results estimates of temperatures and flows were generated for all stages and then the calculation method for regeneration column was changed to rate-based.

A countercurrent model would be the best flow model for packed columns, but these simulations did not converge with that flow model. When using the countercurrent model the RateSep convergence iterations showed an Err/Tol which reached a fixed value. Even the changing of the reaction condition factor from the default 0.5 to 1.0 did not solve the problem but it still reached a fixed value. So instead of the countercurrent flow model the Vplug is used as the flow model in both of the columns. When dealing with convergence problems the Mixed flow model might be useful since it is simpler and easier to convergence than the Vplug. The Discrxn model is used to calculate the film resistance in the liquid phases. This model discretizes the film and calculates reaction rates in each film region and usually it is used with fast reactions. Instead of the Discrxn model the Filmrxn model, which also considers reactions inside the film and in the bulk phase, might be used.

When performing the simulations with higher MDEA concentrations (0.6 M PZ/ 4.0 M MDEA and only MDEA) configuration problems occurred with the absorber diameter so the diameter was set to 0.2 m after which the simulation converged. Also, when modelling the regeneration efficiency of the process using only MDEA the highest reboiler duty to converge was 11.5 kW with the system including a separate water washing section connected to the absorber.

14.2 Simulation results

14.2.1 Absorber and stripper performances with PZ/MDEA systems

The amount of amine solution feed was varied while the flue gas feed (Table 17) and the reboiler duty were kept constant and the performances of the absorber and stripper were observed. In Figure 24 CO_2 loadings achieved in the absorber with different amine flows are illustrated.

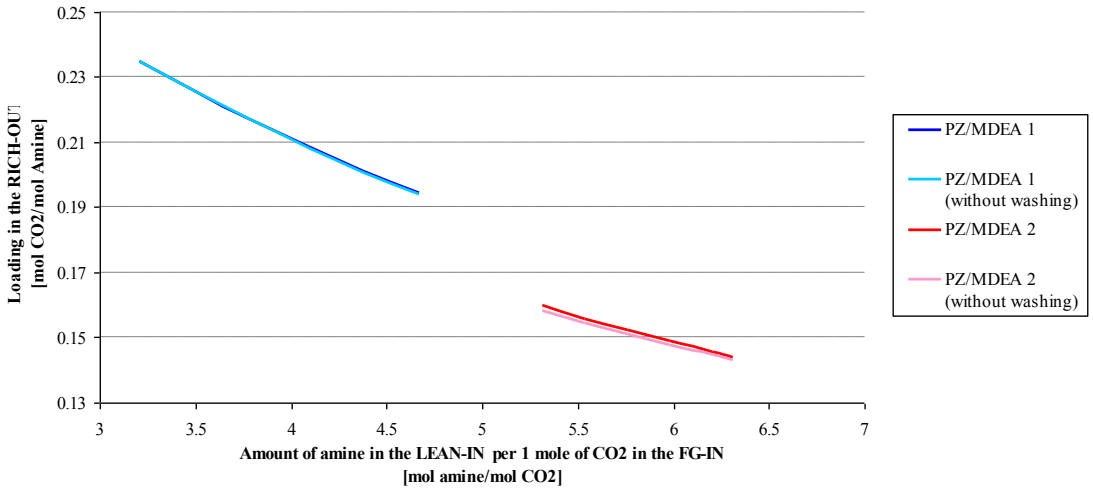

Figure 24 Loading in the RICH-OUT achieved with different feed flows in the absorber with and without the water washing section.

When the amine flow is increased there are more amines per one mole of CO_2 in the absorber. Figure 24 displays that the loading achieved in the absorber decreases while the amine flow is increased. PZ/MDEA 2 results in lower loadings than PZ/MDEA 1. It seems that PZ/MDEA 1 would result in higher loadings in the case where the results are extrapolated to cover the same ratio of amines and CO_2. It can be concluded that with PZ/MDEA 1 one mole of amine captures more CO_2. When observing Figure 24 it can also be noticed that the loading achieved without the water washing section is lower than the loading achieved with the water washing section.

In Figure 25 the CO_2 removal efficiency for the absorber and stripper and the overall removal efficiency are presented as a function of mole ratio of amines and CO_2 in the feeds. As is illustrated in Figure 25 it is evident that the CO_2 capture efficiency in the absorber increases while more amine is fed per one mole of CO_2. When taking this into account while observing Figure 24 it can be concluded that with a low loading in the exiting RICH-OUT stream there is a high CO_2 capture efficiency in the absorber. At the same time it can be seen that the stripper performance decreases while the amount of amines per one mole of CO_2 increases. Thus it can be said that the higher the loading in the RICH-IN, the better the CO_2 recovery in the stripper. The overall CO_2 recovery depends of course on both the CO_2 capture efficiency in the absorber and the CO_2 removal efficiency in the stripper. With similar absorber efficiencies PZ/MDEA 2 results in better overall efficiency since the stripper efficiency seems to be about 2 % higher than with PZ/MDEA 1.

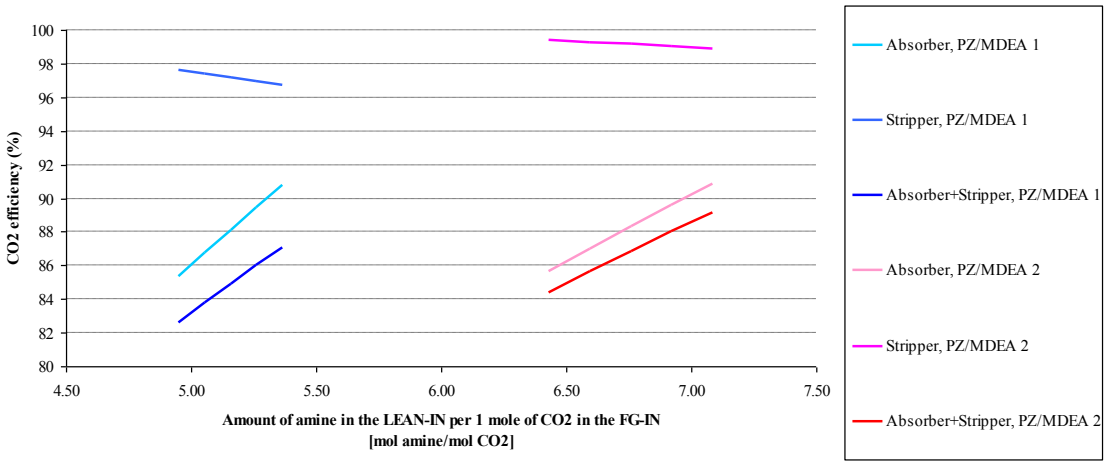

Figure 25 Performance of the CO_2 removal process with the water washing section as a function of mole ratio of amine and CO_2 in the feeds of the absorber. Absorber+Stripper presents the CO_2 capture percentage of the overall process.

The water washing section at the top of the absorber affects the amount of amines in the flue gas exiting the absorber. The effect is made evident in Figure 26. Even a small water circulation (2.47 m^3/h per m^2 in the case of PZ/MDEA 1 and MEA, and 0.97 m^3/h per m^2 in the case of PZ/MDEA 2) more than halves the amount of amines in the FG-OUT. The results of a similar MEA process are presented in the same figure to be able to compare the processes.

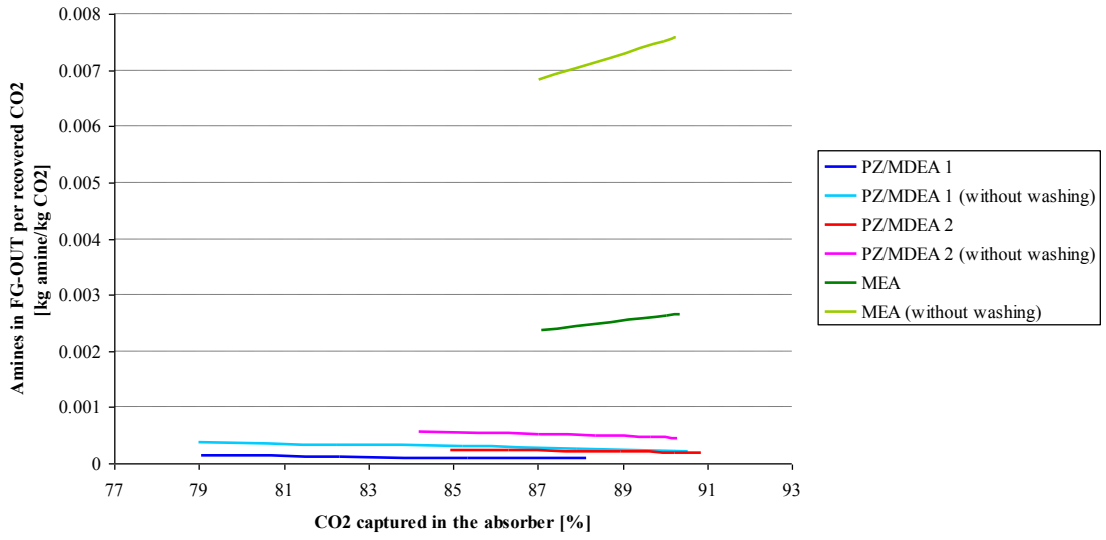

Figure 26 Amines in the exiting flue gas per recovered CO_2 as a function of absorber performance.

Figure 26 shows that with the PZ/MDEA systems the amount of amines exiting the absorber in the FG-OUT stream is significantly smaller than in the case of the MEA

system. An interesting issue to be taken into account is that when the amount of MEA flow is increased to improve the absorber performance the loading decreases where as the amount of amines in the flue gas increases. Due to this behaviour the MEA process was also simulated with a shorter column, which height was 5 m instead of 15 m, in order to see if this behaviour results from the too height column. There was no considerable difference between the results. Somehow in the case of MEA the extra amine solution is released to flue gas. From the environmental point of view the PZ/MDEA 1 system would be better than the PZ/MDEA 2 system.

In Table 18 the calculated amine emissions are summarized. It is assumed that the large scale absorber, which feed is as presented in Table 15, results in similar parameters i.e. that when for example the absorber CO_2 removal efficiency is approximately 90 % or a bit more it results with same amount of amines per captured CO_2 kg in the FG-OUT. In the MEA system without water washing the amine emissions are noticeable bigger than those of the PZ/MDEA 1 and PZ/MDEA 2 systems with water washing. When observing the findings of Figure 26 and Table 18 it should be remembered that in the real process the degradation products of amines can be more volatile than the original ones and they also affect the amount of amines in the flue gas.

Table 18 Amount of amines in the FG-OUT when the amount of FG-IN is as big as in a real coal fired power plant. The mass flow of CO_2 in the FG-IN is then 427680 kg/h. Results marked with * are from the simulations without a water washing section in the absorber.

	CO_2 removal efficiency (%)	Amines in the FG-OUT per kg of captured CO_2 [kg Amine/kg CO_2]	Amines in the exiting flue gas [kg/h]
PZ/MDEA 1	90.79	0.000085	33.0
PZ/MDEA 1*	90.53*	0.000205*	79.4*
PZ/MDEA 2	90.87	0.000192	74.6
PZ/MDEA 2*	90.28*	0.000450*	173.8*
MEA	90.35	0.003255	1257.8
MEA*	90.27*	0.009169*	3539.8*

In Appendix 5 more detailed absorber profiles with and without the separate water washing section are presented. The flow ratio used results in about 90 % of CO_2 capture efficiency in the absorber.

14.2.2 Comparison with MDEA and MEA systems

In addition to the previous results the absorber performance was investigated also with the MEA and MDEA solutions. The simulation scheme was as illustrated in Figure 22.

The results of the MEA and MDEA simulations are compared with the PZ/MDEA results in Figures 27 and 28.

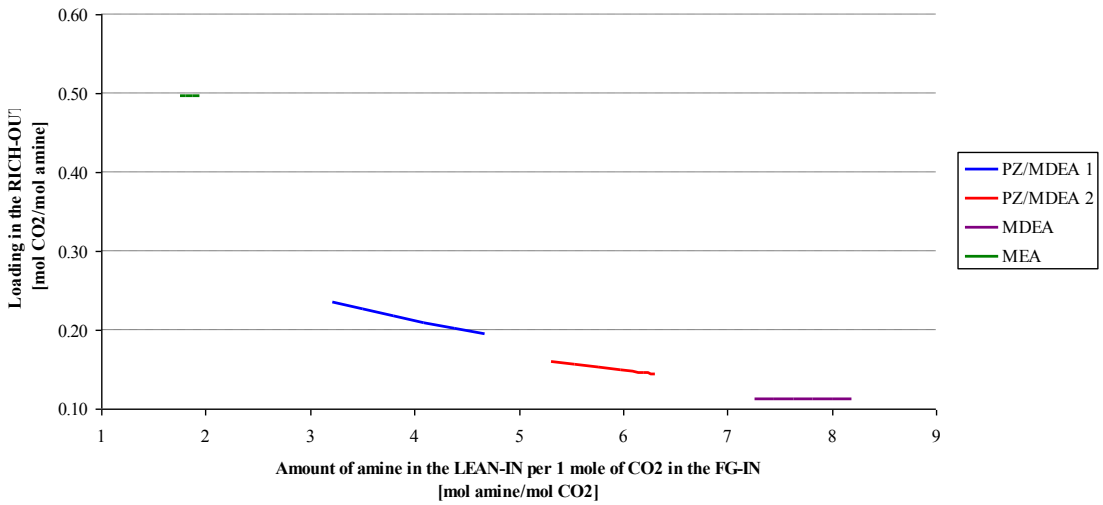

Figure 27 Comparison of the feeds and their loadings in RICH-OUT stream.

From Figure 27 it can be seen that with the MEA the highest loading is achieved where as the MDEA results in the lowest loading. Usually relatively low loadings (α is around 0.20) are preferred since the corrosiveness of the solution increases with the loading. As mentioned before the absorber column is too large (i.e. too effective) for the MEA process. This can also be noticed from the absorber profiles presented in Figures 5 and 6 in Appendix 5. Subsequently the MEA process results in the maximum loading for primary alkanolamines (see page 20). Similarly it can be assumed that the column is too small for the plain MDEA and it results in a low loading regardless of the lean amine flow. These results confirm the fact that the MEA solution can be considered a more effective absorber than the MDEA solution.

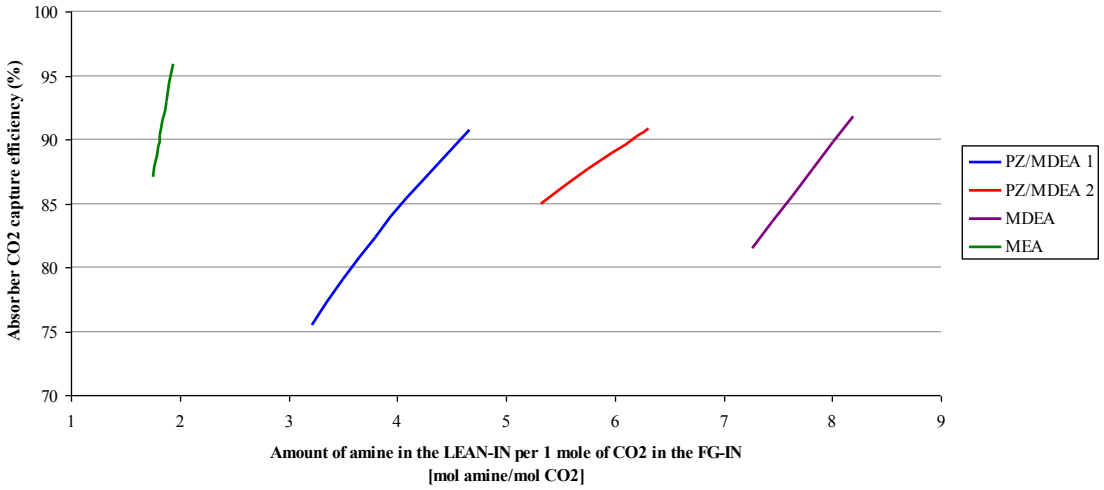

Figure 28 CO_2 capture efficiency in the absorber as a function of mole ratio between amines and CO_2 in the feeds.

With the MEA solution the CO_2 capture efficiency in the absorber is higher than with the PZ/MDEA and MDEA solutions. In addition Figure 28 illustrates that in the presence of piperazine less amine is needed to achieve the same CO_2 capture percentage in the absorber. Thus it can be stated that in the absorber the addition of PZ improves the efficiency and fastens the reactions.

In general around 90 % of CO_2 is captured in the absorber. The flows for further simulations were chosen according to that and the details are gathered to Table 19. The concentration of amines in the lean amine solution varies widely from 30 % to over 50 % by weight. The lean amine solutions fed to the process do not contain any impurities. When comparing the feed specifications in Table 19 it should be noticed that the flow of LEAN-IN is much smaller in the case of MEA and at the same time the loading of the RICH-OUT stream is much higher as could be concluded from Figures 27 and 28.

Table 19 Specifications for the FG-IN and LEAN-IN streams.

Stream ID	FG-IN	PZ/MDEA 1	PZ/MDEA 2	MDEA	MEA
Temperature [K]	323.15	323.15	323.15	323.15	323.15
Pressure [kPa]	101.325	101.325	101.325	101.325	101.325
Total flow [kg/h]	46	320	285	430	75.25
Mass-Frac					
MDEA	0	0.31	0.466	0.45	0
MEA	0	0	0	0	0.3
PZ	0	0.031	0.05	0	0
H_2O	0.068	0.659	0.484	0.55	0.7
CO_2	0.194	0	0	0	0
N_2	0.694	0	0	0	0
O_2	0.044	0	0	0	0
CO_2 captured in the absorber (%)	-	90.79	90.87	89.78	90.27
Loading in RICH-OUT [mol CO_2/mol amine]	-	0.1944	0.144	0.4963	0.1122

One important parameter to describe the regeneration performance is the energy consumption of the stripper i.e. how much energy is needed to recover 1 kg of pure CO_2. The smaller the amount of energy needed the more favourable the process from the economic point of view. The energy consumption of the stripper is in inverse relation to the lean amine loading exiting in the stripper bottom. So the energy consumption per recovered CO_2 increases while the lean-CO_2 loading decreases. The partial pressure of CO_2 diminishes while the loading decreases and this makes the separation difficult at the low loading region.

Sakwattanapong et al. (2005) have presented that when the loading of lean amine solvent exiting the stripper is presented as a function of energy consumption per recovered CO_2 two different regions can be distinguished. The first region can be considered as an unfavourable operation region that consumes excessive energy during solvent regeneration. In this region, recognized at very low loadings, the energy consumption per recovered CO_2 is highly sensitive to the change in lean amine loading. This means that a significant amount of energy is needed for a small change in the lean amine loading. In the second region the energy consumption per recovered CO_2 is less and less sensitive to the change in the lean amine loading. After a certain phase only a small addition in the reboiler duty is required to achieve a noticeable reduction in the lean amine loading. Thus this second region is more favourable as an operating region. In Figure 29 the lean-CO_2 loadings are presented as a function of the energy consumption.

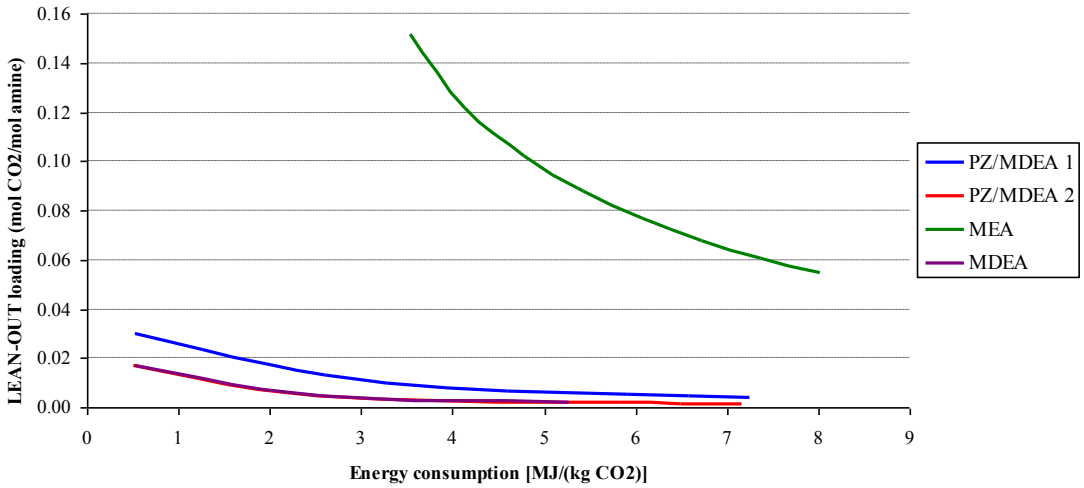

Figure 29 Loading of the lean amine solution exiting from the stripper bottom as a function of energy consumption per recovered CO_2.

The results of the PZ/MDEA 2 and plain MDEA are almost equal. The energy consumption of the PZ/MDEA 2 is slightly smaller. The energy consumption of the PZ/MDEA 1 is a bit larger whereas the energy consumption of the MEA is significantly larger. When considering the concentrations of the amine solutions the order is reasonable. The PZ/MDEA 2 is the most concentrated solution, but because of the PZ content the energy consumption is at the same level than with the little less concentrated plain MDEA. The PZ/MDEA 1 is less concentrated and includes more PZ. Similar findings were achieved in the solubility simulations. The MEA is the least concentrated amine solution but in addition MEA has a higher heat of reaction with CO_2 than MDEA and this causes the large difference in the energy consumption. The stripper CO_2 removal efficiency is directly proportional to the achieved lean amine loading since it describes how many percentages of incoming CO_2 have been stripped out. Due to this high stripper efficiencies are hard to achieve as the extremely low lean-CO_2 contents.

In the next chapter the same process is simulated so that the lean amine solution gained from the stripper is cooled down and returned to the absorber. According to Figure 29 it is chosen that the PZ/MDEA 1 and PZ/MDEA 2 processes are simulated with energy consumption of approximately 4 MJ/ (kg CO_2) that was achieved with the reboiler duty of 8.5 kW. It seems that in that point the PZ/MDEA systems are moving from the district two to district one. The amine solution recycled should be as free from CO_2 as possible; otherwise the absorber efficiency will decrease. In Figure 29 the calculated energy consumption includes only the energy consumed in the reboiler i.e. the reboiler

duty. Energies consumed in the pumps or in other additional process equipments are not taken into account. Detailed stripper profiles with the reboiler duty of 8.5 kW are presented in Appendix 6.

In the literature some references about the energy consumption of the MEA process are presented. For example Kothandamaran (2010) reported reboiler duty of 4.250 MJ/(kg CO_2) for gas from a coal fired power plant with a 85 % CO_2 capture with lean loading. Kothandamaran (2010) has researched that the increase in loading increases the reboiler duty in the case of MEA system; a higher rich loading leads to a lower steam requirement since the equilibrium partial pressure of CO_2 increases with loading and hence, there is less steam that leaves the desorber with the CO_2. Chapel et al. (1999) reported that well designed Econamine FG plants, apparently using MEA, have been proven to use less than 4.2 MJ/(kg CO_2) while Aroonwilas and Veawab (2007) reported a conventional MEA process to use 4.8 MJ/(kg CO_2). The CO_2 capture percentage and the achieved lean amine CO_2 loading have been reported in neither of the references. Due to this the comparison of the results with the literature is impossible. References concerning the reboiler duties in MDEA or PZ/MDEA processes were not found from the literature.

15 Modelling of process with amine circulation

When observing the real amine based CO_2 absorption process, they are always almost closed systems i.e. the amine regenerated in the stripper is returned to the absorber as the lean-in solution. The simulation flow sheet used is presented in Figure 30 below.

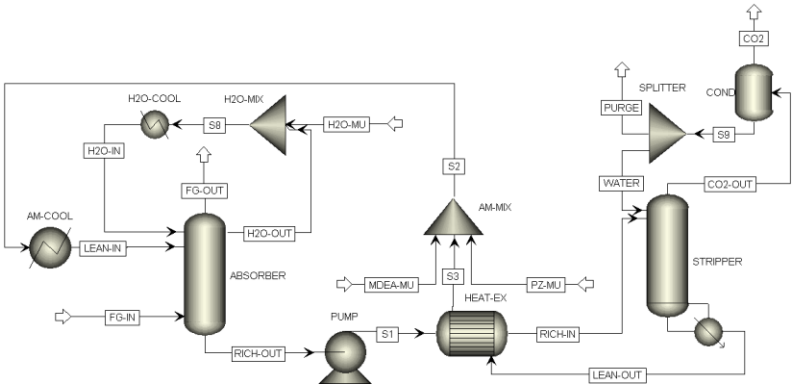

Figure 30 Simulation scheme with closed amine circulation.

The simulation scheme presented in Figure 30 was further built from the simulation scheme presented in Figure 22. The Broyden method was chosen as the default convergence method, but also the direct substitution method could have been used in this case. In order to help the overall convergence the tear convergence tolerance was set to 1E-04 to be looser than in the columns (1E-05) and in the flash convergence (1E-06). It should be noticed that too loose tear convergence tolerance may lead to convergence problems.

Besides the amine circulation there are also some other differences compared to the process scheme presented before. The condensate (S9) exiting the condenser of the stripper is split into two separate streams; PURGE and WATER. The purge stream takes the extra water resulting from the washing section out of the process in addition to the water leaving with FG-OUT and CO2 streams. The amount of the purge stream is determined so that about 10 % of the water circulation in the washing section is renewed. The LEAN-OUT stream heats up the rich-in stream in the heat recovery exchanger (HEAT-EX). It is determined that the temperature difference between the hot outlet stream and the cold inlet stream is 1 °C so that as much energy as possible is used from the LEAN-OUT solution. Then two amine streams are mixed to the flow to make up the MDEA and PZ losses of the process. There are two design specification blocks used to determine the flows of PZ-MU and MDEA-MU so that they are equal to the PZ

and MDEA losses of the process. Amine losses occur within FG-OUT, CO2 and PURGE streams. In the PURGE stream amines can be lost in addition in an ionized form so the total amine was calculated using the WAPP (apparent component mass flow) property set for the total flow of amine in all speciated forms. Also there is a standard balance block to determine the right mass flow rate for the H2O-MU stream so that the water inlets (FG-IN and H2O-MU) and the water outlets (FG-OUT, CO2 and PURGE) are in a mass balance. The LEAN-IN stream is cooled down in AM-COOL to 323.15 K, which was the original temperature of the lean amine solution and also the pressure is decreased to 101.325 kPa from 202.65 kPa, which was the pressure in the stripper. Looser damping methods were used with absorber and stripper than in the previous simulations to enable faster convergence. The amine circulation was built up with the tear stream function of the Aspen Plus. The original LEAN-IN stream was deleted and initial values of it were set as the starting values for the stream exiting the AM-COOL heat exchanger. The stream was connected to the absorber and renamed to a new lean-in stream. In the convergence menu of the Aspen Plus the new LEAN-IN stream was set as a tear stream and then the calculation was performed. Modelling of the whole process was performed with PZ/MDEA 1 and PZ/MDEA 2.

The input specifications of the closed systems are presented in Table 20. From the streams only the FG-IN is really determined. The LEAN-IN streams have been calculated by Aspen Plus, based on the original lean-in streams, which were presented in Table 19. Major difference between Tables 19 and 20 is the CO_2 loading present in the recycled LEAN-IN stream in the closed system. The flows and compositions are almost equal.

Table 20 Specifications for the FG-IN and LEAN-IN streams.

Stream ID	FG-IN	PZ/MDEA 1	PZ/MDEA 2
Temperature [K]	323.15	323.15	323.15
Pressure [kPa]	101.325	101.325	101.325
Total flow [kg/h]	46	321.0351	285.4285
Mass-Frac			
MDEA	0	0.3089	0.4649
PZ	0	0.0324	0.0511
H_2O	0.068	0.6569	0.4834
CO_2	0.194	0.0018	0.0006
N_2	0.694	0	0
O_2	0.044	0	0
CO_2 loading [(mol CO_2)/(mol amine)]	-	0.0212	0.0057

In the case of PZ/MDEA 2 the recycled lean in solution has a lower CO_2 loading; only a bit over a quarter of the CO_2 loading of the LEAN-IN solution in the case of PZ/MDEA 1, based on the better stripper performance.

In Table 21 the key simulation results are presented. With recycled amine streams the CO_2 capture efficiency in the absorber has decreased in both cases. This results from the existing CO_2 loading in the recycled lean solution. In Table 19 it was presented that the absorber efficiencies with similar amine feeds were 90.79 % in the case of PZ/MDEA 1 and 90.87 % in the case of PZ/MDEA 2. The decrease is about 6 % in the case of PZ/MDEA 1 and 3 % in the case of PZ/MDEA 2. The explanation for the bigger decrease in the case of PZ/MDEA 1 is the higher CO_2 loading in the LEAN-IN solution as was presented in Table 20 and the loading of the RICH-OUT stream has increased only slightly when comparing the results in Tables 19 and 21. The stripper CO_2 removal efficiencies are almost 100 %, since there is the lean-CO_2 loading existing, which is not meant to be removed, and is not taken into account in this case. If the stripper efficiency would be less than 100 % there would be CO_2 accumulation in the recycled amine stream.

Table 21 Key simulation results of the closed system.

	PZ/MDEA 1	PZMDEA 2
CO_2 mole fraction in FG-OUT	0.0219	0.0165
CO_2 absorber efficiency (%)	84.55	88.07
CO_2 stripper efficiency (%)	99.94	99.94
CO_2 recovery (%)	84.50	88.02
Loading of RICH-OUT [(mol CO_2)/(mol amine)]	0.2022	0.1452
Stripper Reboiler duty [kW]	8.5	8.5
Stripper Condenser duty [kW]	-4.64	-3.95
Specific Energy Requirement of The Reboiler [MJ/(kg CO_2)]	4.06	3.89
Make-up H_2O [kg/h]	2.7061	3.0055
Make-up MDEA [kg/h]	0.0033	0.0045
Make-up PZ [kg/h]	0.0002	0.0002
Heat recovery exchanger duty [kW]	20.24	16.71

The cyclic capacity of the solvent can be calculated from the rich and lean amine solutions, as mentioned in Chapter 3.2. The information needed is presented in the Tables above. In the case of PZ/MDEA 1 the cyclic capacity is 0.18 (mol CO_2)/ (mol amine) and in the case of PZ/MDEA 2 it is 0.14 (mol CO_2)/ (mol amine).

The make-up streams presented in Table 21 are keeping the process in balance. The make-up H_2O stream is determined with the balance block and the amine make-up

streams are determined with the design specs as explained before. In the case of PZ/MDEA 2 there is more water in the FG-OUT so the amount of make-up water is larger than in the case of PZ/MDEA 1 even though the amine circulation is larger with the PZ/MDEA 1. Similarly there are more amines in the purge stream of PZ/MDEA 2 so the MDEA make-up stream is larger. Detailed stream results of the PZ/MDEA 1 are presented in Appendix 7 and the results of PZ/MDEA 2 are presented in Appendix 8. The heat recover exchanger duty in Table 21 represents the duty of the heat exchanger where the hot lean amine solution exiting the stripper column heats up the rich amine solution exiting the absorber column. The flows in the case of PZ/MDEA 1 are bigger than in the case of PZ/MDEA 2 and the heat exchanger results in a higher duty.

Because the energy consumption of the regeneration process has gained interest in this thesis, the most important issue to be taken into account from Table 21 is that PZ/MDEA 2 has over 3.5 % better CO_2 recovery than PZ/MDEA 1 and at the same time it has 0.17 MJ smaller specific energy requirement of the reboiler per 1 kg of recovered CO_2.

In addition to the key simulation results it is interesting to see if the amount of amines in the exiting flue gas changes and if there is some amine accumulation in the water circulation after closing the system. In Table 22 the mass fractions of the H2O-OUT streams before and after closing the system are compared. The amines in the FG-OUT are discussed in Chapter 15.3.

Table 22 Comparison of the mass fraction of H2O-OUT stream before and after closing the amine circulation.

	PZ/MDEA 1	PZ/MDEA 1 (before circulation)	PZ/MDEA 2	PZ/MDEA 2 (before circulation)
Mass-Frac				
MDEA	0.000172	0.000232	0.000489	0.000507
PZ	0.000032	0.000048	0.000048	0.000049
H_2O	0.999667	0.999569	0.999222	0.999212
CO_2	0.000117	0.000138	0.000230	0.000220
N_2	0.000011	0.000011	0.000011	0.000010
O_2	0.000001	0.000001	0.000001	0.000001

Table 22 shows that actually the mass fraction of amines in the H2O-OUT decreases after closing the amine circulation, so no accumulation of amines into the water circulation can be detected. The decrease in the amine mass fraction in the water

circulation may be due to the fact that in the lean amine solution, which is circulated, there are more substances as ions than in the lean solution which would be fed as a raw material to the process. The amount of other substances in the washing water also remains constant except that with PZ/MDEA 2 after closing the system the mass fraction of nitrogen in the water circulation is 1E-6 bigger.

Temperature profiles of the absorber are illustrated in Figure 31. The figure validates that there is some heat evolved due to the physical solution and the exothermic reactions. Both of the inlet streams are fed at the temperature of 323.15 K as well as the circulated washing water. The water washing section starts from the top of the absorber and continues until the actual absorber packing starts at 0.42 m. The highest temperatures achieved in the absorbers are around 348 K in the case of the PZ/MDEA 2 and 346 K in the case of the PZ/MDEA 1. The highest temperatures are achieved in the upper parts of the column. Temperature difference between the two systems results from the differences between the lean amine solutions.

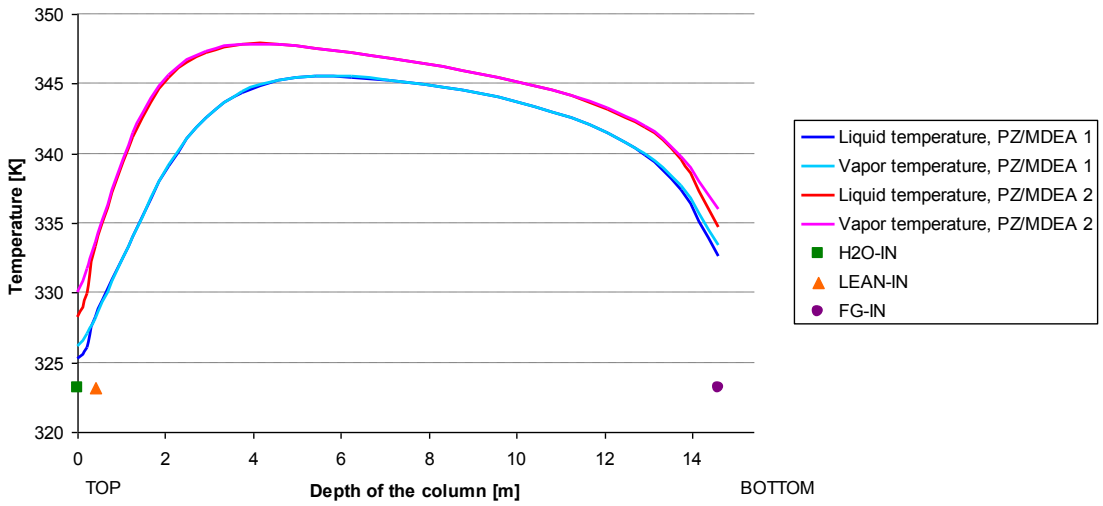

Figure 31 Temperature profiles of the absorbers. Washing water is fed to the top and removed from the depth of 0.21 m. The lean amine solution is fed to the depth of 0.42 m and flue gas to the depth of 14.59 m. The Rich amine solution is taken out from the bottom and the exiting flue gas from the top.

Temperature profiles of the stripper are presented in Figure 32. Reactions occurring in the stripper are endothermic so heat is generated only at the bottom of the stripper in the reboiler. The duty of the reboiler is the same in both cases. Temperatures above 393.15 K are really sensitive to thermal degradation of amines. Figure 32 illustrates that

the temperature rises above that close to the reboiler. This may cause thermal degradation and the formation of heat stable salts.

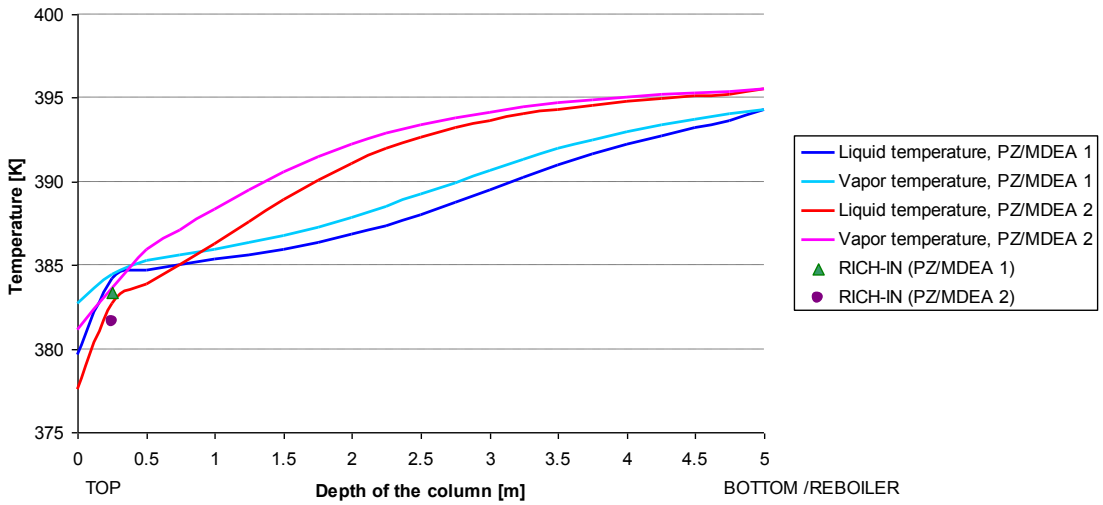

Figure 32 Temperature profiles of the strippers. The rich solution is fed to the depth of 0.25 m. The overhead product to the condenser is removed from the top and the condensate (WATER) is returned to the top at the temperature of 313.15 K. The lean amine solution is taken out from the bottom of the column from the reboiler.

Vapour stream rich in CO_2 is taken out from the top of the regeneration column (CO2-OUT) from where it is further fed to condenser to remove extra water and possible impurities. Recovered CO_2 which is going for further handling or storage is the vapour stream from the condenser (CO2) the extra water in the recovered CO_2 in order to prevent corrosion and formation of ice and hydrates in the further treatments. The quality requirements for the recovered CO_2 are set according to the transport and storage methods, but some approximate figures are gathered for example by Teir et al. (2009). The mole fractions of the streams before and after the condenser are presented in Table 23.

Table 23 Mole fraction of the recovered CO_2 before and after the condenser.

Stream ID	PZ/MDEA 1 CO2	CO2-OUT	PZ/MDEA 2 CO2	CO2-OUT
Total flow [kg/h]	7.6653	14.1371	7.9832	13.4716
Mole fractions				
MDEA	5.06E-12	0.000134	1.01E-11	0.000182
PZ	5.55E-13	1.04E-05	5.92E-13	7.87E-06
H2O	0.037032	0.679444	0.037026	0.63398
CO2	0.962348	0.320206	0.962557	0.365673
N2	0.000563	1.87E-04	0.000379	0.000144
O2	5.63E-05	1.87E-05	3.76E-05	1.43E-05

Teir et al. (2009) have reported that the amount of volatile compounds (N_2, O_2, Ar, H_2 and CH_4) should be less than 0.2-4 %, the amount of water less than 20-500 ppm, and the amount of CO_2 more than 95.5 %. In addition there are limitations given for the amount of hazardous compounds (H_2S, CO) and sulphur and nitrogen oxides (NO_x, SO_2). No recommendation for the amine content was found. The purity of recovered CO_2 fulfils the approximate figures given for the volatile compounds instead the amount of water is still, after the condenser, way more than it should be. The mole fraction of carbon dioxide in the streams going for further processing is over 96 % in both cases which is an acceptable concentration and in addition the amount of amines is extremely low.

15.1 About energy consumption

To clarify the order of the energy consumption in the stripper Figure 33 presents how three pumps are added to the process scheme.

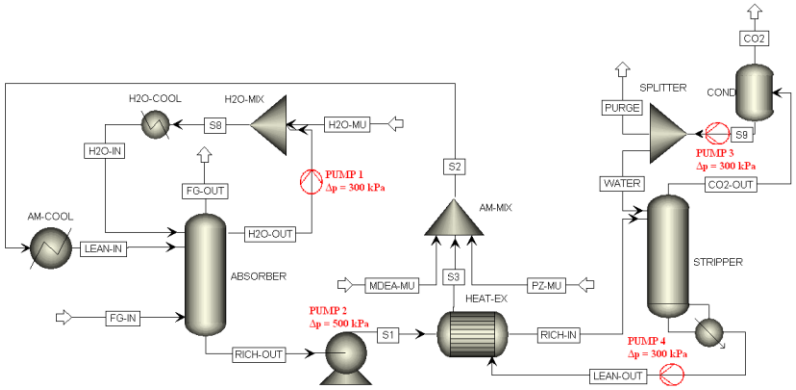

Figure 33 Process scheme with three additional pumps.

The locations of the pumps are chosen according to the true processes. The pressure demands for pumps are roughly estimated by taking into account the pressure

differences and equipments like control valves. Other terms affecting the lifting height like frictional losses are not taken into account. The flue gas fan is not taken into account either. The power demand of the pump can be calculated with the help of efficiency, which takes into account all the losses from the power cable to the pump shaft, as follows:

$$P_E = \frac{\dot{V} \cdot \Delta p}{\eta_{TOT}} \tag{102}$$

where P_E is the electrical power of the pump [W],
$\dot{V}$ is the volumetric flow [m^3/s],
Δp is the pressure difference [Pa], and
η_{TOT} is the efficiency [-].

In Table 24 the energy demands of the pumps presented in Figure 33 are calculated by using Equation (102). Originally the flue gas flow was 46 kg/h but the calculations are performed assuming that the mass flow of CO_2 in the FG-IN is 427680 kg/h, which corresponds to the flow from a true power plant. The increase is taken into account by multiplying every stream with a factor 9297.4.

Table 24 Energy demands of the pumps calculated according to Equation 102.

	PZ/MDEA 1			
	PUMP 1	PUMP 2	PUMP 3	PUMP 4
η_{TOT}	0.6	0.6	0.6	0.6
Δp [kPa]	300	500	300	300
V [m^3/s]	7.07E-02	8.27E-01	1.69E-02	8.63E-01
P_E [kW]	35.3327	689.0185	8.4340	431.3964
Energy consumption per day [MJ]	3052.7427	59531.1965	728.6953	37272.6467
	PZ/MDEA 2			
	PUMP 1	PUMP 2	PUMP 3	PUMP 4
η_{TOT}	0.6	0.6	0.6	0.6
Δp [kPa]	300	500	300	300
V [m^3/s]	7.08E-02	7.29E-01	1.43E-02	7.64E-01
P_E [kW]	35.3978	607.5217	7.1507	382.0183
Energy consumption per day [MJ]	3058.3657	52489.8730	617.8239	33006.3825

In the process simulated in this chapter PZ/MDEA 1 would recover 8673350.4 kg of CO_2 per day and it makes the specific energy requirement of the reboiler about 3.52E+7 MJ/d whereas PZ/MDEA 2 would recover 9034654.5 kg of CO_2 per day resulting in the

specific energy requirement of the reboiler of about 3.51E+7 MJ/d. PZ/MDEA 2 recovers over 15000 kg more CO_2 per day with a slightly smaller specific energy requirement and a smaller energy requirement of the pumps.

In the case of PZ/MDEA 1 the energy needed in pumps is only about 0.28 % of the total energy consumption when taking into account the reboiler and the pumps. The same percentage for PZ/MDEA 2 is about 0.25 %. The energy requirement per kg of recovered CO_2 is 4.07 MJ in the case of PZ/MDEA 1 and 3.90 MJ in the case of PZ/MDEA 2. The addition of the pumps increases the energy requirement per kg of CO_2 about one hundredth of a MJ. Above all these results support the theory that the energy consumption of the CO_2 capture process is highly dependent on the regeneration process. Plant economics of the CO_2 recovery unit have been discussed in the literature for example by Tellini and Manenti (2012).

15.2 Salt formation

As discussed in Chapter 3 the thermal degradation and the salt formation are important issues to be taken into account in the real process. Thermal degradation restricts the temperature used in the regeneration process. Closmann et al. (2009) have investigated that 7 m MDEA/2 m piperazine blend is resistant to thermal degradation up to 120 °C at a loading of 0.2. Since the concentration used in this study is different it is assumed that thermal degradation occurs and at the same time heat stable salts are formed although the flue gas fed to the process does not contain any impurities. The heat-stable salts must be removed from the process to prevent them from accumulation. An additional purge stream (PURGE-2) to remove these heat-stable salts is added to the process after the regeneration of the amine as can be seen in Figure 34. In the process descriptions this process unit is usually referred as the amine reclaimer. In addition in this simulation the flow in the washing section is 10 m^3/h per cross-sectional area m^2 i.e. about 310 kg/h (PZ/MDEA 2_2). In the previous simulations the renewal of the washing stream was about 10 %, but in this case only 1 % of the washing water is constantly renewed due to the convergence problems in the simulation. With bigger purge streams the lean-in flow decreased in every iteration round, which caused that no mass balance was achieved in separate process units and the convergence was not achieved. Although the design specs and the water balance were determined. In the absorber the desired CO_2 capture efficiency is about 90 %. Since the efficiencies stayed below that in the previous

simulations the amine circulation was increased to 310 kg/h to achieve the goal (PZ/MDEA 2_3).

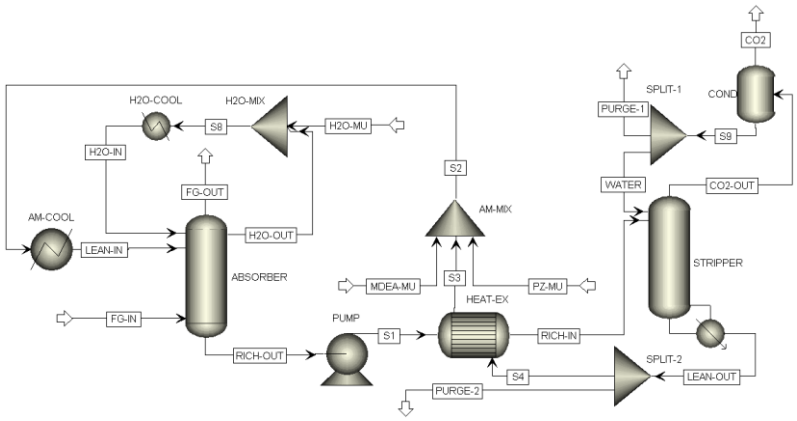

Figure 34 Process scheme with the additional purge stream (PURGE-2) for the removal of the heat-stable salts.

The amount of amines which forms heat-stable salts in the process and are useless in the recycling is impossible to estimate since the simulation base does not include the information needed to calculate the formation. As mentioned in the previous chapter the increase in the flows of the purge streams caused convergence problems. Due to that the amount of the PURGE-2 is only about 1 % of the LEAN-OUT stream. Feed specifications and the key simulation results are presented in Tables 25 and 26. The specifications for the FG-IN stream are the same as in Table 20.

From Tables 26 and 27 it can be calculated that in the case of PZ/MDEA 2_2 there is about 132.0 kg/h of MDEA in the LEAN-IN circulation stream of which 1.05 % is renewed constantly and the circulation of PZ is about 14.4 kg/h of which 1.05 % is renewed constantly where as in the case of PZ/MDEA 2_3 the same numbers are about 144.3 kg/h for MDEA with the renewal state of 0.96 % and about 16.0 kg/h for PZ with the renewal state of 0.94 %. With the state of renewal used in the simulations the amount of amines forming heat stable salts should be under 1 % of the total amount of amines in order to prevent the heat stable salts from accumulating into the process.

When comparing the results of PZ/MDEA 2 in Table 21 and the results of PZ/MDEA 2_2 in Table 26 it can be concluded that the increase in the washing water worsens the results slightly. The increase in the amine flow (PZ/MDEA 2_3) increased the absorber CO_2 capture efficiency close to 90 %, but since the reboiler duty was kept constant the

stripper efficiency decreased 0.04 % and raised the amine loading in the LEAN-IN solution to 0.0087 (mol CO_2)/(mol amine).

Table 25 Specifications for the FG-IN and LEAN-IN streams.

Stream ID	LEAN-IN PZ/MDEA 2_2	LEAN-IN PZ/MDEA 2_3
Temperature [K]	323.15	323.15
Pressure [kPa]	101.325	101.325
Total flow [kg/h]	285.3432	310.6203
Mass-Frac		
MDEA	0.4625	0.4647
PZ	0.0503	0.0514
H_2O	0.4857	0.4829
CO_2	0.0014	0.0010
N_2	0	0
O_2	0	0
CO_2 loading [(mol CO_2)/(mol amine)]	0.0059	0.0087

The specific energy requirement of the reboiler decreases when the amine circulation is increased. As a result of the amine increase the absorber efficiency is improved and the total CO_2 recovery process is improved and furthermore the amount of energy needed per recovered kg of CO_2 is decreased and also the fraction of CO_2 in the exiting flue gas stream (FG-OUT) is decreased. The mass fraction of carbon dioxide in the CO2 stream is almost unchanged when comparing the results of Tables 23 and 26. The increase in the amount of washing in the absorber does not affect to the final purity of CO_2.

Table 26 Key simulation results of the process scheme presented in Figure 36.

	PZ/MDEA 2_2	PZ/MDEA 2_3
CO_2 mole fraction in FG-OUT	0.0170	0.0146
CO_2 absorber efficiency (%)	88.01	89.80
CO_2 stripper efficiency (%)	99.94	99.90
CO_2 recovery (%)	87.96	89.71
Loading of RICH-OUT [mol CO_2/mol Amine]	0.1454	0.1394
Stripper Reboiler duty [kW]	8.5	8.5
Stripper Condenser duty [kW]	-3.77	-3.65
Specific Energy requirement of the reboiler [MJ/kg CO_2]	3.90	3.82
Makeup H_2O [kg/h]	2.6396	2.4175
Makeup MDEA [kg/h]	1.3902	1.3898
Makeup PZ [kg/h]	0.1506	0.1506
Heat recovery exchanger duty [kW]	16.62	17.79
CO_2 mass fraction in CO2	0.9842	0.9842

Detailed stream results of the most important streams of PZ/MDEA 2_2 are presented in Appendix 9 and of PZ/MDEA 2_3 the important streams are presented in Appendix 10.

15.3 Amines in the exiting flue gas

In Figure 26 the amount of amines in the FG-OUT per CO_2 captured in the absorber was presented as a function of absorber performance. The amount of amines in the FG-OUT was less than 0.0003 kg of amine per kg of captured CO_2 in the case of the PZ/MDEA systems with washing. The simulations in Chapter 14 were performed with the same parameters i.e. the same inlet stream specifications and the same amount of washing where as the simulations in this chapter were performed with a bigger washing stream and with bigger washing and amine streams. The amount of LEAN-IN solution was specified so that approximately 90 % of the CO_2 capture was achieved in the absorber. The amounts of amines in the FG-OUT streams are presented in Table 27. Table 28 presents three different results of PZ/MDEA 2; PZ/MDEA 2 represents the case in Chapter 14, PZ/MDEA 2_2 represents the case where the amount of washing stream is increased 310 kg/h, but the amount of the inlet stream is the same as in the case of PZ/MDEA 2. The PZ/MDEA 2_3 represents the case where the washing circulation is 310 kg/h and the amount of the inlet flow was specified so that 90 % of the absorber efficiency is achieved.

Table 27 Amount of amines in the FG-OUT.

	PZ/MDEA 1	PZ/MDEA 2	PZ/MDEA 2_2	PZ/MDEA 2_3
CO_2 captured in the absorber [kg/h]	7.548271	7.861668	7.857058	8.016241
MDEA in FG-OUT [kg/h]	0.000467	0.001317	0.001636	0.001332
PZ in FG-OUT [kg/h]	0.000065	0.000104	0.000134	0.000111
Amines in FG-OUT per CO_2 captured in the absorber [(kg Amine)/(kg CO_2)]	0.000070	0.000181	0.000225	0.000180

According to the results presented in Table 27 the amine circulation diminishes the amount of amines in the FG-OUT stream when comparing the results in Table 27 and Figure 26. Also the amine emissions in the case of PZ/MDEA 1 are smaller than in the cases of PZ/MDEA 2. A really interesting thing in the results is that actually the amount of amines in the FG-OUT increases while the washing is increased. This can be noticed in Table 28 when comparing the results of PZ/MDEA 2 and PZ/MDEA 2_2. There is no clear reason for this kind of behaviour since the key simulation results of these two cases are really close to each other. The differences are only some hundredths of the given values. Only bigger difference between PZ/MDEA 2 and PZ/MDEA 2_2 is that with larger washing there are more amines in the circulating water. When the amount of

lean amine solution is increased, (PZ/MDEA 2_3), the amount of amines in the FG-OUT returns to the same level as in the case of PZ/MDEA 2. The amount of amines in FG-OUT per CO_2 captured in the absorber is smaller in the case of PZ/MDEA 2_3 since the absorber efficiency is increased and more CO_2 is captured in the absorber. As mentioned in Chapter 3.2.3 Svendsen et al. (2011) have reported that with the washing section in the absorber amount of amines in the exiting flue gas could be decreased to as low level as 0.01-0.05 ppm. In the case of PZ/MDEA 1 the achieved level is about 3 ppm and in the case of PZ/MDEA 2_3 the level is about 9 ppm on the molarity basis. The reason for this might be the fact that the washing circulation is not renewed enough.

16 Conclusions and proposals for further studies

In this work the ability of Aspen Plus V7.3.2 to model the CO_2 capture process with mixed PZ and MDEA solutions was investigated.

The solubility of CO_2 into the amine solution at equilibrium was investigated with a flash tank. It was concluded that the simulation results corresponded to the literature values relatively well especially with lower loadings which are more interesting in this case. Nevertheless it was impossible to find clear consistency from the solubility simulations since depending on the amine concentrations and temperature the simulated partial pressures were either bigger or smaller than the literature values. In certain cases the simulation results were also almost equal to the literature values.

Some of the reactions occurring in the alkanolamine absorption are so fast that it can be assumed that they reach chemical equilibrium and some of the reactions are kinetically controlled. Reactions 34, 38, 88, 90 and 92 are handled as equilibrium reactions also in the rate-based model. There are deviations between the results of the equilibrium constant simulations and the correlations given in the literature. The deviations occurred mainly with reactions including piperazine but also with all the reactions when the temperature was raised above 100 °C. This deviation may cause disturbances in the regeneration column which is operated at high temperatures.

The deviation between the literature values and the physical property simulation results varied depending on the amine concentration and temperature. However the deviation is not too large so consequently it can be stated that Aspen Plus models the physical properties of unloaded amine solutions with a sufficient accuracy.

Since there is no experimental data available on the real PZ/MDEA processes and there were a lot of assumptions and simplifications in the process simulations, the validity of the simulation results is debatable. Despite, the simulation results are still promising. PZ accelerates the absorption of CO_2 into MDEA without increasing the energy consumption in the regeneration column too much. The energy requirement of the pumps is so small compared to the specific energy requirement of the reboiler that from the energy usage point of view it is more beneficial to use a bigger flow of PZ/MDEA

than a small flow MEA. In the case of PZ/MDEA systems low lean amine CO_2 loadings can be achieved with acceptable energy requirements and this enables the lean amine solution recycling. Amine emissions from the top of the absorber are smaller when using PZ activated MDEA solutions than when using MEA solutions. With an ordinary condenser at the top of the stripper column the CO_2 purity can be raised to an acceptable level. Only the amount of water should be further decreased.

In order to improve the validity of the results some further studies should be performed. An optimal ratio and concentration of PZ and MDEA are important so that the amine consumption could be minimized. The optimum should be determined according to the absorber and stripper performances, but in addition it should take into account the decomposition and the emissions. The optimal cyclic capacity of the PZ/MDEA system should be determined in order to avoid too effective stripper performance. The solubility of CO_2 into the PZ/MDEA solutions in the stripper conditions have gained too few interest in spite of the fact that regeneration of the amine solution and desorption of CO_2 are as important factors of the process as the CO_2 absorption. The accuracy of the equilibrium constants of the piperazine reactions should also be checked.

In this work it was assumed that there are some heat stable salts formed in the process but the thermal degradation of amines was not taken into account. To improve the simulation model the formation of HSS should be included in the process as well as the thermal degradation of amines. The flue gas to be treated always includes some impurities. To bring the simulation to bear reality it must be known how the impurities affect the amine circulation. Some other questions can be arisen such as; Are they affecting the circulation rate by reacting with amines? Are they accumulated in the process or can they be removed similarly as the degradation products?

It was proven that the washing section at the top of the absorber decreases the amine emissions. To be able to optimize the washing it should be studied which is the optimal flow for the washing water. It should be known how the degradation products and other impurities are acting in order to know how big portion of the washing water should be renewed constantly. The effect of the number stages used in the simulations of packed columns should be checked. With smaller segments more valid approximation of a real structured packing would be achieved but meanwhile it could cause severe convergence problems. Last but not least the optimal sizing for the columns should be performed.

References

Ahmady, A., Hashim, M. A. & Aroua, M. K. (2012) Kinetics of Carbon Dioxide absorption into aqueous MDEA + [bmim][BF_4] solutions from 303 to 333 K. *Chemical Engineering Journal,* 200–202**,** 317-328.

Al-Ghawas, H. A., Hagewiesche, D. P., Ruiz-Ibanez, G. & Sandall, O. C. (1989) Physicochemical properties important for carbon dioxide absorption in aqueous methyldiethanolamine. *Journal of Chemical & Engineering Data,* 34**,** 385-391.

Appl, M., Wagner, U., Henrici, H. J., Kuessner, K., Volkamer, K. & Fuerst, E. (1982) Removal of CO_2 and/or H_2S and/or COS from gases containing these constituents. United States, BASF Aktiengesellschaft (DE).

Arcis, H., Rodier, L., Ballerat-Busserolles, K. & Coxam, J.-Y. (2009) Modeling of (vapor+liquid) equilibrium and enthalpy of solution of carbon dioxide (CO_2) in aqueous methyldiethanolamine (MDEA) solutions. *The Journal of Chemical Thermodynamics,* 41**,** 783-789.

Aroonwilas, A. & Veawab, A. (2007) Integration of CO_2 capture unit using single- and blended-amines into supercritical coal-fired power plants: Implications for emission and energy management. *International Journal of Greenhouse Gas Control,* 1**,** 143-150.

Aspen Technology (2010-2012). Rate-Based Model of the CO_2 Capture Process by Mixed PZ and MDEA Using Aspen Plus. Burlington, MA, USA: Aspen Technology, Inc. Available: http://www.aspentech.com [Accessed August 2012].

Astarita, G. (1967) *Mass transfer with chemical reaction,* Amsterdam, Elsevier.

Astarita, G., Savage, D. W. & Bisio, A. (1983) *Gas treating with chemical solvents,* New York, N.Y. , Wiley-Interscience.

Austgen, D. M., Rochelle, G. T., Peng, X. & Chen, C. C. (1989) Model of vapor-liquid equilibria for aqueous acid gas-alkanolamine systems using the electrolyte-NRTL equation. *Industrial & Engineering Chemistry Research,* 28**,** 1060-1073.

Baugh, L. S., Kortunov, P. & Siskin, M. (2012) Ionic Liquids for Removal of Carbon Dioxide. IN APPLICATION, U. S. P. (Ed.) United States, EXXONMOBIL RESEARCH AND ENGINEERING COMPANY

Bishnoi, S. (2000) *Carbon Dioxide Absorption and Solution Equilibrium in Piperazine Activated Methyldiethanolamine.* Ph.D. Dissertation, The University of Texas at Austin.

Bishnoi, S. & Rochelle, G. T. (2000) Absorption of carbon dioxide into aqueous piperazine: reaction kinetics, mass transfer and solubility. *Chemical Engineering Science,* 55**,** 5531-5543.

Bishnoi, S. & Rochelle, G. T. (2002a) Absorption of carbon dioxide in aqueous piperazine/methyldiethanolamine. *AIChE Journal,* 48**,** 2788-2799.

Bishnoi, S. & Rochelle, G. T. (2002b) Thermodynamics of piperazine/methyldiethanolamine/water/carbon dioxide. *Industrial & Engineering Chemistry Research,* 41**,** 604-612.

Boll, W., Hochgesand, G., Higman, C., Supp, E., Kalteier, P., Müller, W.-D., Kriebel, M., Schlichting, H. & Tanz, H. (2000) Gas Production, 3. Gas Treating. *Ullmann's Encyclopedia of Industrial Chemistry.* Wiley-VCH Verlag GmbH & Co. KGaA.

Bonenfant, D., Mimeault, M. & Hausler, R. (2005) Comparative analysis of the carbon dioxide absorption and recuperation capacities in aqueous 2-(2-aminoethylamino)ethanol (AEE) and blends of aqueous AEE and N-methyldiethanolamine solutions. *Industrial & Engineering Chemistry Research,* 44**,** 3720-3725.

Bonenfant, D., Mimeault, M. & Hausler, R. (2007) Estimation of the CO_2 absorption capacities in aqueous 2-(2-aminoethylamino)ethanol and its blends with MDEA and TEA in the presence of SO_2. *Industrial & Engineering Chemistry Research,* 46**,** 8968-8971.

Böttger, A., Ermatchkov, V. & Maurer, G. (2009) Solubility of carbon dioxide in aqueous solutions of N-methyldiethanolamine and piperazine in the high gas loading region. *Journal of Chemical & Engineering Data,* 54**,** 1905-1909.

Chang, H. T., Posey, M. & Rochelle, G. T. (1993) Thermodynamics of alkanolamine-water solutions from freezing point measurements. *Industrial & Engineering Chemistry Research,* 32**,** 2324-2335.

Chapel, D. G., Mariz, C. L. & Ernest, J. (1999) Recovery of CO_2 from Flue Gases: Commercial Trends. *Canadian Society of Chemical Engineers annual meeting.* Saskatchewan, Canada.

Chen, C.-C., Britt, H. I., Boston, J. F. & Evans, L. B. (1982) Local composition model for excess Gibbs energy of electrolyte systems. Part I: Single solvent, single completely dissociated electrolyte systems. *AIChE Journal,* 28**,** 588-596.

Chen, C.-C. & Evans, L. B. (1986) A local composition model for the excess Gibbs energy of aqueous electrolyte systems. *AIChE Journal,* 32**,** 444-454.

Chen, X. (2011) *Carbon dioxide thermodynamics, Kinetic and mass transfer in aqueous piperazine derivates and other amines.* Ph. D. Dissertation, The University of Texas at Austin.

Chen, Y.-R., Caparanga, A. R., Soriano, A. N. & Li, M.-H. (2010) Liquid heat capacity of the solvent system (piperazine + n-methyldiethanolamine + water). *The Journal of Chemical Thermodynamics,* 42**,** 54-59.

Clarke, J. K. A. (1964) Kinetics of absorption of cardon dioxide in monoethanolamine solutions at short contact times. *Industrial & Engineering Chemistry Fundamentals,* 3**,** 239-245.

Closmann, F. B. (2011) *Oxidation and thermal degradation of methyldiethanolamine/ piperazine in CO_2 capture.* Ph.D. Dissertation, The University of Texas at Austin.

Closmann, F. B., Nguyen, T. & Rochelle, G. T. (2009) MDEA/Piperazine as a solvent for CO_2 capture. *Energy Procedia,* 1**,** 1351-1357.

Danckwerts, P. V. (1970) *Gas-liquid reactions GBP,* New York, McGraw-Hill Chemical Engineering Series.

Derks, P. W. J. (2006) *Carbon dioxide absorption in piperazine activated N-methyldiethanolamine.* Ph.D. Dissertation.

Derks, P. W. J., Dijkstra, H. B. S., Hogendoorn, J. A. & Versteeg, G. F. (2005) Solubility of carbon dioxide in aqueous piperazine solutions. *AIChE Journal,* 51**,** 2311-2327.

Derks, P. W. J., Hamborg, E. S., Hogendoorn, J. A., Niederer, J. P. M. & Versteeg, G. F. (2008) Densities, viscosities, and liquid diffusivities in aqueous piperazine and aqueous (piperazine + N-methyldiethanolamine) solutions. *Journal of Chemical & Engineering Data,* 53**,** 1179-1185.

Derks, P. W. J., Hogendoorn, J. A. & Versteeg, G. F. (2006a) Solubility of carbon dioxide in aqueous blends of piperazine and N-methyldiethanolamine. Enschede, the Netherlands: CATO Publication. Available: http://www.co2-cato.org/publications/publications/solubility-of-carbon-dioxide-in-aqueous-blends-of-piperazine-and-n-methyldiethanolamine [Accessed 04.09.2012].

Derks, P. W. J., Hogendoorn, J. A. & Versteeg, G. F. (2010) Experimental and theoretical study of the solubility of carbon dioxide in aqueous blends of piperazine and N-methyldiethanolamine. *The Journal of Chemical Thermodynamics,* 42**,** 151-163.

Derks, P. W. J., Kleingeld, T., van Aken, C., Hogendoorn, J. A. & Versteeg, G. F. (2006b) Kinetics of absorption of carbon dioxide in aqueous piperazine solutions. *Chemical Engineering Science,* 61**,** 6837-6854.

Deshmukh, R. D. & Mather, A. E. (1981) A mathematical model for equilibrium solubility of hydrogen sulfide and carbon dioxide in aqueous alkanolamine solutions. *Chemical Engineering Science,* 36**,** 355-362.

Donaldson, T. L. & Nguyen, Y. N. (1980) Carbon dioxide reaction kinetics and transport in aqueous amine membranes. *Industrial & Engineering Chemistry Fundamentals,* 19**,** 260-266.

Dow. *DOW Specialty Amines - Products* [Online]. The Dow Chemical Company (1995-2012). Available: http://www.dow.com/amines/prod/index.htm [Accessed 17.08. 2012].

Dow. (2001) *Ethyleneamines* [Online]. Michigan, U.S.A.: The Dow Chemical Company. Available: http://www.dow.com/amines/pdfs/108-01347.pdf [Accessed 22.08. 2012].

Dow. (2010a) *Product Safety Assessment, DOW™ N-Methyldiethanolamine* [Online]. The Dow Chemical Company. Available: http://msdssearch.dow.com/PublishedLiteratureDOWCOM/dh_0436/0901b80380436ae7.pdf?filepath=productsafety/pdfs/noreg/233-00470.pdf&fromPage=GetDoc [Accessed 31.08. 2012].

Dow. (2010b) *Product Safety Assessment, DOW™ Piperazine* [Online]. The Dow Chemical Company. Available: http://msdssearch.dow.com/PublishedLiteratureDOWCOM/dh_0436/0901b80380436a9e.pdf?filepath=productsafety/pdfs/noreg/233-00304.pdf&fromPage=GetDoc [Accessed 29.08. 2012].

Dow. (2011) *Material Safety Data Sheet, Aminoethylethanolamine* [Online]. The Dow Chemical Company. Available: http://www.dow.com/webapps/msds/ShowPDF.aspx?id=090003e88020458c [Accessed 03.09. 2012].

Edali, M., Idem, R. & Aboudheir, A. (2010) 1D and 2D absorption-rate/kinetic modeling and simulation of carbon dioxide absorption into mixed aqueous solutions of MDEA and PZ in a laminar jet apparatus. *International Journal of Greenhouse Gas Control,* 4**,** 143-151.

Edwards, T. J., Maurer, G., Newman, J. & Prausnitz, J. M. (1978) Vapor-liquid equilibria in multicomponent aqueous solutions of volatile weak electrolytes. *AIChE Journal,* 24**,** 966-976.

Eide-Haugmo, I., Brakstad, O. G., Hoff, K. A., Sørheim, K. R., da Silva, E. F. & Svendsen, H. F. (2009) Environmental impact of amines. *Energy Procedia,* 1**,** 1297-1304.

Ermatchkov, V. & Maurer, G. (2011) Solubility of carbon dioxide in aqueous solutions of N-methyldiethanolamine and piperazine: Prediction and correlation. *Fluid Phase Equilibria,* 302**,** 338-346.

Ermatchkov, V., Pérez-Salado Kamps, Á. & Maurer, G. (2003) Chemical equilibrium constants for the formation of carbamates in (carbon dioxide +piperazine + water) from 1H-NMR-spectroscopy. *The Journal of Chemical Thermodynamics,* 35**,** 1277-1289.

Feng, Z., Cheng-Gang, F., You-Ting, W., Yuan-Tao, W., Ai-Min, L. & Zhi-Bing, Z. (2010) Absorption of CO_2 in the aqueous solutions of functionalized ionic liquids and MDEA. *Chemical Engineering Journal,* 160**,** 691-697.

FLUOR. (2004) *Improvement in Power Generation with Post-Combustion Capture of CO_2 (Report Number PH4/33)* [Online]. The International Energy Agency Greenhouse Gas R&D Programme. Available: http://www.canadiancleanpowercoalition.com/pdf/AS5%20-%20PH4-33%20post%20combustion.pdf [Accessed 17.08. 2012].

Giardina, J., Maginn, E. J. & Lang, D. (2010) *Ionic Liquids: Breakthrough Absorption Technology for Post-Combustion CO_2 Capture* [Online]. University of Notre Dame. Available: http://www.netl.doe.gov/technologies/coalpower/ewr/co2/pubs/43091%20University%20of%20Notre%20Dame%20Ionic%20Liquid%20Absorption.pdf [Accessed 14.09. 2012].

Glasscock, D. A. (1990) *Modelling and experimental study of carbon dioxide absorption into aqueous alkanolamines.* Ph. D. Dissertation, University of Texas at Austin.

Harned, H. S. & Robinson, R. A. (1940) A note on the temperature variation of the ionisation constants of weak electrolytes. *Transactions of the Faraday Society,* 36**,** 973-978.

Harned, H. S. & Scholes, S. R. (1941) The ionization constant of HCO_3^- from 0 to 50°. *Journal of the American Chemical Society,* 63**,** 1706-1709.

Hessen, E. T., Haug-Warberg, T. & Svendsen, H. F. (2010) The refined e-NRTL model applied to CO_2–H_2O–alkanolamine systems. *Chemical Engineering Science,* 65**,** 3638-3648.

Huang, Y.-M., Soriano, A. N., Caparanga, A. R. & Li, M.-H. (2011) Kinetics of absorption of carbon dioxide in 2-amino-2-methyl-l-propanol + N-methyldiethanolamine + water. *Journal of the Taiwan Institute of Chemical Engineers,* 42**,** 76-85.

Idem, R., Edali, M. & Aboudheir, A. (2009) Kinetics, modeling, and simulation of the experimental kinetics data of carbon dioxide absorption into mixed aqueous solutions of MDEA and PZ using laminar jet apparatus with a numerically solved absorption-rate/kinetic model. *Energy Procedia,* 1**,** 1343-1350.

Ilme, J. (1997) *Estimating plate efficiencies in simulation of industrial scale distillation columns,* Lappeenranta, Lappeenranta University of Technology.

Irons, R., Sekkapan, G., Panesar, R., Gibbins, J. & Lucquiaud, M. (2007) *CO_2 Capture Ready Plants (Report Number: 2007/4)* [Online]. The International Energy Agency Greenhouse Gas R&D Programme. Available: http://www.iea.org/papers/2007/CO2_capture_ready_plants.pdf [Accessed 17.08. 2012].

Kalliola, L. (2007) *Purification of synthesis gas produced in biomass gasification by physical absorption.* Master's thesis, Helsinki University of Technology.

Kenig, E. Y., Schneider, R. & Górak, A. (2001) Reactive absorption: Optimal process design via optimal modelling. *Chemical Engineering Science,* 56**,** 343-350.

Kent, R. L. & Eisenberg, B. (1976) Better data for amine treating. *Hydrocarbon Processing,* 55**,** 87-90.

Kierzkowska-Pawlak, H. & Chacuk, A. (2010) Kinetics of carbon dioxide absorption into aqueous MDEA solutions. *Ecological Chemistry and Engineering,* 17.

Kim, I., Hessen, E. T., Haug-Warberg, T. & Svendsen, H. F. (2009a) Enthalpies of absorption of CO_2 in aqueous alkanolamine solutions from e-NRTL model. *Energy Procedia,* 1**,** 829-835.

Kim, I., Hoff, K. A., Hessen, E. T., Haug-Warberg, T. & Svendsen, H. F. (2009b) Enthalpy of absorption of CO_2 with alkanolamine solutions predicted from reaction equilibrium constants. *Chemical Engineering Science,* 64**,** 2027-2038.

Kim, I. & Svendsen, H. F. (2011) Comparative study of the heats of absorption of post-combustion CO_2 absorbents. *International Journal of Greenhouse Gas Control,* 5**,** 390-395.

Ko, J.-J. & Li, M.-H. (2000) Kinetics of absorption of carbon dioxide into solutions of N-methyldiethanolamine+water. *Chemical Engineering Science,* 55**,** 4139-4147.

Kohl, A. L. (1987) Absorption and Stripping. IN ROUSSEAU, R. W. (Ed.) *Handbook of Separation Process Technology.* New York, Wiley-Interscience.

Kohl, A. L. & Nielsen, R. B. (1997) *Gas Purification (5th Edition),* Houston, Gulf Professional Publishing.

Komati, S. & Suresh, A. K. (2008) CO_2 absorption into amine solutions: a novel strategy for intensification based on the addition of ferrofluids. *Journal of Chemical Technology & Biotechnology,* 83**,** 1094-1100.

Kothandaraman, A. (2010) *Carbon Dioxide Capture by Chemical Absorption: A Solvent Comparison Study.* Ph.D. Dissertation, Massachusetts Institute of Technology.

Krishna, R. & Wesselingh, J. A. (1997) The Maxwell-Stefan approach to mass transfer. *Chemical Engineering Science,* 52**,** 861-911.

Kucka, L., Müller, I., Kenig, E. Y. & Górak, A. (2003) On the modelling and simulation of sour gas absorption by aqueous amine solutions. *Chemical Engineering Science,* 58**,** 3571-3578.

Lewis, W. K. & Whitman, W. G. (1924) Principles of gas absorption. *Industrial & Engineering Chemistry,* 16**,** 1215-1220.

Liu, H.-B., Zhang, C.-F. & Xu, G.-W. (1999) A study on equilibrium solubility for carbon dioxide in methyldiethanolamine−piperazine−water solution. *Industrial & Engineering Chemistry Research,* 38**,** 4032-4036.

Lu, Wang, Sun, Li & Liu (2005) Absorption of CO_2 into aqueous solutions of methyldiethanolamine and activated methyldiethanolamine from a gas mixture in a hollow fiber contactor. *Industrial & Engineering Chemistry Research,* 44**,** 9230-9238.

Lu, J.-G., Zheng, Y.-F., Cheng, M.-D. & Wang, L.-J. (2007) Effects of activators on mass-transfer enhancement in a hollow fiber contactor using activated alkanolamine solutions. *Journal of Membrane Science,* 289**,** 138-149.

MAK (2002) Methyldiethanolamine [MAK Value Documentation, 1998]. *The MAK-Collection for Occupational Health and Safety.* Wiley-VCH Verlag GmbH & Co. KGaA.

McCabe, W. L., Smith, J. C. & Harriott, P. (2001) *Unit Operations of Chemical Engineering,* New York, McGraw-Hill Chemical Engineering Series.

McCann, N., Maeder, M. & Attalla, M. (2008) Simulation of Enthalpy and Capacity of CO_2 Absorption by Aqueous Amine Systems. *Industrial & Engineering Chemistry Research,* 47**,** 2002-2009.

Metz, B. (2005) *IPCC Special Report on Carbon Dioxide Capture and Storage,* Cambridge, Cambridge University Press, for the Intergovernmental Panel on Climate Change.

Mofarahi, M., Khojasteh, Y., Khaledi, H. & Farahnak, A. (2008) Design of CO_2 absorption plant for recovery of CO_2 from flue gases of gas turbine. *Energy,* 33**,** 1311-1319.

Muhammad, A., Mutalib, M. I. A., Murugesan, T. & Shafeeq, A. (2009) Thermophysical properties of aqueous piperazine and aqueous (N-

methyldiethanolamine + piperazine) solutions at temperatures (298.15 to 338.15) K. *Journal of Chemical & Engineering Data,* 54**,** 2317-2321.

Nguyen, T., Hilliard, M. & Rochelle, G. (2011) Volatility of aqueous amines in CO_2 capture. *Energy Procedia,* 4**,** 1624-1630.

Nguyen, T., Hilliard, M. & Rochelle, G. T. (2010) Amine volatility in CO_2 capture. *International Journal of Greenhouse Gas Control,* 4**,** 707-715.

Noeres, C., Kenig, E. Y. & Górak, A. (2003) Modelling of reactive separation processes: reactive absorption and reactive distillation. *Chemical Engineering and Processing: Process Intensification,* 42**,** 157-178.

Oexmann, J. (2011) *Post Combustion CO_2 Capture: Energetic Evaluation of Chemical Absorption Processes in Coal-Fired Steam Power Plants.* D.Eng. Dissertation, Technischen Universität Hamburg-Harburg.

Olajire, A. A. (2010) CO_2 capture and separation technologies for end-of-pipe applications – A review. *Energy,* 35**,** 2610-2628.

Olofsson, G. & Hepler, L. G. (1975) Thermodynamics of ionization of water over wide ranges of temperature and pressure. *Journal of Solution Chemistry,* 4**,** 127-143.

Oyenekan, B. A. (2007) *Modeling of Strippers for CO_2 Capture by Aqueous Amines.* Ph.D. Dissertation, The University of Texas at Austin.

Oyenekan, B. A. & Rochelle, G. T. (2007) Alternative stripper configurations for CO_2 capture by aqueous amines. *AIChE Journal,* 53**,** 3144-3154.

Pacheco, M. A. (1998) *Mass Transfer, Kinetics and Rate-based Modeling of Reactive Absorption.* Ph.D. Dissertation, The University of Texas at Austin.

Pacheco, M. A., Kaganoi, S. & Rochelle, G. T. (2000) CO_2 absorption into aqueous mixtures of diglycolamine® and methyldiethanolamine. *Chemical Engineering Science,* 55**,** 5125-5140.

Pagano, J. M., Goldberg, D. E. & Fernelius, W. C. (1961) A thermodynamic study of homopiperazine, piperazine and N-(2-aminoethyl)-piperazine and their complexes with copper(II) ion. *The Journal of Physical Chemistry,* 65**,** 1062-1064.

Pani, F., Gaunand, A., Cadours, R., Bouallou, C. & Richon, D. (1997) Kinetics of absorption of CO_2 in concentrated aqueous methyldiethanolamine solutions in the range 296 K to 343 K. *Journal of Chemical & Engineering Data,* 42**,** 353-359.

Paul, S. & Mandal, B. (2006a) Density and viscosity of aqueous solutions of (2-piperidineethanol + piperazine) from (288 to 333) K and surface tension of aqueous solutions of (N-methyldiethanolamine + piperazine), (2-amino-2-methyl-1-propanol + piperazine), and (2-piperidineethanol + piperazine) from (293 to 323) K. *Journal of Chemical & Engineering Data,* 51**,** 2242-2245.

Paul, S. & Mandal, B. (2006b) Density and viscosity of aqueous solutions of (N-methyldiethanolamine + piperazine) and (2-amino-2-methyl-1-propanol + piperazine) from (288 to 333) K. *Journal of Chemical & Engineering Data,* 51**,** 1808-1810.

Penders-van Elk, N. J. M. C., Derks, P. W. J., Fradette, S. & Versteeg, G. F. (2012) Kinetics of absorption of carbon dioxide in aqueous MDEA solutions with carbonic anhydrase at 298 K. *International Journal of Greenhouse Gas Control,* 9**,** 385-392.

Peng, J., Lextrait, S., Edgar, T. F. & Eldridge, R. B. (2002) A Comparison of Steady-State Equilibrium and Rate-Based Models for Packed Reactive Distillation Columns. *Industrial & Engineering Chemistry Research,* 41**,** 2735-2744.

Pérez-Salado Kamps, Á., Xia, J. & Maurer, G. (2003) Solubility of CO_2 in (H_2O+piperazine) and in (H_2O+MDEA+piperazine). *AIChE Journal,* 49**,** 2662-2670.

Pinsent, B. R. W., Pearson, L. & Roughton, F. J. W. (1956) The kinetics of combination of carbon dioxide with hydroxide ions. *Transactions of the Faraday Society,* 52**,** 1512-1520.

Piperazine - Why It's Used and How It Works. (2008) *The Contactor*^{TM} [Online]. Houston, Texas: Optimized Gas Treating, Inc. Available: http://www.ogtrt.com/files/contactors/vol_2_issue_4.pdf.

Posey, M. L. & Rochelle, G. T. (1997) A thermodynamic model of methyldiethanolamine−CO_2−H_2S−water. *Industrial & Engineering Chemistry Research,* 36**,** 3944-3953.

Prausnitz, J. M. (1977) Equilibrium properties from activity coefficient correlations. IN HENLEY, E. J. & SEADER, J. D. (Eds.) *Equilibrium-Stage Separation Operations in Chemical Engineering.* New York, Wiley.

Puxty, G., Rowland, R., Allport, A., Yang, Q., Bown, M., Burns, R., Maeder, M. & Attalla, M. (2009) Carbon dioxide postcombustion capture: A novel screening study of the carbon dioxide absorption performance of 76 amines. *Environmental Science & Technology,* 43**,** 6427-6433.

Rao, A. B. & Rubin, E. S. (2002) A technical, economic, and environmental assessment of amine-based CO_2 capture technology for power plant greenhouse gas control. *Environmental Science & Technology,* 36**,** 4467-4475.

Read, A. J. (1975) The first ionization constant of carbonic acid from 25 to 250 °C and to 2000 bar. *Journal of Solution Chemistry,* 4**,** 53-70.

Renon, H. & Prausnitz, J. M. (1968) Local compositions in thermodynamic excess functions for liquid mixtures. *AIChE Journal,* 14**,** 135-144.

Rinker, E. B., Ashour, S. S. & Sandall, O. C. (1997) Acid gas treating with aqueous alkanolamines - Part III: Experimental absorption rate measurements and reaction kinetics for H_2S and CO_2 in aqueous DEA, MDEA, and blends of DEA and MDEA. Gas Processing Association (GPA) Research Report, No. 159.

Rinker, E. B., Sami, S. A. & Sandall, O. C. (1995) Kinetics and modelling of carbon dioxide absorption into aqueous solutions of N-methyldiethanolamine. *Chemical Engineering Science,* 50**,** 755-768.

Rochelle, G. T. (2012) Thermal degradation of amines for CO_2 capture. *Current Opinion in Chemical Engineering,* 1**,** 183-190.

Rufford, T. E., Smart, S., Watson, G. C. Y., Graham, B. F., Boxall, J., Diniz da Costa, J. C. & May, E. F. (2012) The removal of CO_2 and N_2 from natural gas: A review of conventional and emerging process technologies. *Journal of Petroleum Science and Engineering,* 94–95**,** 123-154.

Sakwattanapong, R., Aroonwilas, A. & Veawab, A. (2005) Behavior of reboiler heat duty for CO_2 capture plants using regenerable single and blended alkanolamines. *Industrial & Engineering Chemistry Research,* 44**,** 4465-4473.

Samanta, A. & Bandyopadhyay, S. S. (2007) Kinetics and modeling of carbon dioxide absorption into aqueous solutions of piperazine. *Chemical Engineering Science,* 62**,** 7312-7319.

Samanta, A. & Bandyopadhyay, S. S. (2011) Absorption of carbon dioxide into piperazine activated aqueous N-methyldiethanolamine. *Chemical Engineering Journal,* 171**,** 734-741.

Samanta, A., Roy, S. & Bandyopadhyay, S. S. (2007) Physical solubility and diffusivity of N_2O and CO_2 in aqueous solutions of piperazine and (N-methyldiethanolamine + piperazine). *Journal of Chemical & Engineering Data,* 52**,** 1381-1385.

Schäfer, B., Mather, A. E. & Marsh, K. N. (2002) Enthalpies of solution of carbon dioxide in mixed solvents. *Fluid Phase Equilibria,* 194–197**,** 929-935.

Schenkel, R. & Day, C. (2005) *European Union Risk Assessment Report - Piperazine* [Online]. Sweden: European Chemicals Bureau, Institute for Health and Consumer Protection. Available: http://esis.jrc.ec.europa.eu/doc/risk_assessment/REPORT/piperazinereport324.pdf [Accessed 29.08. 2012].

Schubert, S., Grünewald, M. & Agar, D. W. (2001) Enhancement of carbon dioxide absorption into aqueous methyldiethanolamine using immobilised activators. *Chemical Engineering Science,* 56**,** 6211-6216.

ScienceLab. *Piperazine, anhydrous MSDS* [Online]. Sciencelab.com, Inc. Available: http://www.sciencelab.com/msds.php?msdsId=9926575 [Accessed 09.01. 2013].

Si Ali, B. & Aroua, M. K. (2004) Effect of piperazine on CO_2 loading in aqueous solutions of MDEA at low pressure. *International Journal of Thermophysics,* 25**,** 1863-1870.

Snijder, E. D., te Riele, M. J. M., Versteeg, G. F. & van Swaaij, W. P. M. (1993) Diffusion coefficients of several aqueous alkanolamine solutions. *Journal of Chemical & Engineering Data,* 38**,** 475-480.

Speyer, D., Ermatchkov, V. & Maurer, G. (2010) Solubility of carbon dioxide in aqueous solutions of N-methyldiethanolamine and piperazine in the low gas loading region. *Journal of Chemical & Engineering Data,* 55**,** 283-290.

Svendsen, H. F., Hessen, E. T. & Mejdell, T. (2011) Carbon dioxide capture by absorption, challenges and possibilities. *Chemical Engineering Journal,* 171**,** 718-724.

Taylor, R. & Krishna, R. (1993) *Multicomponent Mass Transfer,* New York, Wiley & Sons.

Teir, S., Tsupari, E., Koljonen, T., Pikkarainen, T., Arasto, A., Tourunen, A., Kärki, J., Kujanpää, L., Nieminen, M. & Aatos, S. (2009) *Hiilidioksidin talteenotto ja varastointi (CCS),* Helsinki, VTT Technical Research Centre of Finland.

Tellini, M. & Manenti, F. (2012) Low-pressure absorption of CO_2 fom flue gas: Plant economics with incentives. *Hydrocarbon Processing,* November**,** 71-76.

Thiele, R. & Löning, J.-M. (2006) Industrial Absorption Current Status and Future Aspects. *Symposium Series No. 152.* IChemE.

Vahidi, M., Matin, N. S., Goharrokhi, M., Jenab, M. H., Abdi, M. A. & Najibi, S. H. (2009) Correlation of CO_2 solubility in N-methyldiethanolamine + piperazine aqueous solutions using extended Debye–Hückel model. *The Journal of Chemical Thermodynamics,* 41**,** 1272-1278.

Vaidya, P. D. & Kenig, E. Y. (2007) CO_2-alkanolamine reaction kinetics: A review of recent studies. *Chemical Engineering & Technology,* 30**,** 1467-1474.

van Loo, S., van Elk, E. P. & Versteeg, G. F. (2007) The removal of carbon dioxide with activated solutions of methyl-diethanol-amine. *Journal of Petroleum Science and Engineering,* 55**,** 135-145.

Veltman, K., Singh, B. & Hertwich, E. G. (2010) Human and environmental impact assessment of postcombustion CO_2 capture focusing on emissions from amine-based scrubbing solvents to air. *Environmental Science & Technology,* 44**,** 1496-1502.

Versteeg, G. F. & van Swaaij, W. P. M. (1988a) On the kinetics between CO_2 and alkanolamines both in aqueous and non-aqueous solutions—II. Tertiary amines. *Chemical Engineering Science,* 43**,** 587-591.

Versteeg, G. F. & van Swaaij, W. P. M. (1988b) Solubility and diffusivity of acid gases (carbon dioxide, nitrous oxide) in aqueous alkanolamine solutions. *Journal of Chemical & Engineering Data,* 33**,** 29-34.

Wang, R., Li, D. F. & Liang, D. T. (2004) Modeling of CO_2 capture by three typical amine solutions in hollow fiber membrane contactors. *Chemical Engineering and Processing: Process Intensification,* 43**,** 849-856.

Weiland, R. H. & Sivasubramanian, M. S. (2004) *Effect of Heat-Stable Salts on Amine Absorber and Regenerator Performance* [Online]. Austin, Texas: Optimized Gas Treating, Inc. Available: http://www.ogtrt.com/files/publications/AIChE_Austin.pdf [Accessed 14.12. 2012].

Xu, G.-W., Zhang, C.-F., Qin, S.-J., Gao, W.-H. & Liu, H.-B. (1998) Gas−liquid equilibrium in a CO_2−MDEA−H_2O system and the effect of piperazine on it. *Industrial & Engineering Chemistry Research,* 37**,** 1473-1477.

Xu, G.-W., Zhang, C.-F., Qin, S.-J. & Zhu, B.-C. (1995) Desorption of CO_2 from MDEA and activated MDEA solutions. *Industrial & Engineering Chemistry Research,* 34**,** 874-880.

Xu, G.-W., Zhang, C., Qin, S. & Wang, Y. (1992) Kinetics study on absorption of carbon dioxide into solutions of activated methyldiethanolamine. *Industrial & Engineering Chemistry Research,* 31**,** 921-927.

Zhang, X., Zhang, C.-F., Qin, S.-J. & Zheng, Z.-S. (2001a) A kinetics study on the absorption of carbon dioxide into a mixed aqueous solution of methyldiethanolamine and piperazine. *Industrial & Engineering Chemistry Research,* 40**,** 3785-3791.

Zhang, X., Zhang, C.-F., Xu, G.-W., Gao, W.-H. & Wu, Y.-Q. (2001b) An experimental apparatus to mimic CO_2 removal and optimum concentration of MDEA aqueous solution. *Industrial & Engineering Chemistry Research,* 40**,** 898-901.

Zhang, Y. & Chen, C.-C. (2010) Thermodynamic modeling for CO_2 absorption in aqueous MDEA solution with electrolyte NRTL model. *Industrial & Engineering Chemistry Research,* 50**,** 163-175.

Zhi, Q. & Kai, G. (2009) Modeling and kinetic study on absorption of CO_2 by aqueous solutions of N-methyldiethanolamine in a modified wetted wall column. *Chinese Journal of Chemical Engineering,* 17**,** 571-579.

Zoghi, A. T., Feyzi, F. & Zarrinpashneh, S. (2012) Experimental investigation on the effect of addition of amine activators to aqueous solutions of N-methyldiethanolamine on the rate of carbon dioxide absorption. *International Journal of Greenhouse Gas Control,* 7**,** 12-19.

APPENDIX 1 Results of the solubility simulations (1/3)

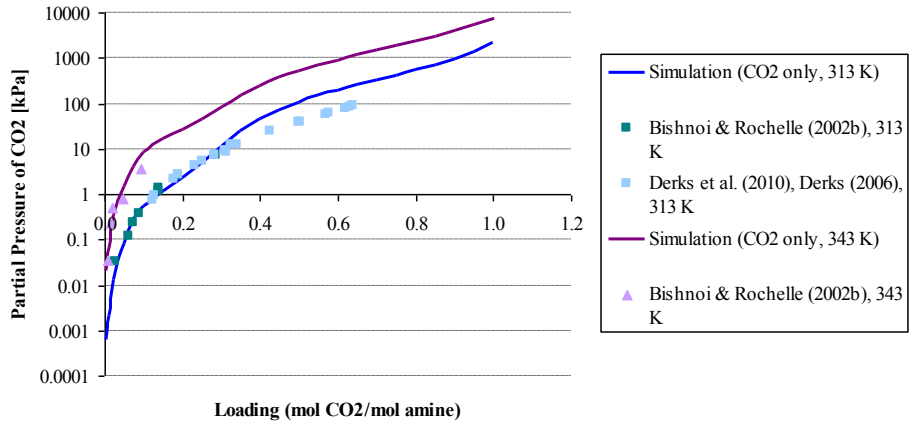

Figure 1 Solubility of CO_2 into aqueous 4 kmol/ m^3 MDEA and 0.6 kmol/ m^3 PZ solution.

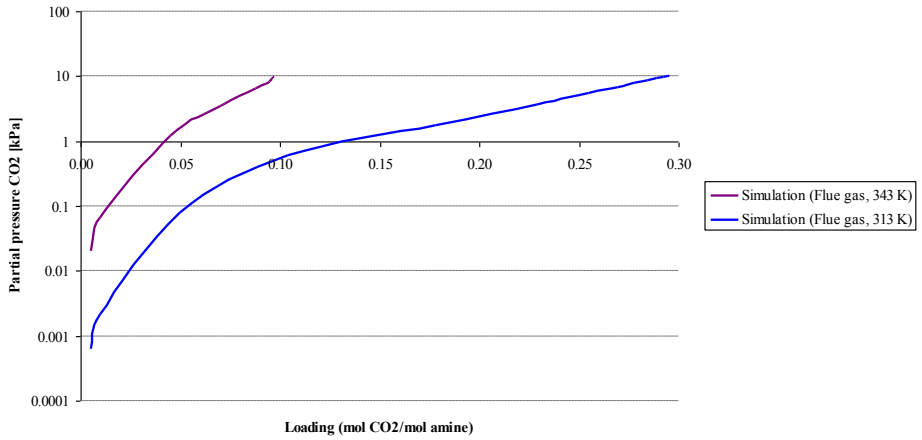

Figure 2 Solubility of CO_2 with flue gas composition into aqueous 4 kmol/ m^3 MDEA and 0.6 kmol/ m^3 PZ solution.

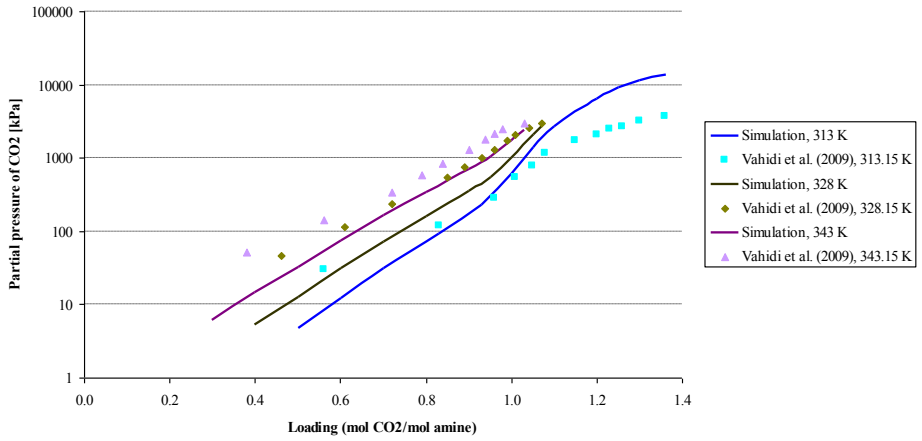

Figure 3 Solubility of CO_2 into aqueous 2 kmol/ m^3 MDEA and 1.36 kmol/ m^3 PZ solution.

APPENDIX 1 Results of the solubility simulations (2/3)

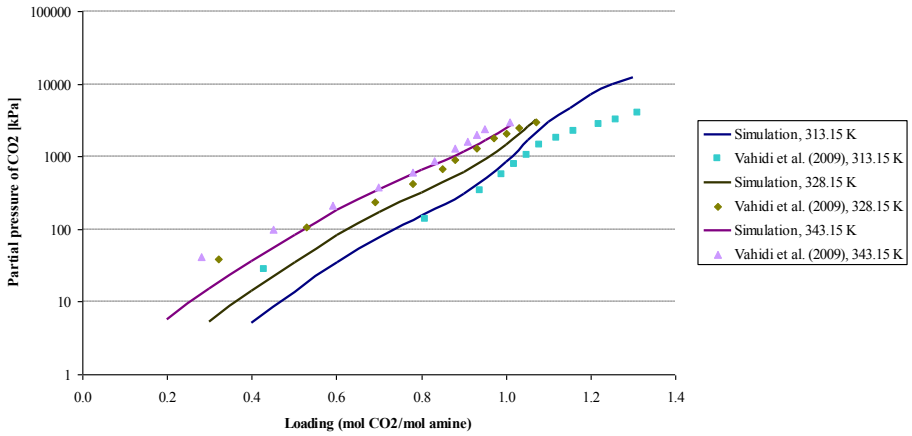

Figure 4 Solubility of CO_2 into aqueous 2.5 kmol/ m^3 MDEA and 0.86 kmol/ m^3 PZ solution.

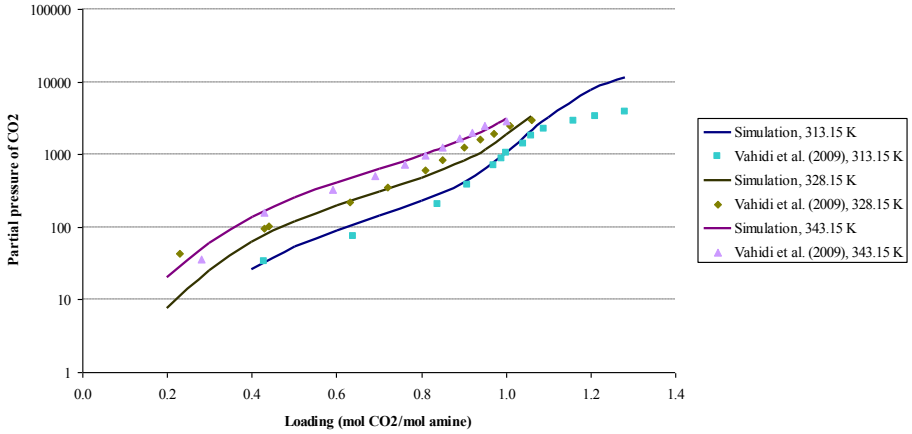

Figure 5 Solubility of CO_2 into aqueous 3 kmol/ m^3 MDEA and 0.36 kmol/ m^3 PZ solution.

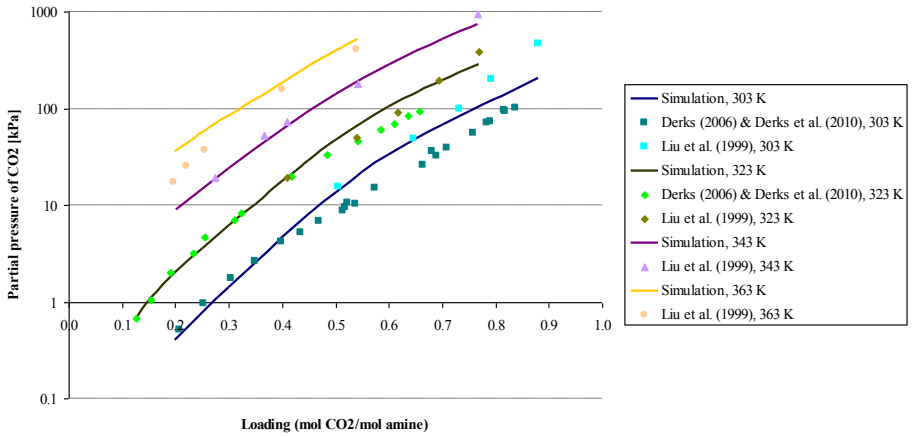

Figure 6 Solubility of CO_2 into aqueous 2.8 kmol/ m^3 MDEA and 0.7 kmol/ m^3 PZ solution.

APPENDIX 1 Results of the solubility simulations (3/3)

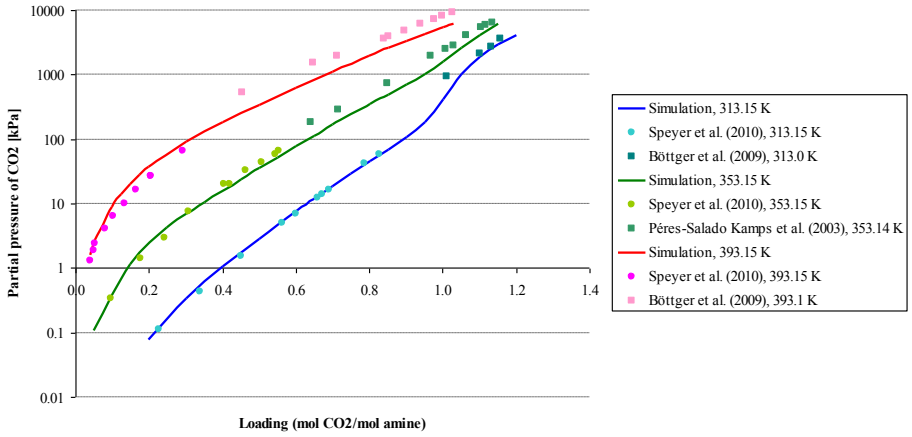

Figure 7 Solubility of CO_2 into aqueous 1.44 kmol/ m^3 MDEA and 1.44 kmol/ m^3 PZ solution. Molalities roughly 2 mol/ (kg water) MDEA and 2 mol/ (kg water) PZ.

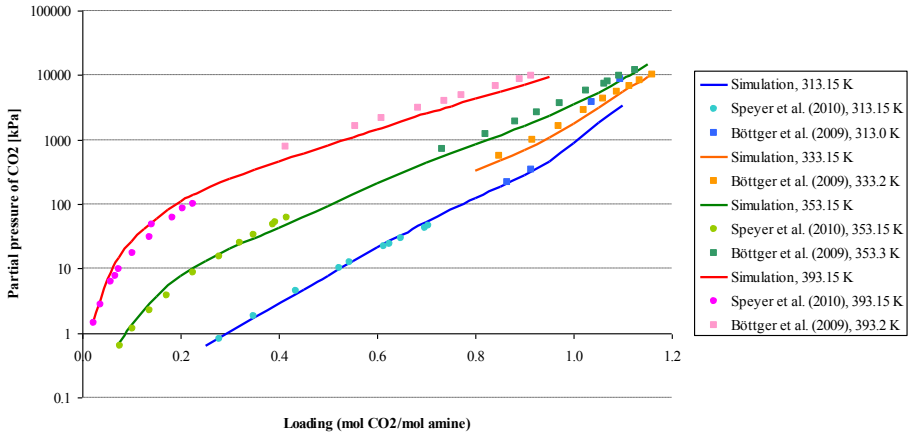

Figure 8 Solubility of CO_2 into aqueous 2.48 kmol/ m^3 MDEA and 1.24 kmol/ m^3 PZ solution. Molalities are roughly 4 mol/ (kg water) MDEA and 2 mol/ (kg water) PZ.

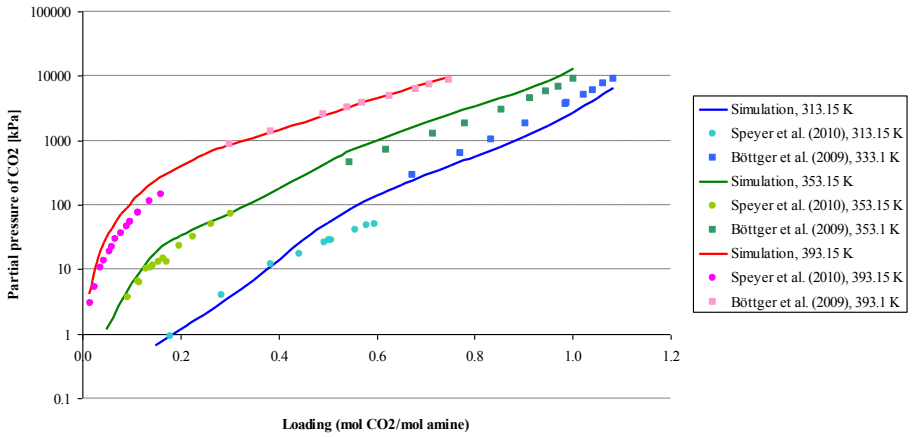

Figure 9 Solubility of CO_2 into aqueous 3.88 kmol/ m^3 MDEA and 0.97 kmol/ m^3 PZ solution. Molalities roughly 8 mol/ (kg water) MDEA and 2 mol/ (kg water) PZ.

APPENDIX 2 Results of the density simulations

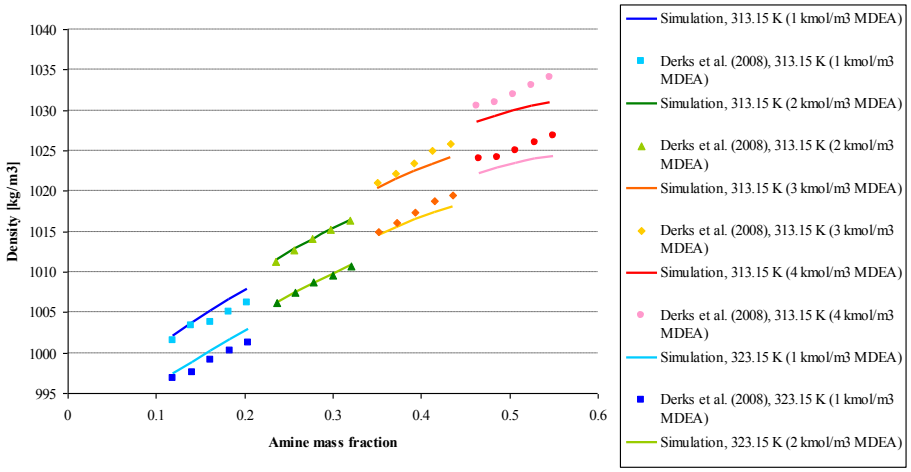

Figure 1 Densities of unloaded aqueous PZ+MDEA solutions at two temperatures. The concentrations of MDEA has been kept constant at (1, 2, 3 and 4) kmol/m^3 and the concentration of PZ has been varied (0, 0.25, 0.50, 0.75 and 1) kmol/m^3.

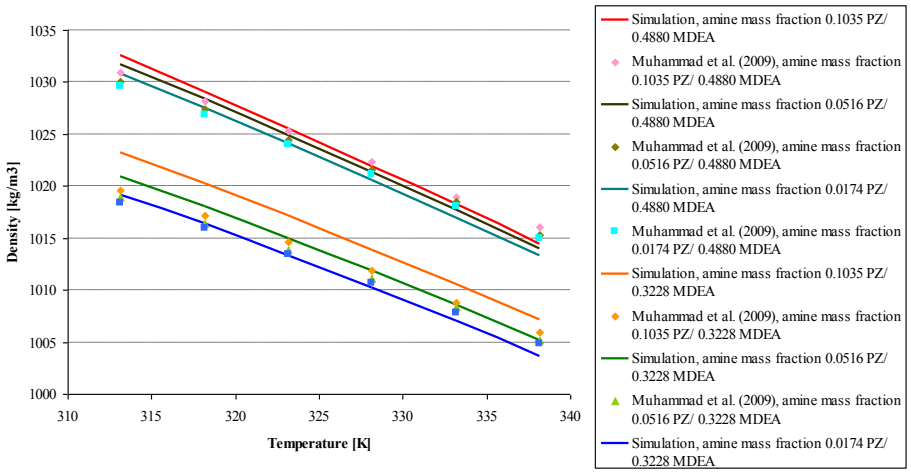

Figure 2 Densities unloaded amine concentrations as a function of temperature.

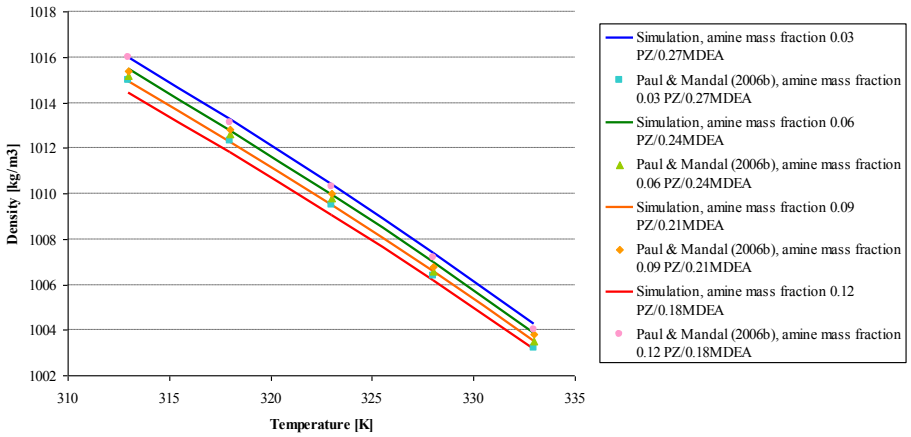

Figure 3 Densities of unloaded amine concentrations as a function of temperature.

APPENDIX 3 Results of the viscosity simulations

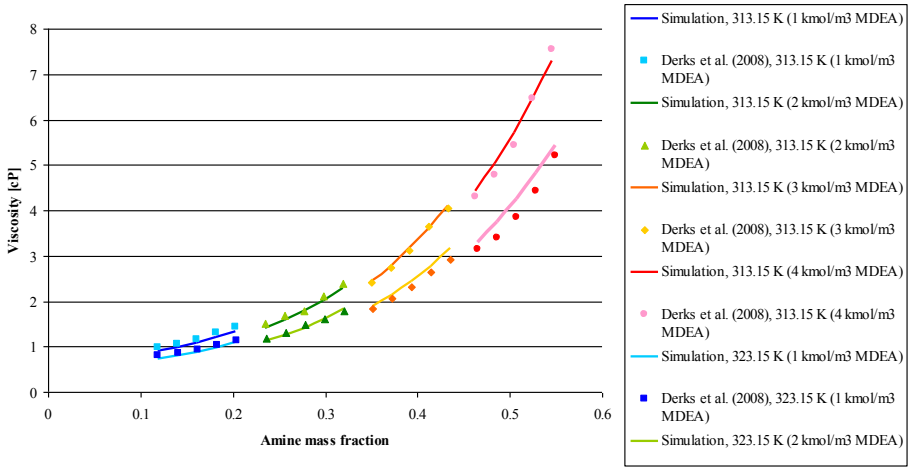

Figure 1 Viscosities of unloaded aqueous PZ+MDEA solutions at two temperatures. The concentrations of MDEA has been kept constant at (1, 2, 3 and 4) kmol/m^3 and the concentration of PZ has been varied (0, 0.25, 0.50, 0.75 and 1) kmol/m^3.

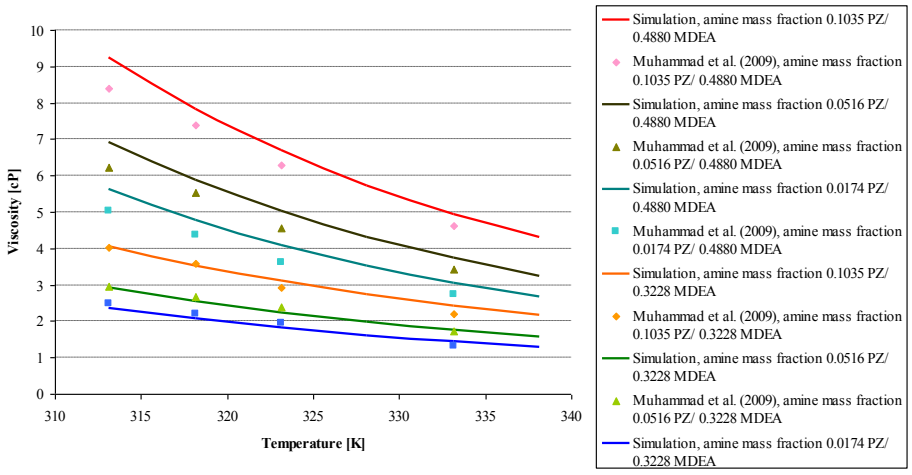

Figure 2 Viscosities of unloaded amine solutions as a function of temperature.

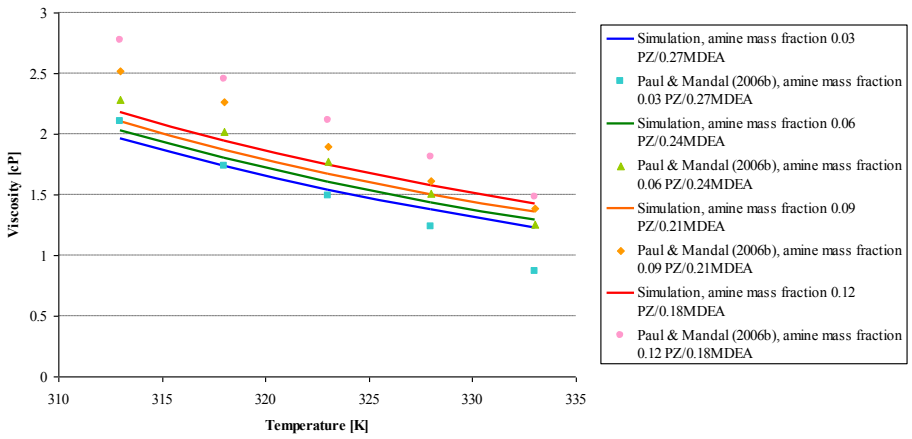

Figure 3 Viscosities of unloaded amine solutions as a function of temperature.

APPENDIX 4 Results of the surface tension and heat capacity simulations

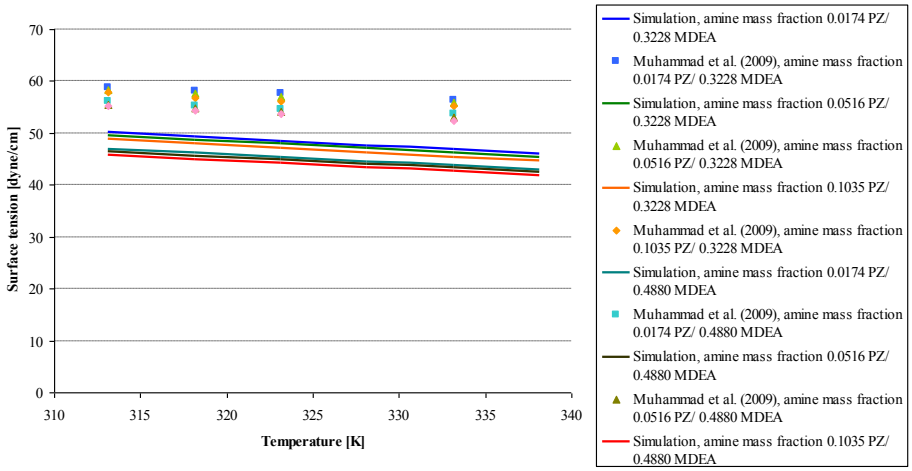

Figure 1 Surface tensions of unloaded amine solutions as a function of temperature.

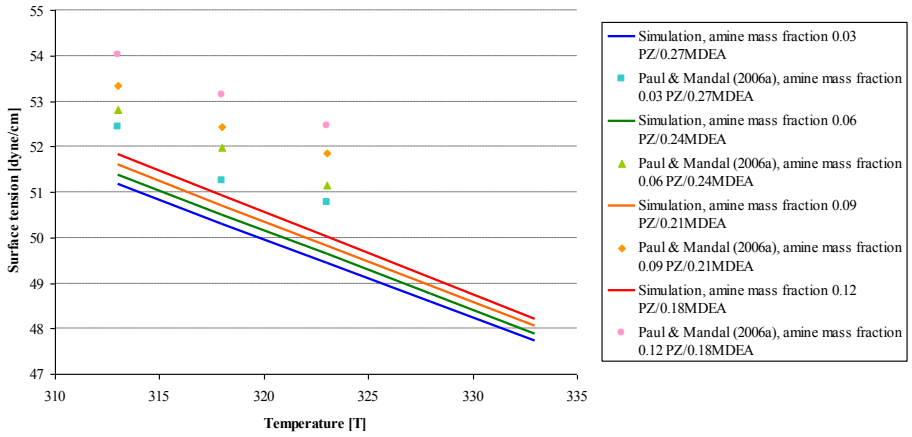

Figure 2 Surface tensions of unloaded amine solutions as a function of temperature.

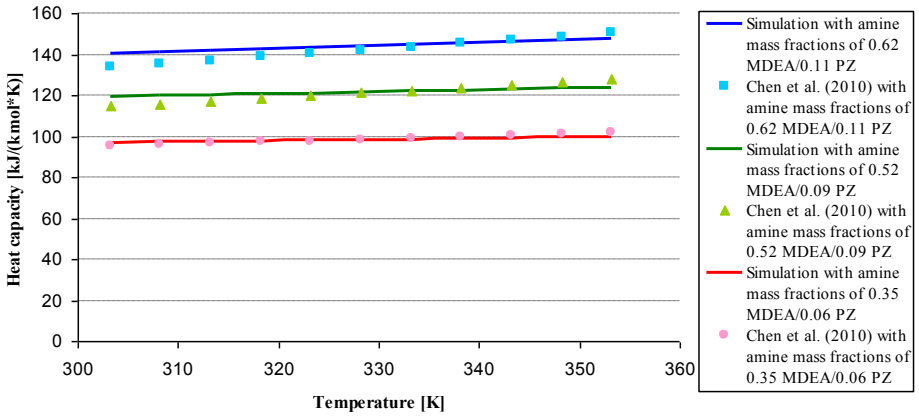

Figure 3 Heat capacities of various unloaded amine solutions as a function of temperature.

APPENDIX 5 Absorber profiles with and without the water washing section (1/3)

In the figures of this appendix following abbreviations are used:
PZ/MDEA 1 = 0.365 M PZ/2.635 M MDEA, PZ/MDEA 2 = 0.6 M PZ/4.0 M MDEA, MDEA = concentration of MDEA is 45% by weight, MEA = concentration of MEA is 30% by weight. The flow rates used were PZ/MDEA 1 = 320 kg/h, PZ/MDEA 2 = 285 kg/h, MDEA = 430 kg/h and MEA = 75.25 kg/h. In the case of the absorber with washing section the column height was 0.42 m/20 m instead of 0.42 m/15m with MDEA. With PZ/MDEA 2 and MDEA the column diameter was 0.2 m instead of 0.125 m in both of the cases.

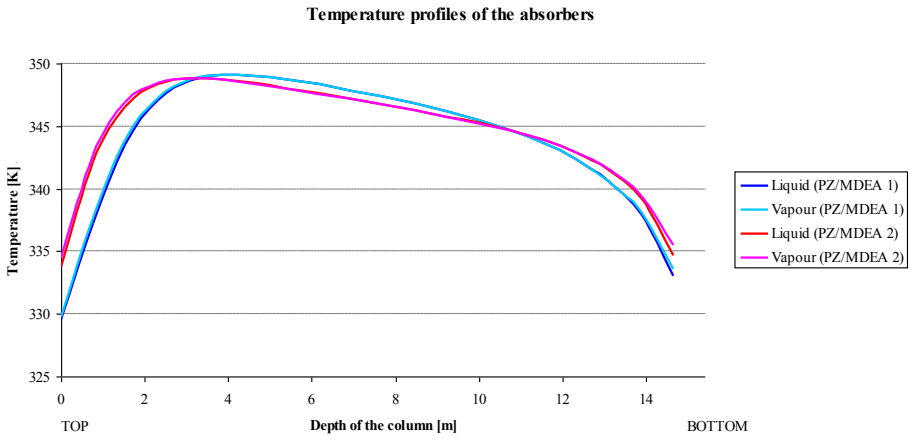

Figure 1 Temperature profiles of the absorbers without water washing section.

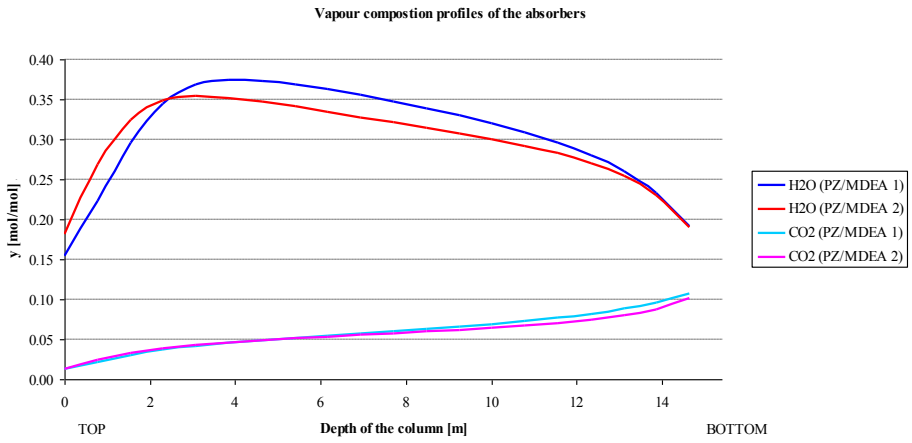

Figure 2 Vapour composition profiles of the absorbers without water washing section.

APPENDIX 5 Absorber profiles with and without the water washing section (2/3)

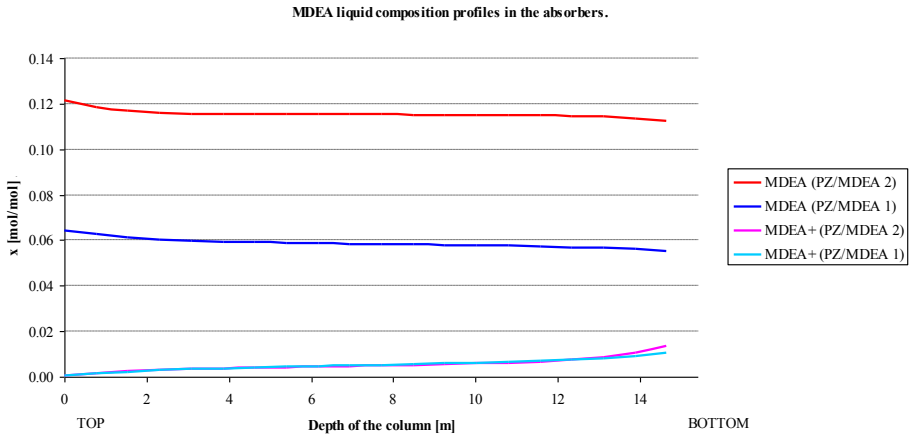

Figure 3 MDEA composition profiles in the absorbers without water washing section.

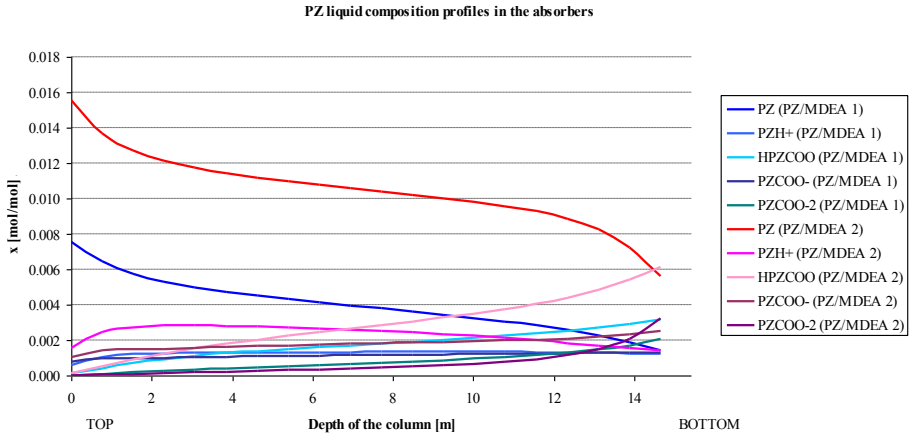

Figure 4 PZ composition profiles in the absorbers without water washing section.

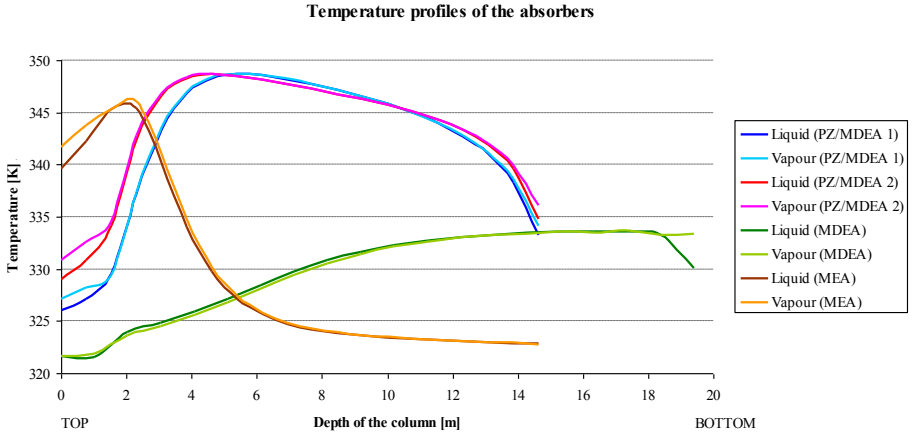

Figure 5 Temperature profiles of the absorbers with water washing section.

APPENDIX 5 Absorber profiles with and without the water washing section (3/3)

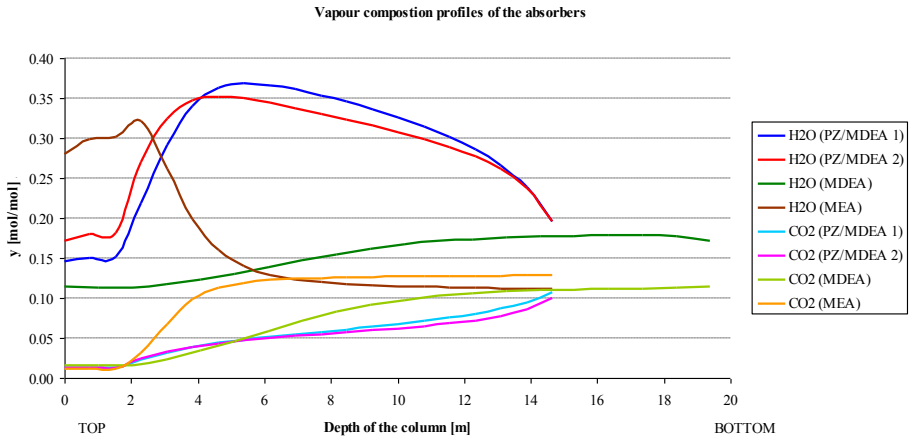

Figure 6 Vapour composition profiles of the absorbers with water washing section.

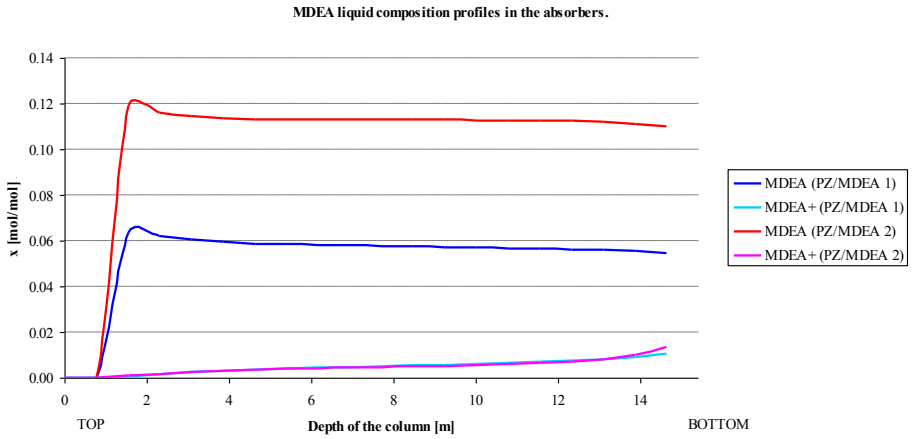

Figure 7 MDEA composition profiles in the absorbers with water washing section.

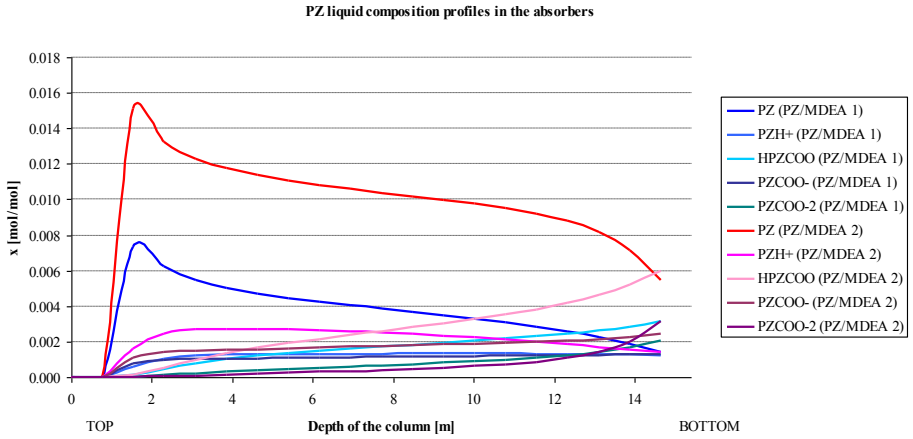

Figure 8 PZ composition profiles in the absorbers with water washing section.

APPENDIX 6 Stripper profiles (1/2)

In the figures of this appendix following abbreviations are used:

PZ/MDEA 1 = 0.365 M PZ/2.635 M MDEA, PZ/MDEA 2 = 0.6 M PZ/4.0 M MDEA, MDEA = concentration of MDEA is 45% by weight, MEA = concentration of MEA is 30% by weight. The flow rates used were PZ/MDEA 1 = 320 kg/h, PZ/MDEA 2 = 285 kg/h, MDEA = 430 kg/h and MEA = 75.25 kg/h.

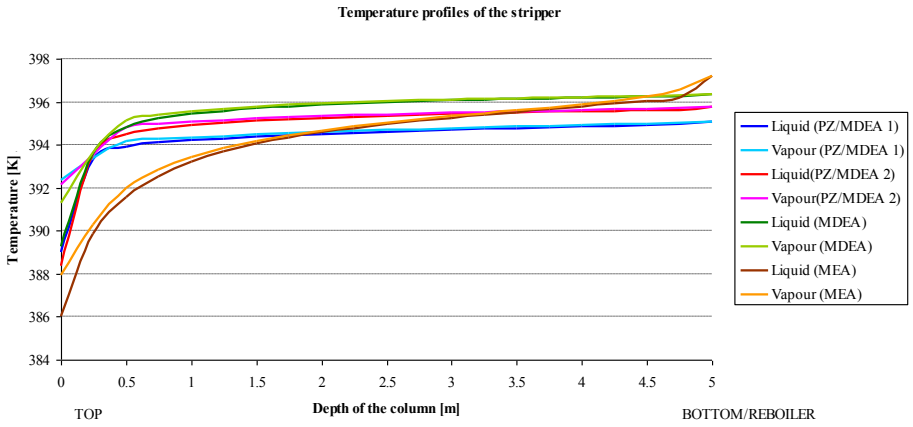

Figure 1 Temperature profiles of the stripper.

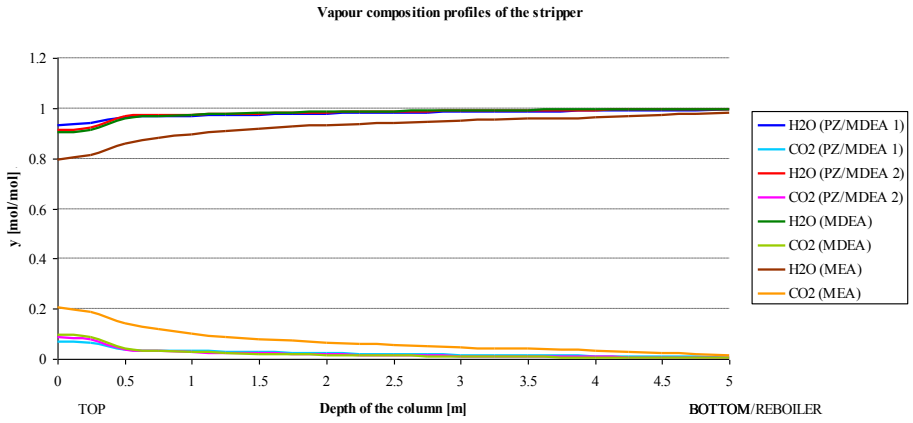

Figure 2 Vapour composition profiles of the stripper.

APPENDIX 6 Stripper profiles (2/2)

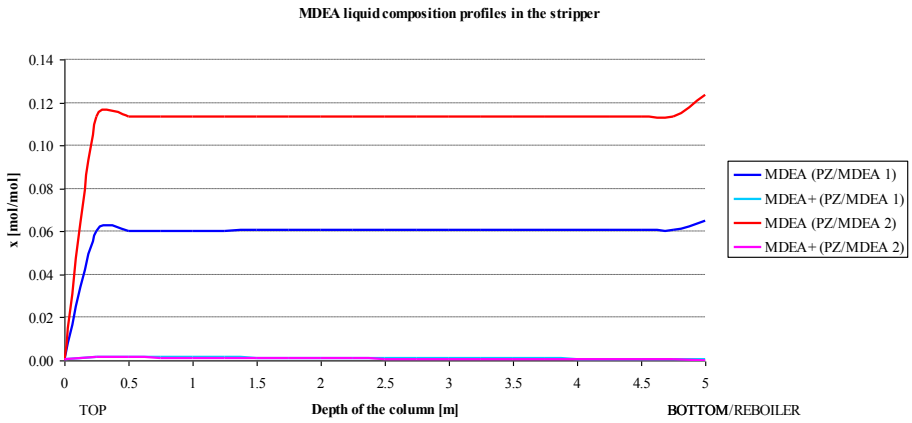

Figure 3 MDEA liquid composition profiles of the stripper.

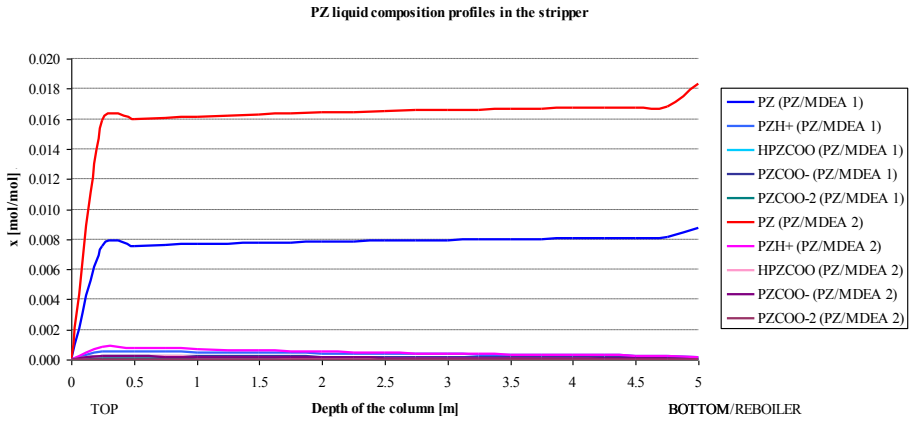

Figure 4 PZ liquid composition profiles of the stripper.

APPENDIX 7 Stream results of the PZ/MDEA 1

STREAM ID	CO2	CO2-OUT	FG-IN	FG-OUT	H2O-IN	H2O-MU	H2O-OUT	LEAN-IN	LEAN-OUT	MDEA-MU	PURGE	PZ-MU	RICH-IN	RICH-OUT	WATER
Mole Flow [kmol/h]															
MDEA	9.02E-13	7.18E-05	0	3.92E-06	2.92E-06	0	3.22E-06	0.8228	0.8188	2.76E-05	6.45E-08	0	0.7548	0.6898	1.31E-07
PZ	9.89E-14	5.60E-06	0	7.56E-07	7.48E-08	0	8.71E-08	0.0938	0.1063	0	3.67E-10	2.61E-06	0.0624	0.0159	7.45E-10
H_2O	0.0066	0.3645	0.1744	0.1999	1.6484	0.1502	1.4982	11.7055	11.6989	0	0.1181	0	11.7656	11.7606	0.2397161
CO_2	0.1714	0.1718	0.2028	0.0313	9.50E-06	0	9.81E-06	2.50E-06	3.39E-04	0	9.27E-05	0	0.0765	0.0005	1.88E-04
H3O+	0	0	0	0	3.22E-09	6.09E-10	2.94E-09	4.70E-11	2.25E-09	0	4.59E-09	0	6.85E-09	1.06E-09	9.33E-09
OH-	0	0	0	0	1.52E-08	6.09E-10	1.63E-08	7.15E-05	8.97E-05	0	3.41E-11	0	2.82E-05	1.32E-05	6.92E-11
HCO3-	0	0	0	0	4.51E-05	0	4.48E-05	0.0078	0.0157	0	2.53E-05	0	0.0729	0.0719	5.14E-05
CO3-2	0	0	0	0	3.16E-08	0	3.20E-08	0.0017	2.35E-04	0	1.07E-09	0	1.09E-03	0.0072	2.16E-09
MDEA+	0	0	0	0	3.57E-05	0	3.54E-05	0.0094	0.0134	0	2.36E-05	0	0.0774	0.1424	4.80E-05
PZH+	0	0	0	0	9.57E-06	0	9.53E-06	0.0111	0.0053	0	1.69E-06	0	0.0168	0.0149	3.42E-06
PZH+2	0	0	0	0	0	0	0	0	0	0	0	0	0	0	0
HPZCOO	0	0	0	0	1.36E-07	0	1.57E-07	0.0014	0.0013	0	1.62E-07	0	0.0220	0.0411	3.29E-07
PZCOO-	0	0	0	0	1.01E-09	0	1.26E-09	0.0089	0.0023	0	5.27E-11	0	0.0090	0.0159	1.07E-10
PZCOO-2	0	0	0	0	3.31E-12	0	4.55E-12	1.86E-04	9.03E-05	0	1.66E-12	0	0.0050	0.0275	3.37E-12
N_2	1.00E-04	1.00E-04	1.1389	1.1388	1.06E-05	0	1.06E-05	0	5.03E-17	0	1.34E-09	0	1.00E-04	1.00E-04	2.72E-09
O_2	1.00E-05	1.00E-05	0.0634	0.0633	1.08E-06	0	1.08E-06	0	1.25E-17	0	2.53E-10	0	1.00E-05	1.00E-05	5.14E-10
CO	0	0	0	0	0	0	0	0	0	0	0	0	0	0	0
H_2	0	0	0	0	0	0	0	0	0	0	0	0	0	0	0
Mass Flow [kg/h]															
MDEA	1.07E-10	0.0086	0	4.67E-04	3.48E-04	0	3.84E-04	98.0504	97.5679	0.00329035	7.69E-06	0	89.9460	82.2027	1.56E-05
PZ	8.52E-12	4.82E-04	0	6.51E-05	6.45E-06	0	7.50E-06	8.0772	9.1528	0	3.16E-08	2.25E-04	5.3712	1.3701	6.42E-08
H_2O	0.1188	6.5658	3.1411	3.6012	29.6971	2.7061	26.9910	210.8770	210.7595	0	2.1270	0	211.9612	211.8703	4.3186
CO_2	7.5434	7.5591	8.9271	1.3788	0.0004	0	0.0004	1.10E-04	0.0149	0	0.0041	0	3.3651	0.0225	0.0083
H3O+	0	0	0	0	6.12E-08	1.16E-08	5.59E-08	8.95E-10	4.29E-08	0	8.74E-08	0	1.30E-07	2.02E-08	1.77E-07
OH-	0	0	0	0	2.59E-07	1.04E-08	2.77E-07	0.00121622	0.0015	0	5.80E-10	0	4.79E-04	2.25E-04	1.18E-09
HCO3-	0	0	0	0	0.0028	0	0.0027	0.4766	0.9599	0	0.0015	0	4.4506	4.3844	0.0031
CO3-2	0	0	0	0	1.90E-06	0	1.92E-06	0.0993	0.0141	0	6.40E-08	0	0.0654	0.4339	1.30E-07
MDEA+	0	0	0	0	0.0043	0	0.0042	1.1307	1.6141	0	0.0028	0	9.3031	17.1118	0.0058
PZH+	0	0	0	0	0.0008	0	0.0008	0.9636	0.4627	0	1.47E-04	0	1.4666	1.2970	2.98E-04
PZH+2	0	0	0	0	0	0	0	0	0	0	0	0	0	0	0
HPZCOO	0	0	0	0	1.77E-05	0	2.04E-05	0.1772	0.1756	0	2.11E-05	0	2.8669	5.3452	4.29E-05
PZCOO-	0	0	0	0	1.30E-07	0	1.63E-07	1.1498	0.2931	0	6.80E-09	0	1.1661	2.0518	1.38E-08
PZCOO-2	0	0	0	0	5.70E-10	0	7.82E-10	0.0320	0.0155	0	2.86E-10	0	0.8665	4.7391	5.80E-10
N_2	0.0028	0.0028	31.9045	31.9017	0.0003	0	0.0003	0	1.41E-15	0	3.75E-08	0	0.0028	0.0028	7.62E-08
O_2	3.21E-04	3.21E-04	2.0273	2.0270	3.46E-05	0	3.46E-05	0	4.01E-16	0	8.10E-09	0	3.21E-04	3.21E-04	1.64E-08
CO	0	0	0	0	0	0	0	0	0	0	0	0	0	0	0
H_2	0	0	0	0	0	0	0	0	0	0	0	0	0	0	0
Total Flow [kmol/h]	0.1781	0.5364	1.5795	1.4334	1.6486	0.1502	1.4983	12.6625	12.6628	2.76E-05	0.1182	2.61E-06	12.8638	12.7878	0.2400
Total Flow [kg/h]	7.6653	14.1371	46	38.9092	29.7061	2.7061	27	321.0351	321.0316	0.0033	2.1357	0.0002	330.8322	330.8322	4.3361
Total Flow [m^3/h]	2.2672	8.2766	41.8166	38.2982	0.0301	0.0027	0.0274	0.3161	0.3341	0.0000	0.0022	0.0000	3.7882	0.3202	0.0044
Temperature [K]	313.15	382.72	323.15	326.13	323.15	323.15	326.03	323.15	394.25	323.15	313.15	323.15	383.34	332.62	313.15
Pressure [kPa]	202.65	202.65	101.325	101.325	101.325	101.325	101.325	101.325	202.65	101.325	202.65	101.325	202.65	101.325	202.65

APPENDIX 8 Stream results of the PZ/MDEA 2

STREAM ID	CO2	CO2-OUT	FG-IN	FG-OUT	H2O-IN	H2O-MU	H2O-OUT	LEAN-IN	LEAN-OUT	MDEA-MU	PURGE	PZ-MU	RICH-IN	RICH-OUT	WATER
Mole Flow [kmol/h]															
MDEA	1.87E-12	8.88E-05	0	1.11E-05	2.50E-05	0	2.64E-05	1.1115	1.1094	3.77E-05	9.86E-08	0	1.0594	0.9905	2.30E-07
PZ	1.10E-13	3.85E-06	0	1.21E-06	3.86E-07	0	4.59E-07	0.1573	0.1634	0	3.03E-10	2.37E-06	0.1113	0.0487	7.06E-10
H_2O	0.0069	0.3101	0.1744	0.2434	1.6644	0.1668	1.4976	7.6583	7.6551	0	0.0909	0	7.6934	7.7081	0.2122
CO_2	0.1785	0.1789	0.2028	0.0242	0	0	6.92E-06	2.36E-07	1.47E-04	0	7.14E-05	0	0.0854	4.65E-04	1.67E-04
H3O+	0	0	0	0	9.03E-10	6.77E-10	9.85E-10	6.89E-12	1.26E-09	0	2.60E-09	0	7.06E-09	6.25E-10	6.06E-09
OH-	0	0	0	0	5.75E-08	6.77E-10	6.30E-08	8.67E-05	4.96E-05	0	3.71E-11	0	1.18E-05	1.21E-05	8.66E-11
HCO3-	0	0	0	0	9.81E-05	0	9.67E-05	0.002685	0.0061	0	2.76E-05	0	0.0655	0.0462	6.43E-05
CO3-2	0	0	0	0	2.67E-07	0	2.28E-07	2.33E-04	1.72E-05	0	1.71E-09	0	2.42E-04	0.0048	3.99E-09
MDEA+	0	0	0	0	8.50E-05	0	8.36E-05	0.002065	0.0042	0	2.65E-05	0	0.0542	0.1231	6.19E-05
PZH+	0	0	0	0	1.37E-05	0	1.36E-05	0.0054	0.0027	0	1.02E-06	0	0.0227	0.0129	2.38E-06
PZH+2	0	0	0	0	0	0	0	0	0	0	0	0	0	0	0
HPZCOO	0	0	0	0	4.03E-07	0	4.67E-07	1.39E-04	3.35E-04	0	1.35E-07	0	0.0239	0.0543	3.14E-07
PZCOO-	0	0	0	0	1.12E-08	0	1.30E-08	0.0042	6.62E-04	0	6.13E-11	0	0.0074	0.0222	1.43E-10
PZCOO-2	0	0	0	0	8.24E-11	0	1.07E-10	3.40E-06	2.48E-06	0	2.84E-12	0	0.0017	0.0290	6.63E-12
N_2	7.03E-05	7.03E-05	1.1389	1.1388	1.02E-05	0	1.02E-05	0	8.54E-16	0	6.99E-10	0	7.03E-05	7.03E-05	1.63E-09
O_2	6.98E-06	6.98E-06	0.0634	0.0633	1.03E-06	0	1.03E-06	0	1.09E-16	0	1.31E-10	0	6.98E-06	6.98E-06	3.06E-10
CO	0	0	0	0	0	0	0	0	0	0	0	0	0	0	0
H_2	0	0	0	0	0	0	0	0	0	0	0	0	0	0	0
Mass Flow [kg/h]															
MDEA	2.22E-10	0.0106	0	0.0013	0.0030	0	0.0031	132.4536	132.1958	0.0045	1.17E-05	0	126.2410	118.0274	2.74E-05
PZ	9.45E-12	0.0003	0	0.0001	3.33E-05	0	3.96E-05	13.5473	14.0712	0	2.61E-08	2.04E-04	9.5887	4.1937	6.09E-08
H_2O	0.1237	5.5866	3.1411	4.3846	29.9845	3.0055	26.9790	137.9659	137.9086	0	1.6384	0	138.5982	138.8634	3.8229
CO_2	7.8573	7.8718	8.9271	1.0654	0.0002	0	0.0003	1.04E-05	0.0065	0	0.0031	0	3.7589	0.0205	0.0073
H3O+	0	0	0	0	1.72E-08	1.29E-08	1.87E-08	1.31E-10	2.39E-08	0	4.94E-08	0	1.34E-07	1.19E-08	1.15E-07
OH-	0	0	0	0	9.78E-07	1.15E-08	1.07E-06	0.0015	8.43E-04	0	6.32E-10	0	2.01E-04	2.06E-04	1.47E-09
HCO3-	0	0	0	0	0.0060	0	0.0059	0.1639	0.3733	0	0.0017	0	3.9955	2.8190	0.0039
CO3-2	0	0	0	0	1.60E-05	0	1.37E-05	0.0140	0.0010	0	1.03E-07	0	0.0145	0.2882	2.40E-07
MDEA+	0	0	0	0	0.0102	0	0.0101	0.2481	0.5036	0	0.0032	0	6.5119	14.7949	0.0074
PZH+	0	0	0	0	0.0012	0	0.0012	0.4706	0.2334	0	8.89E-05	0	1.9741	1.1233	0.0002
PZH+2	0	0	0	0	0	0	0	0	0	0	0	0	0	0	0
HPZCOO	0	0	0	0	5.25E-05	0	6.08E-05	0.0180	0.0436	0	1.75E-05	0	3.1130	7.0618	4.09E-05
PZCOO-	0	0	0	0	1.45E-06	0	1.68E-06	0.5450	0.0855	0	7.92E-09	0	0.9589	2.8680	1.85E-08
PZCOO-2	0	0	0	0	1.42E-08	0	1.84E-08	5.85E-04	4.27E-04	0	4.89E-10	0	0.2960	4.9904	1.14E-09
N_2	0.0020	0.0020	31.9045	31.9025	0.0003	0	0.0003	0.00E+00	2.39E-14	0	1.96E-08	0	0.0020	0.0020	4.57E-08
O_2	0.0002	0.0002	2.0273	2.0271	3.29E-05	0	3.29E-05	0.00E+00	3.48E-15	0	4.20E-09	0	2.23E-04	2.23E-04	9.79E-09
CO	0	0	0	0	0	0	0	0	0	0	0	0	0	0	0
H_2	0	0	0	0	0	0	0	0	0	0	0	0	0	0	0
Total Flow [kmol/h]	0.1855	0.4891	1.5795	1.4698	1.6646	0.1668	1.4978	8.9419	8.9420	3.77E-05	0.0911	2.37E-06	9.1252	9.0403	0.2125
Total Flow [kg/h]	7.9832	13.4716	46	39.3810	30.0055	3.0055	27	285.4285	285.4238	0.0045	1.6465	0.0002	295.0530	295.0530	3.8419
Total Flow [m^3/h]	2.3610	7.5248	41.8166	39.7313	0.0304	0.0030	0.0274	0.2786	0.2958	4.45E-06	0.0017	2.28E-07	3.5114	0.2823	0.0039
Temperature [K]	313.15	381.13	323.15	330.05	323.15	323.15	329.96	323.15	395.52	323.15	313.15	323.15	381.60	334.73	313.15
Pressure [kPa]	202.65	202.65	101.325	101.325	101.325	101.325	101.325	101.325	202.65	101.325	202.65	101.325	202.65	101.325	202.65

APPENDIX 9 Stream results of the PZ/MDEA 2_2

STREAM ID	CO2	CO2-OUT	FG-IN	FG-OUT	H2O-IN	H2O-MU	H2O-OUT	LEAN-IN	LEAN-OUT	MDEA-MU	PURGE-1	PURGE-2	PZ-MU	RICH-IN	RICH-OUT	WATER
Mole Flow [kmol/h]																
MDEA	1.97E-12	8.70E-05	0	1.37E-05	1.36E-04	0	1.43E-04	1.1111	1.1088	0.0117	3.16E-08	0.0116	0	1.0583	0.9899	2.99E-07
PZ	1.16E-13	3.79E-06	0	1.55E-06	1.97E-06	0	2.15E-06	0.1568	0.1631	0	9.72E-11	0.0017	0.0017	0.1107	0.0486	9.19E-10
H_2O	0.0069	0.2956	0.1744	0.2055	17.1774	0.1465	17.0309	7.6554	7.7329	0	0.0276	0.0809	0	7.7076	7.7227	0.2610
CO_2	0.1784	0.1787	0.2028	0.0243	8.62E-05	0	9.32E-05	2.54E-07	1.57E-04	0	2.17E-05	1.64E-06	0	0.0845	0.0005	0.0002
H3O+	0	0	0	0	1.58E-08	5.95E-10	1.59E-08	7.17E-12	1.31E-09	0.00E+00	7.69E-10	1.37E-11	0.00E+00	7.06E-09	6.27E-10	7.27E-09
OH-	0	0	0	0	3.48E-07	5.95E-10	3.79E-07	8.42E-05	4.93E-05	0.00E+00	1.16E-11	5.16E-07	0.00E+00	1.18E-05	1.21E-05	1.10E-10
HCO3-	0	0	0	0	0.0009	0	0.0009	0.0028	0.0064	0	8.61E-06	6.74E-05	0	0.0660	0.0463	8.14E-05
CO3-2	0	0	0	0	1.42E-06	0	1.41E-06	2.39E-04	1.85E-05	0	5.52E-10	1.93E-07	0	2.48E-04	0.0048	5.22E-09
MDEA+	0	0	0	0	7.83E-04	0	0.0007762	0.0021464	0.0044	0	8.29E-06	4.62E-05	0	0.0549	0.1233	7.84E-05
PZH+	0	0	0	0	1.19E-04	0	1.18E-04	5.63E-03	2.81E-03	0	3.19E-07	2.94E-05	0.00E+00	0.022656	0.012916	3.02E-06
PZH+2	0	0	0	0	0	0	0	0	0	0	0	0	0	0	0	0
HPZCOO	0	0	0	0	3.11E-06	0	3.42E-06	1.49E-04	3.63E-04	0	4.33E-08	3.79E-06	0	0.0244	0.0543	4.09E-07
PZCOO-	0	0	0	0	5.07E-08	0	5.77E-08	4.40E-03	7.00E-04	0	2.03E-11	7.32E-06	0	0.0075	0.0222	1.91E-10
PZCOO-2	0	0	0	0	3.28E-10	0	3.88E-10	3.74E-06	2.85E-06	0	9.69E-13	2.98E-08	0	0.0018	0.0290	9.16E-12
N_2	7.04E-05	7.04E-05	1.1389	1.1388	1.25E-04	0	1.25E-04	0.00E+00	9.07E-16	0	2.13E-10	9.49E-18	0	7.04E-05	7.04E-05	2.01E-09
O_2	6.99E-06	6.99E-06	0.0634	0.0633	1.28E-05	0	1.28E-05	0.00E+00	1.15E-16	0	3.99E-11	1.21E-18	0	6.99E-06	6.99E-06	3.78E-10
CO	0	0	0	0	0	0	0	0	0	0	0	0	0	0	0	0
H_2	0	0	0	0	0	0	0	0	0	0	0	0	0	0	0	0
Mass Flow [kg/h]																
MDEA	2.34E-10	0.0104	0	0.0016	0.0162	0	0.0170	132.3987	132.1251	1.3902	3.76E-06	1.3821	0	126.1117	117.9578	3.56E-05
PZ	9.99E-12	0.0003	0	0.0001	1.70E-04	0	1.85E-04	1.35E+01	14.04993	0	8.37E-09	0.1470	0.1506	9.5324	4.1830	7.91E-08
H_2O	0.1236	5.3248	3.1411	3.7028	309.4557	2.6396	306.8163	137.9137	139.3096	0	0.4975	1.4572	0	138.8549	139.1269	4.7020
CO_2	7.8522	7.8662	8.9271	1.0700	0.0038	0	0.0041	1.12E-05	0.0069	0	0.0010	7.23E-05	0	3.7173	0.0205	9.02E-03
H3O+	0	0	0	0	3.01E-07	1.13E-08	3.03E-07	1.36E-10	2.50E-08	0	1.46E-08	2.61E-10	0	1.34E-07	1.19E-08	1.38E-07
OH-	0	0	0	0	5.91E-06	1.01E-08	6.44E-06	1.43E-03	0.0008	0	1.97E-10	8.77E-06	0	0.0002	0.0002	1.87E-09
HCO3-	0	0	0	0	0.0548	0	0.0544	0.1713	0.3929	0	0.0005	0.0041	0	4.0251	2.8253	0.0050
CO3-2	0	0	0	0	8.55E-05	0	8.44E-05	1.43E-02	0.0011101	0	3.31E-08	1.16E-05	0	0.0149	0.2890	3.13E-07
MDEA+	0	0	0	0	0.0941	0	0.0933	0.2579	0.5312	0	0.0010	0.0056	0	6.5964	14.8193	0.0094
PZH+	0	0	0	0	0.0103	0	0.0103	0.4907	0.2449	0	2.78E-05	2.56E-03	0	1.9743	1.1256	0.0003
PZH+2	0	0	0	0	0	0	0	0	0	0	0	0	0	0	0	0
HPZCOO	0	0	0	0	4.05E-04	0	4.45E-04	0.0193	0.0472	0	5.63E-06	4.94E-04	0	3.1730	7.0617	5.32E-05
PZCOO-	0	0	0	0	6.55E-06	0	7.45E-06	5.68E-01	0.0904	0	2.62E-09	9.46E-04	0	0.9683	2.8683	2.47E-08
PZCOO-2	0	0	0	0	5.65E-08	0	6.67E-08	6.43E-04	0.0005	0	1.67E-10	5.14E-06	0	0.3077	4.9986	1.58E-09
N_2	0.0020	0.0020	31.9045	31.9025	0.0035	0	0.0035	0	2.54E-14	0	5.96E-09	2.66E-16	0	1.97E-03	0.0020	5.64E-08
O_2	0.0002	0.0002	2.0273	2.0271	4.10E-04	0	4.10E-04	0	3.70E-15	0	1.28E-09	3.87E-17	0	2.24E-04	0.0002	1.21E-08
CO	0	0	0	0	0	0	0	0	0	0	0	0	0	0	0	0
H_2	0	0	0	0	0	0	0	0	0	0	0	0	0	0	0	0
Total Flow [kmol/h]	0.1854	0.4745	1.5795	1.4320	17.1796	0.1465	17.0331	8.9387	9.0197	0.0117	0.0277	0.0943	0.0017	9.1386	9.0546	0.2614
Total Flow [kg/h]	7.9780	13.2038	46	38.7042	309.6396	2.6396	307	285.3432	286.8006	1.3902	0.5	3	0.1506	295.2784	295.2784	4.7258
Total Flow [m^3/h]	2.3595	7.2930	41.8166	38.4375	0.3133	0.0027	0.3110	0.2785	0.2973	0.0014	5.04E-04	3.11E-03	1.68E-04	3.4460	0.2825	0.0048
Temperature [K]	313.15	380.71	323.15	327.63	323.15	323.15	325.09	323.15	395.48	323.15	313.15	395.48	323.15	381.46	334.72	313.15
Pressure [kPa]	202.65	202.65	101.325	101.325	101.325	101.325	101.325	101.325	202.65	101.325	202.65	202.65	101.325	202.65	101.325	202.65

APPENDIX 10 Stream results of the PZ/MDEA 2_3

STREAM ID	CO2	CO2-OUT	FG-IN	FG-OUT	H2O-IN	H2O-MU	H2O-OUT	LEAN-IN	LEAN-OUT	MDEA-MU	PURGE-1	PURGE-2	PZ-MU	RICH-IN	RICH-OUT	WATER
Mole Flow [kmol/h]																
MDEA	1.85E-12	8.07E-05	0	1.12E-05	1.58E-04	0	1.66E-04	1.2079	1.2044	0.0117	2.91E-08	0.0116	0	1.1530	1.0848	2.66E-07
PZ	1.06E-13	3.41E-06	0	1.29E-06	2.36E-06	0	2.53E-06	0.1656	0.1755	0	8.73E-11	0.0017	1.75E-03	0.1218	0.0567	7.97E-10
H_2O	0.0070	0.2866	0.1744	0.1932	17.1652	0.1342	17.0310	8.3266	8.4023	0	0.0276	0.0808	0	8.3761	8.3931	0.2519
CO_2	0.1820	0.1823	0.2028	0.0207	7.02E-05	0	7.76E-05	5.38E-07	3.08E-04	0	2.17E-05	2.96E-06	0	0.0862	0.0005	1.98E-04
H3O+	0	0	0	0	1.32E-08	5.44E-10	1.30E-08	1.14E-11	2.01E-09	0	8.00E-10	1.93E-11	0	7.69E-09	6.81E-10	7.29E-09
OH-	0	0	0	0	4.16E-07	5.44E-10	4.46E-07	7.03E-05	4.17E-05	0	1.11E-11	4.01E-07	0	1.30E-05	1.34E-05	1.01E-10
HCO3-	0	0	0	0	8.76E-04	0	8.68E-04	0.0046	0.0101	0	8.25E-06	9.69E-05	0	0.0707	0.0493	7.52E-05
CO3-2	0	0	0	0	1.66E-06	0	1.67E-06	3.32E-04	2.54E-05	0	5.03E-10	2.44E-07	0	2.59E-04	0.0047	4.59E-09
MDEA+	0	0	0	0	7.61E-04	0	7.54E-04	0.0033	0.0069	0	7.95E-06	6.60E-05	0	0.0583	0.1264	7.25E-05
PZH+	0	0	0	0	1.19E-04	0	1.18E-04	0.0089	0.0044	0	2.98E-07	4.24E-05	0	0.0246	0.0142	2.72E-06
PZH+2	0	0	0	0	0	0	0	0	0	0	0	0	0	0	0	0
HPZCOO	0	0	0	0	3.04E-06	0	3.48E-06	3.03E-04	0.000725	0	3.88E-08	6.97E-06	0	0.0255	0.0577	3.54E-07
PZCOO-	0	0	0	0	5.93E-08	0	7.07E-08	6.90E-03	0.0011	0	1.74E-11	1.05E-05	0	0.0080	0.0241	1.59E-10
PZCOO-2	0	0	0	0	3.74E-10	0	4.84E-10	9.67E-06	7.14E-06	0	7.94E-13	6.86E-08	0	0.0018	0.0290	7.24E-12
N_2	7.56E-05	7.56E-05	1.1389	1.1388	1.27E-04	0	1.27E-04	0.00E+00	2.29E-15	0	2.24E-10	2.20E-17	0	7.56E-05	7.56E-05	2.04E-09
O_2	7.49E-06	7.49E-06	0.0634	0.0633	1.30E-05	0	1.30E-05	0.00E+00	3.73E-16	0	4.19E-11	3.59E-18	0	7.49E-06	7.49E-06	3.82E-10
CO	0	0	0	0	0	0	0	0	0	0	0	0	0	0	0	0
H_2	0	0	0	0	0	0	0	0	0	0	0	0	0	0	0	0
Mass Flow [kg/h]																
MDEA	2.20E-10	0.0096	0	0.0013	0.0189	0	0.0197	143.9414	143.5200	1.3898	3.47E-06	1.3796	0	137.3939	129.2726	3.17E-05
PZ	9.16E-12	2.94E-04	0	1.11E-04	2.03E-04	0	2.18E-04	14.2645	15.1133	0	7.52E-09	0.1453	0.1506	10.4912	4.8799	6.86E-08
H_2O	0.1261	5.1627	3.1411	3.4798	309.2356	2.4175	306.8183	150.0065	151.3702	0	0.4976	1.4551	0	150.8977	151.2043	4.5375
CO_2	8.0084	8.0217	8.9271	0.9108	0.0031	0	0.0034	2.37E-05	0.0135	0	0.000954	1.30E-04	0	3.7919	0.0221	8.70E-03
H3O+	0	0	0	0	2.51E-07	1.04E-08	2.48E-07	2.17E-10	3.83E-08	0	1.52E-08	3.68E-10	0	1.46E-07	1.29E-08	1.39E-07
OH-	0	0	0	0	7.07E-06	9.26E-09	7.58E-06	0.0012	7.10E-04	0	1.89E-10	6.82E-06	0	2.20E-04	0.0002	1.72E-09
HCO3-	0	0	0	0	0.0534	0	0.0529	0.2787	0.6150	0	5.03E-04	0.0059	0	4.3139	3.0069	0.0046
CO3-2	0	0	0	0	9.96E-05	0	1.00E-04	0.0199	0.0015	0	3.02E-08	1.46E-05	0	0.0156	0.2797	2.75E-07
MDEA+	0	0	0	0	0.0914	0	0.0906	0.4023	0.8249	0	0.0010	0.0079	0	7.0038	15.1938	0.0087
PZH+	0	0	0	0	0.0103	0	0.0103	0.7734	0.3844	0	2.60E-05	0.0037	0	2.1423	1.2410	0.0002
PZH+2	0	0	0	0	0	0	0	0	0	0	0	0	0	0	0	0
HPZCOO	0	0	0	0	3.96E-04	0	4.53E-04	0.0395	0.0943	0	5.05E-06	9.07E-04	0	3.3170	7.5140	4.61E-05
PZCOO-	0	0	0	0	7.65E-06	0	9.12E-06	0.8912	0.1408	0	2.25E-09	0.0014	0	1.0347	3.1067	2.05E-08
PZCOO-2	0	0	0	0	6.43E-08	0	8.33E-08	0.0017	0.0012	0	1.37E-10	1.18E-05	0	0.3117	4.9926	1.25E-09
N_2	0.0021	0.0021	31.9045	31.9024	0.0035	0	0.0035	0	6.41E-14	0	6.27E-09	6.16E-16	0	0.0021	0.0021	5.72E-08
O_2	2.40E-04	2.40E-04	2.0273	2.0270	4.15E-04	0	4.15E-04	0	1.19E-14	0	1.34E-09	1.15E-16	0	2.40E-04	0.00024	1.22E-08
CO	0	0	0	0	0	0	0	0	0	0	0	0	0	0	0	0
H_2	0	0	0	0	0	0	0	0	0	0	0	0	0	0	0	0
Total Flow [kmol/h]	0.1891	0.4690	1.5795	1.4160	17.1673	0.1342	17.0331	9.7246	9.8057	0.0117	0.0277	0.0943	0.0017	9.9263	9.8406	0.2522
Total Flow [kg/h]	8.1368	13.1967	46	38.3216	309.4175	2.4175	307	310.6203	312.0799	1.3898	0.5	3	0.1506	320.7160	320.7160	4.5598
Total Flow [m^3/h]	2.4065	7.1991	41.8166	37.8811	0.3131	0.0024	0.3109	0.3030	0.3232	0.0014	5.04E-04	0.0031	1.68E-04	3.5908	0.3074	0.0046
Temperature [K]	313.15	380.09	323.15	326.50	323.15	323.15	324.42	323.15	395.13	323.15	313.15	395.13	323.15	381.79	335.44	313.15
Pressure [kPa]	202.65	202.65	101.325	101.325	101.325	101.325	101.325	101.325	202.65	101.325	202.65	202.65	101.325	202.65	101.325	202.65